



Università degli Studi di Cagliari

## **DOTTORATO DI RICERCA**

in Ingegneria Elettronica e Informatica

Ciclo XXIII

### **TITOLO TESI**

A GENERALIZED FINITE DIFFERENCE APPROACH TO THE  
COMPUTATION OF MODES

Settore scientifico disciplinari di afferenza

ING-INF/02 Campi Elettromagnetici

|                        |                           |
|------------------------|---------------------------|
| Presentata da:         | Alessandro Fanti          |
| Coordinatore Dottorato | Prof. Alessandro Giua     |
| Tutor/Relatore         | Prof. Giuseppe Mazzarella |

Esame finale anno accademico 2010 - 2011





*Ph.D. in Electronic and Computer Engineering  
Dept. of electrical and Electronic Engineering  
University of Cagliari*



# **A GENERALIZED FINITE DIFFERENCE APPROACH TO THE COMPUTATION OF MODES**

Alessandro Fanti

*Advisor: Prof Giuseppe Mazzearella  
Curriculum: ING-INF/02 Elettromagnetismo  
XXIII Cycle December 2011*



*Dedicated to my parents  
and my grand parents!*



## **Abstract**

This thesis deals with numerical techniques for the computation of modes in electromagnetic structures with arbitrary geometry. The approach proposed in this work is based on the Finite Difference (FD) and Vector Finite Difference (VFD), which are applied to rectangular, circular, elliptical geometries, and to combination of them. The FD is applied using a 2D cartesian, polar and elliptical grid in the waveguide section. A suitable Taylor expansion of the mode function allows, either for scalar and for vector FD, to take exactly into account the boundary condition.

To prevent the raising of spurious modes, the VFD approximation results in a constrained eigenvalue problem, that has been solved using a decomposition method.

All approaches presented have been validated comparing the results to the analytical modes of rectangular and circular waveguide, and to known data for the elliptic case.

The standard calculation of the waveguide modes using FD requires the use of two different grids, namely one for TE modes and the other for TM modes, due to the different boundary condition. It has been shown that a single grid can be used for all modes, thus allowing an effective mode-matching solution.

The FD approach has been extended to waveguides (and apertures) with irregular boundaries, and therefore non-regular discretization grids. It has been shown that a suitable FD approximation of the Laplace operator is still possible. A ridged-waveguide, with trapezoidal ridges, and a rounded-ended waveguide have been considered in detail.





## CONTENTS

|  |           |
|--|-----------|
| List of Tables.....                                    | i         |
| List of Figures.....                                   | iii       |
| <b>I. INTRODUCTION. . . . .</b>                        | <b>1</b>  |
| 1.1) ANALYTICAL TECHNIQUES.....                        | 2         |
| 1.2) SEMI-ANALYTICAL .....                             | 3         |
| 1.3) NUMERICAL METHOD.....                             | 4         |
| 1.3.a) FINITE-ELEMENTS METHOD.....                     | 4         |
| 1.3.b) FINITE-DIFFERENCE METHOD.....                   | 5         |
| <b>II. WAVEGUIDE MODES. . . . .</b>                    | <b>8</b>  |
| INTRODUCTION.....                                      | 8         |
| 2.1) MAXWELL EQUATION .....                            | 8         |
| 2.2) DECOMPOSITION INTO TE AND TM FIELDS .....         | 10        |
| 2.3) TE MODES .....                                    | 11        |
| 2.4) TM MODES .....                                    | 15        |
| <b>III. COMPUTATION OF WAVEGUIDE MODES USING</b>       |           |
| <b>FINITE DIFFERENCE: RECTANGULAR WAVEGUIDES .....</b> | <b>17</b> |
| INTRODUCTION.....                                      | 17        |
| 3.1) FINITE DIFFERENCE SCHEME.....                     | 18        |
| 3.2) STANDARD FINITE DIFFERENCE SCHEME.....            | 22        |
| 3.3) FINITE DIFFERENCE SINGLE GRID TE                  |           |
| EVALUATION OF TE AND TM MODES                          |           |
| IN METALLIC WAVEGUIDES.....                            | 27        |
| 3.4) VECTOR FINITE DIFFERENCE APPROACH:                |           |
| TE MODES .....   | 29        |
| 3.5) VECTOR FINITE DIFFERENCE APPROACH:                |           |
| TM MODES .....   | 35        |
| 3.6) EXTENSION TO 3D PROBLEM .....                     | 37        |

|  |            |
|--|------------|
| <b>IV. FINITE DIFFERENCE IN POLAR AND ELLIPTICAL GRID.....</b> | <b>41</b>  |
| INTRODUCTION.....  | 41         |
| 4.1) POLAR FINITE DIFFERENCE .....                             | 41         |
| 4.2) FINITE DIFFERENCE IN ELLIPTICAL WAVEGUIDE.....            | 50         |
| 4.3) VECTOR POLAR FINITE DIFFERENCE.....                       | 58         |
| 4.4) VECTOR ELLYPTIC FINITE DIFFERENCE.....                    | 67         |
| <b>V. FINITE DIFFERENCE IN RIDGED WAVEGUIDE .....</b>          | <b>70</b>  |
| INTRODUCTION.....  | 70         |
| 5.1) FINITE DIFFERENCE IN RIDGED WAVEGUIDE .....               | 70         |
| 5.2) ROUNDED-END WAVEGUIDE.....                                | 76         |
| <b>VI. NUMERICAL RESULTS.....</b>                              | <b>80</b>  |
| INTRODUCTION.....  | 80         |
| 6.1) FD IN SQUARE AND RECTANGULAR WAVEGUIDE....                | 80         |
| 6.2) FD IN CIRCULAR AND ELLIPTICAL WAVEGUIDE.....              | 97         |
| 6.3) FD IN ROUNDED-END WAVEGUIDE.....                          | 113        |
| 6.4) VECTOR FD IN RECTANGULAR WAVEGUIDE.....                   | 120        |
| 6.5) VECTOR FD IN CIRCULAR WAVEGUIDE.....                      | 123        |
| 6.6) VECTOR FD IN ELLIPTIC WAVEGUIDE.....                      | 124        |
| 6.7) EXTENSION TO 3D PROBLEM.....                              | 128        |
| 6.8) ELABORATION TIME.....                                     | 130        |
| <b>VII. CONCLUSION.....</b>                                    | <b>131</b> |
| <b>Appendix.....</b>   | <b>133</b> |
| I. CONSTRAINED EIGENVALUE PROBLEMS.....                        | 133        |
| <b>List of papers by the author .....</b>                      | <b>135</b> |
| <b>Bibliography.....</b>                                       | <b>137</b> |

## List of Tables

|   |    |
|---|----|
| Table 6.1.1: comparison between our FD code and analytic results for TE and TM modes on TE grid in a square waveguide.....                                | 81 |
| Table 6.1.2: comparison between our FD code and analytic results for TE and TM modes on TM grid in a square waveguide.....                                | 82 |
| Table 6.1.3: comparison between our FD code and analytic results for TE and TM modes on TE grid in a rectangular waveguide.....                           | 84 |
| Table 6.1.4: comparison between our FD code and analytic results for TE and TM modes on TM grid in a rectangular waveguide.....                           | 85 |
| Table 6.1.5: comparison between our FD code and analytic results for TE and TM modes on TE grid in a rectangular waveguide.....                           | 86 |
| Table 6.1.6: comparison between our FD code and analytic results for TE and TM modes on TM grid in a rectangular waveguide.....                           | 87 |
| Table 6.1.7: comparison between our FD code and analytic results for TE on TE grid in rectangular waveguide, when varying $\Delta x = \Delta y$ .....     | 89 |
| Table 6.1.8: comparison between our FD code and analytic results for TM on TE grid in rectangular waveguide, when varying $\Delta x = \Delta y$ .....     | 90 |
| Table 6.1.9: comparison between our FD code and analytic results for TE on TM grid in rectangular waveguide, when varying $\Delta x = \Delta y$ .....     | 91 |
| Table 6.1.10: comparison between our FD code and analytic results for TE on TM grid in rectangular waveguide when varying $\Delta x = \Delta y$ .....     | 92 |
| Table 6.1.11: comparison between our FD code and analytic results for TE on TE grid in rectangular waveguide, when varying $\Delta x \neq \Delta y$ ..... | 93 |
| Table 6.1.12: comparison between our FD code and analytic results for TM on TE grid in rectangular waveguide, when varying $\Delta x \neq \Delta y$ ..... | 94 |
| Table 6.1.13: comparison between our FD code and analytic results for TE on TM grid in rectangular waveguide, when varying $\Delta x \neq \Delta y$ ..... | 95 |
| Table 6.1.14: comparison between our FD code and analytic results for TM on TM grid in rectangular waveguide, when varying $\Delta x \neq \Delta y$ ..... | 96 |

|  |     |
|--|-----|
| Table 6.2.1: comparison between our FD code and analytic results for TE and TM modes on TE grid in circular waveguide.....                                   | 98  |
| Table 6.2.2: comparison between our FD code and analytic results for TE modes on TE grid in circular waveguide , when varying $\Delta r$ .....               | 99  |
| Table 6.2.3: comparison between our FD code and analytic results for TM modes on TE grid in circular waveguide , when varying $\Delta r$ .....               | 100 |
| Table 6.2.4: comparison between our FD code and analytic results for TE modes on TE grid in circular waveguide , when varying $\Delta \theta$ .....          | 101 |
| Table 6.2.5: comparison between our FD code and analytic results for TM modes on TE grid in circular waveguide , when varying $\Delta \theta$ .....          | 102 |
| Table 6.2.6: comparison between our FD code and analytic results for TM modes on TM grid in circular waveguide , when varying $\Delta r$ .....               | 104 |
| Table 6.2.7: comparison between our FD code and analytic results for TE modes on TM grid in circular waveguide , when varying $\Delta r$ .....               | 105 |
| Table 6.2.8: comparison between our FD code and analytic results for TM modes on TM grid in circular waveguide , when varying $\Delta \theta$ .....          | 106 |
| Table 6.2.9: comparison between our FD code and analytic results for TE modes on TM grid in circular waveguide , when varying $\Delta \theta$ .....          | 107 |
| Table 6.2.10: comparison between our FD code and FIT (CST) results for TE and TM modes on TE grid in elliptic waveguide , with different $\Delta u$ .....    | 111 |
| Table 6.2.11: comparison between our FD code and FIT (CST) results for TE and TM modes on TE grid in elliptic waveguide , when varying $\Delta \theta$ ..... | 112 |
| Table 6.4.1: comparison between our vector FD code and analytic results for TE modes on TE grid in square waveguide.....                                     | 121 |
| Table 6.4.2: comparison between our vector FD code and analytic results for TE modes on TE grid in square waveguide.....                                     | 122 |
| Table 6.5.1: comparison between our vector FD code and analytic results for TE modes on TE grid in circular waveguide.....                                   | 123 |

|  |     |
|--|-----|
| Table 6.6.1: comparison between our vector FD code and analytic results for TE modes on TE grid in elliptic waveguide with $\epsilon_x=0,1$ , $\Delta\nu=1^\circ$ and $\Delta u$ variable..... | 125 |
| Table 6.6.2: comparison between our vector FD code and analytic results for TE modes on TE grid in elliptic waveguide with $\epsilon_x=0,5$ , $\Delta\nu=1^\circ$ and $\Delta u$ variable..... | 126 |
| Table 6.6.3: comparison between our vector FD code and analytic results for TE modes on TE grid in elliptic waveguide with $\epsilon_x=0,9$ , $\Delta\nu=1^\circ$ and $\Delta u$ variable..... | 127 |
| Table 6.6.4: comparison between our 3D FD code and analytic results for modes on Newmann grid in a rectangular cavity.....   | 129 |

## List of Figures

|  |    |
|--|----|
| Fig. 1.3.1 a) Division of a region into square elements. b) Division of a region into right Isosceles triangles. c) Division of a region into triangles and squares. d) Division of an irregular region into triangles. .... | 4  |
| Fig. 1.4.1 Division of a region into square cells.....   | 6  |
| Fig. 2.3.1. Position of versors from the contour of the conductor.....   | 14 |
| Fig. 3.1.1. Monodimension grid for the Dirichlet problem.....  | 20 |
| Fig. 3.2.1 Internal point of grid TE and TM.....   | 23 |
| Fig. 3.2.3. Standard TE and TM grid, as suggested from BC.....   | 25 |
| Fig. 3.2.4. Boundary point for TE case and TM case.....  | 25 |
| Fig. 3.3.1. Boundary point TM case.....  | 28 |
| Fig. 3.4.1. Vectors geometry with respect to the contour of the conductor.....   | 30 |
| Fig. 3.4.2. Boundary point of TE grids.....  | 33 |
| Fig. 3.6.1. Standard Newmann and Dirichlet grid, as suggested from BC .....  | 38 |
| Fig. 3.6.2. Internal point of 3D Newmann grid.....   | 38 |
| Fig. 3.6.3. Boundary point of 3D Newmann grid.....   | 38 |
| Fig. 4.1.1. Standard TE and TM grid, as suggested from BC.....   | 43 |
| Fig. 4.1.2. Internal point of grid TE and TM.....  | 44 |
| Fig. 4.1.3. Center of circle.....  | 46 |
| Fig. 4.1.4. Boundary point of circular waveguide.....  | 47 |
| Fig. 4.2.1. Geometry of the elliptic cylindrical coordinates.....  | 51 |
| Fig. 4.2.2. Internal point of the elliptic cylindrical coordinates grid TE and TM..  | 52 |
| Fig. 4.2.3. point between foci.....  | 53 |
| Fig. 4.2.4. Focus (P) of the ellipse.....  | 54 |
| Fig. 4.2.5. Standard TE and TM grid, as suggested from BC.....   | 55 |

|   |     |
|---|-----|
| Fig. 4.2.6. Boundary point for TE case and TM case.....   | 56  |
| Fig. 4.3.1 Boundary point of polar framework.....   | 60  |
| Fig. 4.3.2 component of $\vec{M}$ between center and next point.....  | 64  |
|   |     |
| Fig. 5.1.1 Waveguides section with trapezoidal ridge, and FD corner mesh grids.....   | 71  |
| Fig. 5.1.2. Generic internal case of five points used to develop FD scheme.....   | 71  |
| Fig. 5.1.3. Boundary Point of trapezoidal ridge.....  | 73  |
| Fig. 5.1.4. Boundary Point of trapezoidal ridge.....  | 74  |
| Fig. 5.2.1 A mixed mesh (cartesian-polar) of non standard waveguide and its dimension.....  | 77  |
| Fig. 5.2.2. (a) Point between Polar and Cartesian framework (b) Boundary point between Polar and Cartesian framework.....   | 78  |
| Fig. 5.2.3. Center Point between Polar and Cartesian framework.....   | 78  |
|   |     |
| Fig. 6.2.1. Comparison between our FD code and analitic results and FIT(CST) results for TE modes in circular wave guide with $r=4$ mm $\Delta r=0.0792$ mm and $\Delta\theta=1^\circ$ .....              | 108 |
| Fig. 6.2. Comparison between our FD code and analitic results and FIT(CST) results for TE modes in circular wave guide with $r=4$ mm $\Delta r=0.0792$ mm and $\Delta\theta=0,5^\circ$ .....              | 109 |
| Fig. 6.3.1. Comparison between our FD code and and FIT (CST) results for TE modes in Rounded-end wave guide with $\Delta x = \Delta y = \Delta r = 0,1569$ mm $D=B=8$ mm and $\Delta\theta=1^\circ$ ..... | 114 |
| Fig. 6.3.2. Comparison between our FD code and FIT (CST) results for TE modes in Rounded-end wave guide with $\Delta x = \Delta y = \Delta r = 0,0792$ mm $D=B=8$ mm and $\Delta\theta=1^\circ$ .....     | 115 |

|  |     |
|--|-----|
| Fig. 6.3.3. Comparison between our FD code and and FIT (CST) results for TE modes in Rounded-end wave guide with $\Delta x = \Delta y = \Delta r = 0,03980$ mm D=B=8 mm and $\theta=1^\circ$ .....       | 116 |
| Fig. 6.3.4. Comparison between our FD code and and FIT (CST) results for TE modes in Rounded-end wave guide with $\Delta x = \Delta y = \Delta r = 0,01995$ mm D=B=8 mm and $\theta=1^\circ$ .....       | 117 |
| Fig. 6.3.5. Comparison between our FD code and and FIT (CST) results for TE modes in Rounded-end wave guide with $\Delta x = \Delta y = \Delta r = 0,0792$ mm D=8 mm B=16 mm and $\theta=1^\circ$ .....  | 118 |
| Fig. 6.3.6. Comparison between our FD code and and FIT (CST) results for TE modes in Rounded-end wave guide with $\Delta x = \Delta y = \Delta r = 0,03980$ mm D=8 mm B=16 mm and $\theta=1^\circ$ ..... | 119 |



## Chapter I

### INTRODUCTION

This thesis deals with numerical techniques for the computation of modes in electromagnetic structures with generic geometry. The structures we analyse are waveguides, and to a smaller extent resonant cavities.

There are many strategies to do this, but a comparative evaluation of the techniques proposed in the literature has selected the finite difference approach (FD) as the most suitable because of its flexibility and low computational cost.

The knowledge of eigenvalues and distribution of field modes of waveguides and resonant cavities is important to design and use such devices, both for standard usages and for other applications, like for the analysis of waveguide junction using mode matching [1-5], or solution of waveguide problems with sources [6]. The same type of information is required in the analysis with the method of moments (MoM), of thick-walled waveguide slot [7,8] and apertures [9]. Indeed, these apertures can be considered as stub waveguide, and the modes of these guides are the natural basic functions for MoM [7].

In literature, different approaches have been proposed to compute the modes of electromagnetic structures:

- Analytical
- Semi-analytical
- Numerical (differential)

## 1.1) ANALYTICAL TECHNIQUES

The method of separation of variables is a convenient method for solving a partial differential equation (PDE). Basically, it entails seeking a solution which breaks up into a product of functions, each of which involves only one of the variables. For an Helmholtz wave equation,

$$1.1.1.) \nabla_t^2 \phi + k_t^2 \phi$$

we can apply the method of separation of variables, letting  $\phi(x_1, x_2) = \varphi(x_1) \cdot \varphi(x_2)$  as long as the chosen reference frame allows separation of the Laplace equation. In this way we obtain two different problems in  $x_1$  and  $x_2$  variables, whose solution gives the modes of the waveguide.

The PDE to be solved is subject to boundary conditions. The equation is separable when these boundary conditions can be transformed so that they can be applied directly to the separated equations. This is the case for three typical waveguides [10]:

- Rectangular
- Circular
- Elliptic

In the rectangular case, the cartesian reference system is used. Separation is easy because trigonometric functions are used. The circular case is a bit more complex because it requires the use of cylindrical coordinates, and the Bessel functions are used. The cutoff frequencies for the circular waveguide can be written in terms of the zeros associated with Bessel functions and derivatives of Bessel functions.

On the other hand in the case of elliptic waveguide, it is used a reference system with elliptic coordinates. A closed form solution has been found by Chu [11] since the 30's. Unfortunately, the field distribution is described by the

Mathieu functions [12] and so the eigenvalues are the zeros of these function. Numerical evaluation of the Mathieu functions is very cumbersome: the best approach [13] seems to be the expansion of those functions in a series of (more tractable) Bessel functions. As a consequence, the eigenvalues of an elliptic guide must be computed numerically, looking for the zeroes of a suitable series of Bessel functions. It is not a surprise, therefore, that the availability of a closed-form solution in this case have not prevented different numerical techniques to be proposed, aiming at a simpler procedure or, even, at a greater accuracy [14-17]. For resonant cavities, the approach is the same, and the allowed geometries are the cylindrical (with a separable section) and the spherical one .

## **1.2) SEMI-ANALYTICAL**

Although in many practical cases analytical solution cannot be obtained, we must resort to numerical approximate solution. Is often possible to replace the problem of integrating a differential equation by the equivalent problem of seeking a function that gives a minimum value of some integral. Problem of this type are called variational methods [18], and be considered as semi analytical.

The eigenvalues of the equation can be expressed as a suitable (quadratic) functional of the eigenfunctions. Such functional reach its extreme value for the true eigenfunction. If we compute the functional in a different function (an approximation of the true eigenfunction), we obtain an approximate value of the eigenvalue which, due to the variational nature of the functional, is quadratic in the approximation error of the function. For waveguide problem, different functionals can be used. Some of them require the approximate function to fulfil the boundary condition, others don't, and are therefore more effective. A drawback of this approach is that it is taylored to evaluate the eigenvalues only.

The Rayleigh - Ritz method is a generalization of this method, which obtain an approximation of both eigenvalues and eigenfunctions. This method is based on pioneering work by Lord Rayleigh in 1870 and improvements by Ritz in 1909.

The test function for the functional is expressed as a linear combination of known functions and the solution consists of determining the parameters in the combination forcing the maximum condition. This determination involves substitution of the linear combination into the functional and then differentiation with respect to each parameter.

### 1.3) NUMERICAL METHOD

The analytical methods are not valid if the integral region of the structure is complex and therefore we are forced to use numerical methods. Since the problem at hand is the solution of partial differential equation (PDE), the most popular numerical methods available for solving PDE are finite-elements method, and finite difference method.

#### 1.3.a) FINITE-ELEMENTS METHOD

The basic concept of the finite-element method [19] is that although the behavior of a function may be complex when viewed over a large region, a simple approximation may suffice for a small subregion. The total region is therefore divided into a number of small non overlapping subregions called *finite elements*. In two dimensions we usually use polygons and the simplest polygons are triangles and squares.

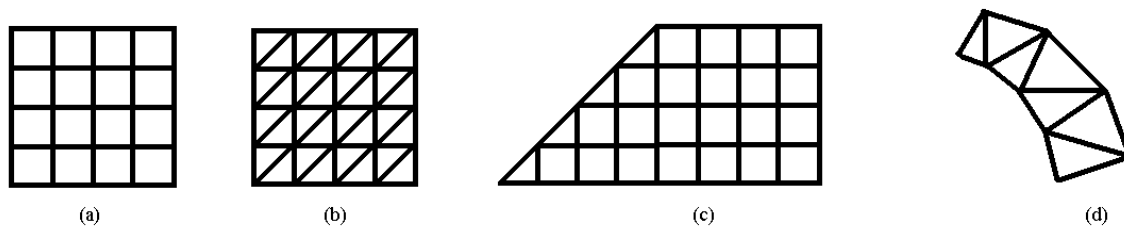


Fig. 1.3.1 a) Division of a region into square elements. b) Division of a region into right Isosceles triangles. c) Division of a region into triangles and squares. d) Division of an irregular region into triangles.

Figure 1.3.1a shows a region divided into squares and Fig. 1.3.1b shows the same region divided into isosceles right triangles. Sometimes as illustrated in Fig. 1.3.1c a combination of triangles and squares is useful. One of the advantages of using triangles is that a fairly arbitrary region can be more easily approximately covered by a set of triangles, as shown in Fig. 1.3.1d. Regardless of the shape of the elements, the field is approximated by a different expression over each element, but where the edges of adjoining elements overlap, the field representations must be chosen as to maintain the continuity of the field. The equations to be solved are usually not stated in terms of the field variables but in terms of an integral-type functional such as energy. The functional is chosen such that the field solution makes the functional stationary. The total functional is the sum of the integral over each element. This technique allow to analyze every type of structure using a suitable “mesh”, but needs a big number of points which leads to an increase in the computational load of the matricial problem, and consequentially an increase of the computational burden. In particular, the more curvilinear is the structure’s edge the more the mesh will be done in those areas, and the more the computational load increases.

### **1.3.b)        FINITE-DIFFERENCE METHOD**

The finite difference approach (FD) is a method for the solution of numerical partial differential equations. It is based on the replacement of the derivatives with a finite approximation [20]. Therefore, the solution is computed only on a finite sets of points (discretization grid, or mesh)

The most popular FD approach is based on the use of a standard four-point FD approximation [21] of the Laplace operator. But it requires a rectangular discretization grid, and therefore a boundary with all sides parallel to the rectangular axes. As a consequence, many geometries cannot be dealt with exactly with this approach, requiring a staircase approximation of the boundaries (see Fig.1.41). In order to achieve good results comparable with

analytic ones, the discretization step should be significantly reduced, and this operation increases the number of points and consequently there's an increase of the computational load. This problem makes the FD standard not suitable for curvilinear edge structures analysis. Moreover, the standard FD approach requires different discretization grids for TE and TM modes. On the other hand, FD methods present many advantages:

- Easy implementation
- Flexibility
- Good precision
- Low computational load compared to FEM methods.

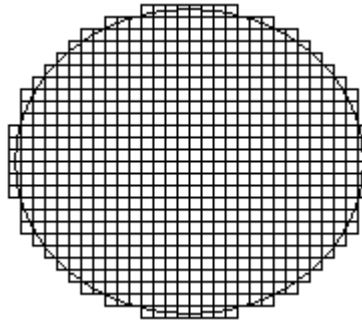


Fig. 1.4.1 Division of a region into square cells

The aim of this thesis is to overcome the drawbacks of FD.

The discretization through a cartesian grid comes from the expression of Laplace operator in (1.1.1) in Cartesian coordinates. It has been tried to use a different grid derived from a form of Laplace operator written in a form suitable to the considered structure.

The first test involved a circular guide, using the Laplace operator and a discretization grid in polar coordinates. We have obtained good results with a low computational load compared to FEM technique and an high precision in the results comparable with analytic results. In particular, as we shall see in chapter

IV, it's been considered the use of circular and elliptic grids for the study of circular [22 - 25] and elliptic [23,25] waveguides.

An other problem, described in chapter 3, is the Laplace operator's redefinition based on boundary conditions in order to use a single grid [26,27]. This is important, e.g. in numerical mode matching analysis of waveguide junctions reducing the computational load (complexity) and the processing time.

The FD is applied to the classical scalar potential, so to compute the waveguide modes numerical derivatives must be used. For regular-shaped guides, the use of numerical derivatives is reasonably accurate and is very easy to implement, but this isn't true for waveguides with irregular section and resonant cavities. In this cases it isn't possible to use the scalar potential, and it is necessary, in order to calculate the modes to introduce a vector FD in this thesis, this problem has been faced introducing the vector finite difference, but in a simplified form respect to the methods present in literature. The computation of the TE and TM modes has been studied by solving the Helmholtz equation using the vectorial finite differences method, reducing to a constrained eigenvalues problems. The vector finite difference approximation of the vector Helmholtz eigenvalues equation on a Cartesian [28,29] an curvilinear grid [23-25] have been considered. In chapter V we present a FD technique for the computation of modes and eigenvalues of a waveguide whose boundary is irregular, such as polygonal, or consisting of segments and circular arcs [22,30], taking exactly into account the boundary of the waveguide and therefore with no loss of accuracy.

## Chapter II

### WAVEGUIDE MODES

#### INTRODUCTION

In this chapter we deal with the propagation in guiding structures. First, we use Maxwell equations to describe the field of these structures and then we decompose in TE, TM field using the boundary conditions. Finally, we explain the TE and TM modes..

#### 2.1) MAXWELL EQUATION

Maxwell equations in the Domain Frequency for an homogeneous material, in the absence of sources, take the form

$$2.1.1.) \quad \begin{cases} \nabla \times \vec{E} = -j\omega\mu\vec{H} \\ \nabla \times \vec{H} = j\omega\varepsilon\vec{E} \end{cases}$$

As we are interested in the study of the propagation in a guiding structure, the direction of propagation, which we assume as “z” direction of a reference system, shall be a preferential direction of the problem. For this reason we decompose all vectors in two components: one transverse and another one alongside “z” :  $\vec{E} = \vec{E}_t + E_z \vec{i}_z$ , and in a similar way for H. It is also convenient to

separate the transverse and longitudinal parts of operator  $\nabla$  :  $\nabla = \vec{\nabla}_t + \frac{\partial}{\partial z} \vec{i}_z$

To solve the (2.1.1), we can use the scalar potentials of Hertz Debye defined for TE and TM fields. For TM field we have  $H_z = 0$ , so that, using the  $\vec{A}$  potential, we can write:



$$2.1.2.) \quad \vec{i}_z \times \vec{H} = \vec{i}_z \cdot (\nabla \times \vec{A}) = \vec{i}_z \cdot (\nabla_t \times \vec{A}_t) = 0$$

Since  $\nabla_t \times \vec{A}_t$  has only the z component, then  $\nabla_t \times \vec{A}_t = 0$  and from this it follows that there exists a longitudinal potential  $\vec{A}$ :

$$2.1.3.) \quad \vec{A} = \vec{i}_z \cdot \mu \Psi$$

that allows we obtain any field TM (with  $\vec{H}_z = 0$ ). We obtained:

$$2.1.4.) \quad \begin{cases} \vec{H}_t = \nabla \times (\Psi \vec{i}_z) = \nabla \Psi \times \vec{i}_z \\ j\omega \epsilon \vec{E} = \nabla \times \vec{H}_t = \nabla \times \nabla \times (\Psi \vec{i}_z) = \nabla \nabla \cdot (\Psi \vec{i}_z) - \nabla^2 \Psi \vec{i}_z = \frac{\partial}{\partial z} \nabla \Psi - \nabla^2 \Psi \vec{i}_z = \frac{\partial}{\partial z} \nabla_t \Psi - \nabla_t^2 \Psi \vec{i}_z \end{cases}$$

The equations (2.1.4) allow also to separate the longitudinal and transverse part of  $\vec{E}$ . To compute  $\Psi$ , we start by Maxwell equation to get:

$$\nabla \times \nabla \times \vec{H} = j\omega \epsilon \nabla \times \vec{E} = j\omega \epsilon (-j\omega \mu \vec{H}) = \beta^2 \vec{H} \quad \text{and substituting the first to (2.1.4)}$$

$$2.1.5.) \quad \nabla \times \nabla \times \nabla \times (\Psi \vec{i}_z) - \beta^2 \nabla \times (\Psi \vec{i}_z) = \nabla \times [\nabla \times \nabla \times (\Psi \vec{i}_z) - \beta^2 (\Psi \vec{i}_z)] = 0$$

the term in the brackets is equal to:

$$2.1.6.) \quad \nabla \nabla \cdot (\Psi \vec{i}_z) - \nabla^2 \Psi \vec{i}_z - \beta^2 \Psi \vec{i}_z = \frac{\partial}{\partial z} \nabla \Psi - \nabla^2 \Psi \vec{i}_z - \beta^2 \Psi \vec{i}_z$$

The rotor of the first term is null and therefore we are left with:

$$2.1.7.) \nabla \times \vec{i}_z [\nabla^2 \Psi + \beta^2 \Psi] = 0$$

Then  $\vec{i}_z [\nabla^2 \Psi + \beta^2 \Psi] = \nabla \chi'$  where  $\chi'$  depends only by  $z$ .

Therefore  $\nabla^2 \Psi + \beta^2 \Psi = f(z)$ . The solution of this equation is the sum of a particular integral (and there is a function only of  $z$ ) and the integral of the general homogeneous. The particular integral isn't part of the field and remains:

$$2.1.8.) \nabla^2 \Psi + \beta^2 \Psi = 0$$

For duality any field TE have a similar expression with a potential  $\phi$  such that  $\nabla^2 \phi + \beta^2 \phi = 0$ , as:

$$2.1.9.) \begin{cases} \vec{E}_t = -\nabla \times (\phi \vec{i}_z) = -\nabla_t \phi \times \vec{i}_z \\ j\omega \varepsilon \vec{H} = -\frac{\partial}{\partial z} \nabla_t \phi - \nabla_t^2 \phi \vec{i}_z \end{cases}$$

## 2.2) DECOMPOSITION INTO TE AND TM FIELDS

Every electromagnetic field can be expressed as the sum of a TE and a TM field (in absence of sources). Let's consider a field with  $E_z \neq 0$ ,  $H_z \neq 0$  and a function  $\tilde{\Psi}$  which satisfies the Poisson equation:

$$2.2.1.) \nabla_t^2 \tilde{\Psi} = -j\omega \varepsilon E_z$$

If  $\tilde{\Psi}$  is considered as Hertz-Debye potential, it allows to determinate a TM-field  $(\vec{E}^{TM}, \vec{H}^{TM})$  with the same z-component of the assigned field. Therefore  $(\vec{E} - \vec{E}^{TM}, \vec{H} - \vec{H}^{TM})$  is a TE-field. Finally, the decomposition is:

$$2.2.2.) \begin{cases} \vec{E} = (\vec{E} - \vec{E}^{TM}) + \vec{E}^{TM} \\ \vec{H} = (\vec{H} - \vec{H}^{TM}) + \vec{H}^{TM} \end{cases}$$

In general, every field can be determined from the potentials  $\Psi, \phi$

$$2.2.3.) \begin{cases} \vec{E}_t = \frac{1}{j\omega\epsilon} \frac{\delta}{\delta z} \nabla_t \Psi - \nabla_t \phi \times \vec{i}_z \\ \vec{H}_t = \nabla_t \Psi \times \vec{i}_z + \frac{1}{j\omega\mu} \frac{\partial}{\partial z} \nabla_t \phi \end{cases} \quad \begin{cases} E_z = -\frac{1}{j\omega\epsilon} \nabla_t^2 \Psi \\ H_z = -\frac{1}{j\omega\mu} \nabla_t^2 \phi \end{cases}$$

### 2.3) TE MODES

The analysis of TEM [31] field is simplified by the possibility of separating the longitudinal variation from the transverse one. In the case of TE or TM [6] fields it's therefore convenient to seek solutions which have an factorized representation

$$2.3.1.) \begin{cases} \vec{E}_t = V(z) \vec{e}(\vec{t}) \\ \vec{H}_t = I(z) \vec{h}(\vec{t}) \end{cases}$$

where V,I have no physical meaning, thus the impedance's choice will be based only on a matter of convenience . In terms of Hertz-Debye potentials

$$2.3.2.) \begin{cases} \vec{E}_t = V(z) \vec{e} = -\nabla_t \phi \times \vec{i}_z \\ \vec{H}_t = I(z) \vec{h} = \frac{1}{j\omega\mu} \frac{\partial}{\partial z} \nabla_t \phi \\ H_z = -\frac{1}{j\omega\mu} \nabla_t^2 \phi \end{cases}$$

The field's factorization implies a similar factorization for the potentials

$\phi = \frac{1}{k_t} \phi_0(\vec{t}) V(z)$ ,  $\frac{1}{k_t} [m^{-1}]$  is an arbitrary constant. Thus

$$2.3.3.) \begin{cases} \vec{e} = -\frac{1}{k_t} \nabla_t \phi_0 \times \vec{i}_z \\ I(z) \vec{h} = \frac{1}{j\omega\mu} \frac{\delta}{\delta z} \nabla_t \phi_0 \frac{dV}{dz} \Rightarrow \vec{h} = -\frac{1}{k_t} \nabla_t \phi_0 \Rightarrow \vec{e} = \vec{h} \times \vec{i}_z \\ -\frac{dV}{dz} = j\omega\mu I \end{cases}$$

From the expression for  $\phi$

$$2.3.4.) V \nabla_t^2 \phi_0 + \phi_0 V'' + \beta^2 V \phi_0 = 0$$

$V''(z)$  is proportional to  $V(z)$ . We can put

$$2.3.5.) V(z) = -\frac{1}{k_z^2} V''(z) = j\omega\mu \frac{1}{k_z^2} \frac{dI}{dz}$$

with  $k_z^2$  constant. We obtain the equations of transmission lines

$$2.3.6.) \begin{cases} -\frac{dV}{dz} = j\omega\mu I \\ -\frac{dI}{dz} = j\frac{k_z^2}{\omega\mu} V \end{cases} \Rightarrow L_{eq} = \mu, \quad C_{eq} = \frac{k_z^2}{\omega^2\mu}$$

$k_z$  is the propagation constant, while the impedance is

$$2.3.7.) Z = \sqrt{\frac{L_{eq}}{C_{eq}}} = \frac{\omega\mu}{k_z}$$

This expression for  $Z$  is directly linked to the choice  $\vec{e} = \vec{h} \times \vec{i}_z$ : in general  $\vec{e} = A\vec{h} \times \vec{i}_z$ , if  $A$  varies properly we can obtain any value for  $Z$ . Thus  $V, I, Z$  are useful in calculations but (for field non-TEM) without any physical meaning.

If we substitute  $V'' = k_z^2 V$  in the  $\phi$  equation

$$2.3.8.) \nabla_t^2 \phi_0 + (\beta^2 - k_z^2) \phi_0 = 0$$

and, if  $k_t = \sqrt{\beta^2 - k_z^2}$

$$2.3.9.) \nabla_t^2 \phi_0 + k_t^2 \phi_0 = 0$$

As regards the boundary conditions (fig. 2.3.1), it must be

$$\vec{e} \cdot \vec{i}_c \Big|_c = 0, \text{ that is } -\vec{h} \times \vec{i}_z \cdot \vec{i}_c \Big|_c = -\vec{h} \cdot \vec{i}_n \Big|_c = -\frac{\delta\phi}{\delta n} \Big|_c = 0.$$

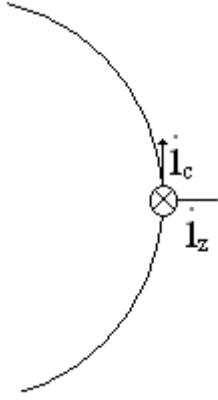


Fig. 2.3.1. Position of versors from the contour of the conductor

So the  $\phi$  potential is obtained by solving the following problem

$$2.3.10.) \quad \begin{cases} \nabla_t^2 \phi + k_t^2 \phi = 0 \\ \left. \frac{\delta \phi}{\delta n} \right|_c = 0 \end{cases}$$

since  $\phi$  must be not identically zero.

(2.3.10) is an eigenvalues problem, its solutions are couples  $(k_{tn}^2, \phi_n)$  eigenvalue-eigenvector such that if  $k_t^2 = k_{tn}^2$  the equation has non-trivial solutions proportional to  $\phi_n$ , while if  $k_t^2 \neq k_{tn}^2, \forall m$  the only solution is  $\phi = 0$ .

It can be shown that the eigenvalues of  $k_t^2$  are real and non negative, and that eigenfunctions and eigenvalues are a countable orthogonal (or at least orthogonalizable) and complete set.

Every function  $\phi$  results in a mode, namely a field which can exist alone in the waveguide. The functions  $V, I$  and the corresponding vectors  $\vec{e}, \vec{h}$  are respectively named scalar and vector mode function.

Finally, we note that  $H_z$  depends on  $V(z)$ :

$$2.3.11.) \quad H_z = -\frac{1}{j\omega\mu} \frac{V(z)}{k_t} \nabla_t^2 \phi_0 = \frac{k_t V(z)}{j\omega\mu} \phi_0$$

## 2.4) TM MODES

For the TM modes, it's possible to achieve a factorized solution. Starting from

$\Psi = \frac{1}{k_t} I(z) \Psi_0(\vec{t})$ , we have:

$$2.4.1.) \quad \begin{cases} \vec{H}_t = I(z) \vec{h} = \frac{1}{k_t} I(z) \Psi_0 \times \vec{i}_z \Rightarrow \vec{h} = \frac{1}{k_t} \nabla_t \Psi_0 \times \vec{i}_z \\ \vec{E}_t = V(z) \vec{e} = \frac{1}{j\omega\mu} \frac{dI}{dz} \frac{1}{k_t} \nabla_t \Psi_0 \Rightarrow \vec{e} = -\frac{1}{k_t} \nabla_t \Psi_0 \Rightarrow \vec{h} = -\vec{e} \times \vec{i}_z \end{cases}$$

Again for the mode scalar function V and I, we have

$$2.4.2.) \quad \begin{cases} -\frac{dI}{dz} = j\omega\epsilon V \\ I'' \nabla_t^2 \Psi_0 + I \nabla_t^2 \Psi_0 + \beta^2 I \Psi_0 = 0 \Rightarrow I'' = k_z^2 I \end{cases}$$

And thus they fulfill the line equations:

$$2.4.3.) \quad \begin{cases} -\frac{dI}{dz} = j\omega\epsilon V \\ -\frac{dV}{dz} = \frac{1}{j\omega\epsilon} (-k_z^2 I) = j \frac{k_z^2}{\omega\epsilon} I \end{cases}$$

with  $L_{eq} = \mu$  ,  $C_{eq} = \frac{k_z^2}{\omega^2 \mu}$  ,  $Z = \frac{k_z}{\omega \epsilon} l$ . Finally:

$$2.4.4.) \nabla_t^2 \Psi_0 + (\beta^2 - k_z^2) \Psi_0 = \nabla_t^2 \Psi_0 + k_t^2 \Psi_0 = 0$$

Since  $\vec{i}_n \times \vec{E}$  has two components (transverse and along z), in this case we have two boundary conditions.

From  $\vec{e} \cdot \vec{i}_c \Big|_c = 0$  we have  $\frac{\partial \Psi_0}{\partial c} \Big|_c = 0$  , that is  $\Psi_0 = 0$  constant on the boundary.

Moreover  $\vec{E}_z = -\frac{1}{j\omega\epsilon} \frac{l(z)}{k_t} \nabla_t^2 \Psi_0 = -\frac{k_t l}{j\omega\epsilon} \Psi_0$  , thus from  $E_z \Big|_c = 0$  we have

$\Psi_0 \Big|_c = 0$  , that is the condition to be imposed ( with  $k_t \neq 0$  , otherwise it would be a TEM mode). A similar reasoning can be made for the TE case.

It is noted that the mode with the smallest  $k_t \neq 0$  is always a TE mode.

Since the discussion is analog to the TE case, we report directly the eigenvalue problem for the TM case.

$$2.4.5.) \begin{cases} \nabla_t^2 \Psi_0 + k_t^2 \Psi_0 = 0 \\ \Psi_0 \Big|_c = 0 \end{cases}$$



## Chapter III

### COMPUTATION OF WAVEGUIDE MODES USING FINITE DIFFERENCE: RECTANGULAR WAVEGUIDES

#### INTRODUCTION

In this chapter we shortly discuss the numerical solution of partial differential equations using finite difference (FD) method. Then, we focus on the eigenvalue problems in particular, we look at the problem of solving the eigenvalue problems (2.3.10) and (2.4.5) in a rectangular waveguide. Since the laplacian operator determines the spatial behavior of solutions, this operator will be approximated in the form best adapted to the problem at hand. The standard calculation of the waveguide modes using FD requires the use of two different grids, namely one for TE modes and the other for TM modes, due to the different boundary condition. In this way, the FD matrix can include the boundary condition, so that the eigenfunction problem reduces to a matrix eigenvalue problem.

After the discussion of this standard solution, we consider a new approximation of Laplacian operator for use on a single grid for the computation of all waveguide modes. This approximation should include the boundary condition, so that the computational burden is the same.

Eigenvalue problems (2.3.10) and (2.4.5) compute the Hertz-Debye potential of waveguide modes. The mode vectors can be computed only using numerical derivatives, which is an operation strongly sensitive to noise. To avoid such derivatives, we present also the direct computation of mode vector in a waveguide, using a finite difference (FD) approximation of the vector Helmholtz equation on a Cartesian grid. Since we are mainly interested in using those modes in MoM, the entire development will be expressed in term of equivalent magnetic surface currents. At variance of the scalar problem, additional

conditions are required on the mode vector. These conditions will be included as constraints into the eigenvalue problem.

### 3.1) FINITE DIFFERENCE SCHEME

The finite difference scheme (FD) is a method for partial differential equations numerical solution and is based on a discrete derivation operator introduction, obtained from the derivative's definition via difference quotients [20].

In a single variable function  $f(x)$ , the first derivate is denoted by:

$$3.1.1.) \quad f'(x) = \frac{df(x)}{dx} \equiv \lim_{h \rightarrow 0} \frac{f(x+h) - f(x)}{h}$$

that can then be reasonably approximated with the only difference quotient:

$$3.1.2.) \quad f'(x) \approx \frac{f(x+h) - f(x)}{h}$$

with  $h$  sufficiently small but finite. The last expression is commonly referred to as forward finite difference as it is evaluated using only values  $\geq x$ .

Similarly it is possible to define the backward approximation of the derivative:

$$3.1.3.) \quad f'(x) \approx \frac{f(x) - f(x-h)}{h}$$

Both equations provide a first order of approximation of  $f'(x)$ , Therefore, the error is proportional to  $h$ . Another possibility is to define a central approximation:

$$3.1.4.) \quad f'(x) \approx \frac{f(x+h) - f(x-h)}{2h}$$

It has an accuracy of second order with an error proportional to  $h^2$ . Similarly, defining higher order derivatives is possible, but following a different approach based on the Taylor expansion, which will be described in detail below, is more convenient.

The approximation of a partial differential equations system by using the finite difference method for solving a problem with the boundary conditions consists of three steps:

- the domain of definition of the continuous problem  $\Omega$ , including the border  $\partial\Omega$ , is replaced by a domain consisting of a discrete finite set of points;
- the derivatives that appear in the expression of the operator are approximated on the discrete domain with finite differences;
- in the discrete approximation of the differential operators the boundary conditions are included.

In this way the continuous problem is approximated with a discrete problem, more specifically with a system of linear equations of finite size, which can be solved with the techniques of classic resolution of linear systems. The finite difference method is particularly effective when the border  $\partial\Omega$  has particular symmetries, otherwise it may be difficult to solve.

Here is an example of this procedure, in particular the solution of a one-dimensional Dirichlet problem;

Determine the function:

$$3.1.5.) \quad u = u(x)$$

defined in the interval  $[0, l]$ , that verifies the equation:

$$3.1.6.) \quad \frac{d^2 u}{dx^2} = \lambda x \quad \text{per } x \in (0, l)$$

with boundary conditions:

$$3.1.7.) \quad \begin{cases} u(0) = g_0 \\ u(l) = g_1 \end{cases}$$

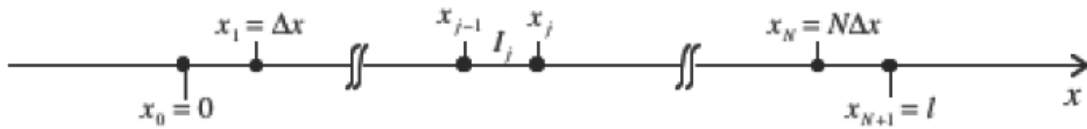


Fig. 3.1.1. Monodimension grid for the Dirichlet problem

We introduce in the range  $[0, l]$  a partition  $I_j = [x_{j-1}, x_j]$  con  $j = 1, 2, \dots, N, N+1$ ,  $x_0 = 0$  e  $x_{N+1} = l$ , (see figures 3.1.1). We assume only for sake of simplicity that the intervals  $I_j$  have all the same lenght  $\Delta x$ ,

$$3.1.8.) \quad \Delta x = \frac{l}{N+1}$$

We indicate with  $u_j = u(x_j)$   $j = 1, 2, \dots, N, N+1$  the sample values of the unknown function  $u(x)$  on grid points of the domain  $[0, l]$ . From the boundary condition (3.1.7) we have:

$$3.1.9.) \quad u_0 = g_0, \quad u_{n+1} = g_1$$

We want to determine  $u_1, u_2, \dots, u_N$  with a numerical method. It is possible to have  $N$  equations for the values  $u_1, u_2, \dots, u_N$  by imposing that (3.1.6) be true in

the grid  $x_1, x_2, \dots, x_N$  and approximating the second derivate through the finite difference. Imposing that the equation (3.1.1) will be verified in the internal grid point  $x_1, x_2, \dots, x_N$  it comes out that:

$$3.1.10.) \quad \left. \frac{d^2 u}{dx^2} \right|_{x=x_i} = \lambda x_i \quad \text{per } i = 1, 2, \dots, N$$

To translate the (3.1.10) into equations (as we will see approximated) for the values  $u_1, u_2, \dots, u_N$  we should express  $\left. \frac{d^2 u}{dx^2} \right|_{x=x_i}$  as a function of samples. If the function  $u$  is sufficiently regular in a neighborhood of the generic point  $\bar{x} \in (0, l)$ , then the operator:

$$3.1.11.) \quad \partial^2 u(\bar{x}) \equiv \frac{u(\bar{x} + \Delta x) - 2u(\bar{x}) + u(\bar{x} - \Delta x)}{\Delta x^2}$$

represents a good approximation of the second derivate. Indeed it has:

$$3.1.12.) \quad \frac{d^2 u}{dx^2} = \partial^2 u(\bar{x}) + O(\Delta x^2)$$

The demonstration of (3.1.12) is quite simple. Developing through the Taylor formula  $u(\bar{x} + \Delta x)$  e  $u(\bar{x} - \Delta x)$  in the neighborhood of  $x = \bar{x}$  we obtain:

$$3.1.13.) \quad u(\bar{x} + \Delta x) = u(\bar{x}) + \left. \frac{du}{dx} \right|_{x=\bar{x}} \cdot \Delta x + \frac{1}{2} \left. \frac{d^2 u}{dx^2} \right|_{x=\bar{x}} \cdot \Delta x^2 + \frac{1}{6} \left. \frac{d^3 u}{dx^3} \right|_{x=\bar{x}} \cdot \Delta x^3$$

$$3.1.14.) \quad u(\bar{x} - \Delta x) = u(\bar{x}) - \left. \frac{du}{dx} \right|_{x=\bar{x}} \cdot \Delta x + \frac{1}{2} \left. \frac{d^2 u}{dx^2} \right|_{x=\bar{x}} \cdot \Delta x^2 - \frac{1}{6} \left. \frac{d^3 u}{dx^3} \right|_{x=\bar{x}} \cdot \Delta x^3$$

Where  $x_+ \in [\bar{x}, \bar{x} + \Delta x]$  and  $x_- \in [\bar{x} - \Delta x, \bar{x}]$ . Summing member to member the (3.1.13) and (3.1.14) we have:

$$3.1.15.) \quad \left. \frac{d^2 u}{dx^2} \right|_{x=\bar{x}} = \frac{u(\bar{x} + \Delta x) - 2u(\bar{x}) + u(\bar{x} - \Delta x)}{\Delta x^2} + O(\Delta x^3)$$

that is:

$$3.1.16.) \quad \left. \frac{d^2 u}{dx^2} \right|_{x=x_i} \cong \frac{u_{i+1} - 2u_i + u_{i-1}}{\Delta x^2}$$

### 3.2) STANDARD FINITE DIFFERENCE SCHEME

Let us consider a rectangular waveguide. As described in chapter II both TE and TM modes can be found from a suitable scalar eigenfunction  $\phi$ , solution of the Helmholtz equation:

$$3.2.1.) \quad \nabla_t^2 \phi + k_t^2 \phi = \frac{\partial^2 \phi}{\partial x^2} + \frac{\partial^2 \phi}{\partial y^2} + k_t^2 \phi = 0$$

with the boundary condition (BC)

$$3.2.2.) \quad \frac{\partial \phi}{\partial n} = 0 \quad \text{TE modes}$$

$$3.2.3.) \quad \phi = 0 \quad \text{TM modes}$$

at the boundary of the rectangular waveguide.

Numerical solution of this eigenvalue problem using the FD approach requires that both the equation (3.2.1) and the BC (3.2.2,3.2.3) are replaced by a discretized version e.g., replacing derivatives with finite approximations. This transforms (3.2.1) into a matrix eigenvalue problem, whose eigenvectors contain the samples of  $\phi$  at the discretization nodes. Assuming a regular Cartesian grid with spacing  $\Delta x, \Delta y$ , and letting  $\phi_{i,j} = \phi(i\Delta x, j\Delta y)$  as sample values of  $\phi(x, y)$ , we need a discretized version of (3.2.1) on each sampling point. For a point P see (fig 3.2.1) we can use a second-order Taylor expression as :

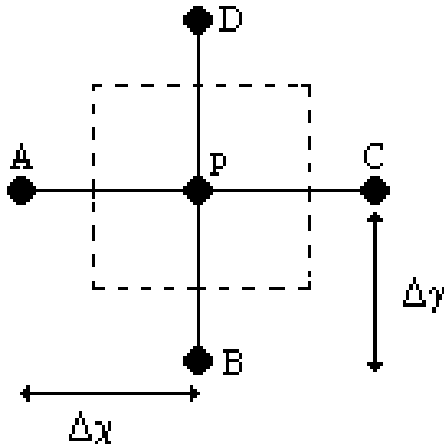


Fig. 3.2.1 Internal point of grid TE and TM

$$3.2.4.) \quad \phi_B = \phi_P + \frac{\partial \phi}{\partial y} \Big|_P \cdot (-\Delta y) + \frac{1}{2} \frac{\partial^2 \phi}{\partial y^2} \Big|_P \cdot (-\Delta y)^2$$

$$3.2.5.) \quad \phi_D = \phi_P + \frac{\partial \phi}{\partial y} \Big|_P \cdot (\Delta y) + \frac{1}{2} \frac{\partial^2 \phi}{\partial y^2} \Big|_P \cdot (\Delta y)^2$$

Adding the two last equations we find:

$$3.2.6.) \quad \frac{\partial^2 \phi}{\partial y^2} \Big|_P = \frac{1}{\Delta y^2} \cdot (\phi_B + \phi_D - 2\phi_P)$$

Likely in x direction

$$3.2.7.) \quad \frac{\partial^2 \phi}{\partial x^2} \Big|_P = \frac{1}{\Delta x^2} \cdot (\phi_A + \phi_C - 2\phi_P)$$

Therefore to be substituted in (3.2.1)

$$3.2.8.) \quad \nabla_t^2 \phi_P = \frac{\phi_A}{\Delta x^2} + \frac{\phi_C}{\Delta x^2} + \frac{\phi_B}{\Delta y^2} + \frac{\phi_D}{\Delta y^2} + \left( \frac{2}{\Delta x^2} + \frac{2}{\Delta y^2} \right) \phi_P$$

This equation can be used for all internal points to get the discretized form of (3.2.1)

$$3.2.9.) \quad \frac{\phi_{i,j-1}}{\Delta x^2} + \frac{\phi_{i,j+1}}{\Delta x^2} + \frac{\phi_{i-1,j}}{\Delta y^2} + \frac{\phi_{i+1,j}}{\Delta y^2} + \left( \frac{2}{\Delta x^2} + \frac{2}{\Delta y^2} \right) \phi_{i,j} = -k_t^2 \phi_{i,j}$$

Equation (3.2.9) cannot be used for boundary points, where BC (3.2.2) or (3.2.3) must be enforced. The standard solution is to use different grids for TE and TM, as in fig (3.2.3).



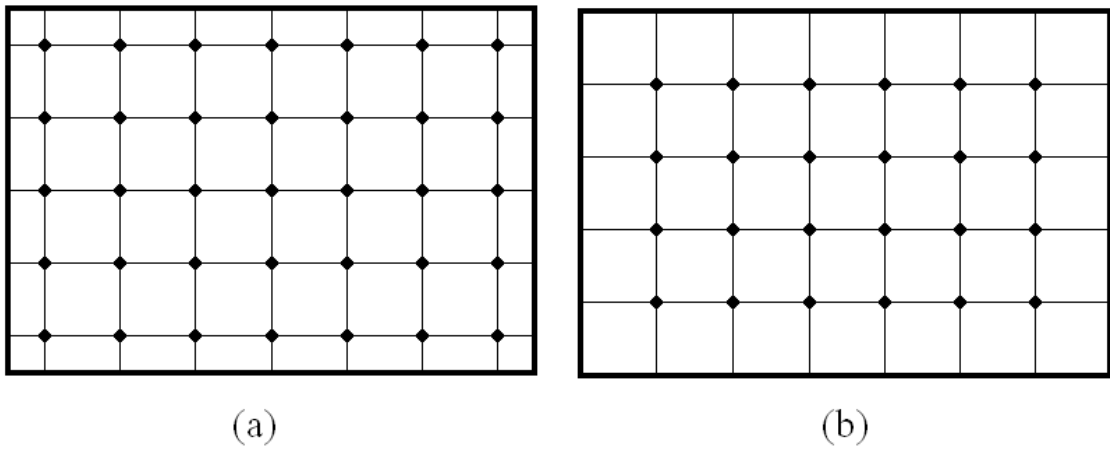


Fig. 3.2.3. Standard TE and TM grid, as suggested from BC

We first discuss for TE case an external point P, we consider the three nearby points A,B and C as shown in fig (3.2.4).

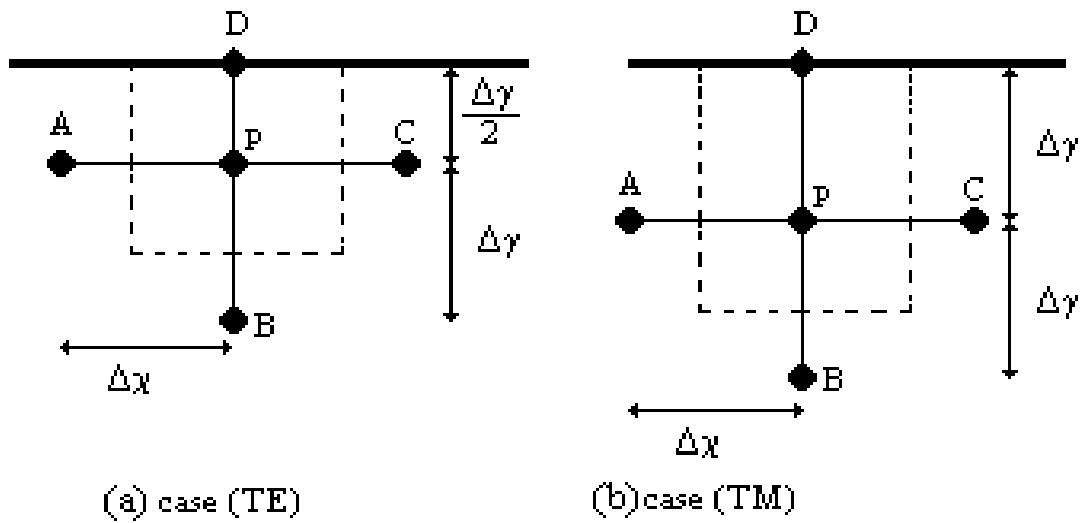


Fig. 3.2.4. Boundary point for TE case and TM case

We can replace (3.2.5) by a first-order approximation  $\phi_P = \phi_D + \frac{\partial \phi}{\partial y} \Big|_D \cdot \left( \frac{\Delta y}{2} \right) = \phi_D$

since the BC require  $\frac{\partial \phi}{\partial y} \Big|_D = 0$ . As a consequence (3.2.6) becomes:

$\frac{\partial^2 \phi}{\partial y^2} \Big|_P = \frac{1}{\Delta y^2} \cdot (\phi_B - \phi_P)$  and (3.2.8) is replaced by:

$$3.2.10.) \quad \frac{\phi_A}{\Delta x^2} + \frac{\phi_C}{\Delta x^2} + \frac{\phi_B}{\Delta y^2} + \left( \frac{2}{\Delta x^2} + \frac{1}{\Delta y^2} \right) \phi_P \quad TE$$

For TM case, on the other hand,  $\phi_d = 0$  and since D is a sampling point, we can put directly in to (3.2.8) to get:

$$3.2.11.) \quad \frac{\phi_A}{\Delta x^2} + \frac{\phi_C}{\Delta x^2} + \frac{\phi_B}{\Delta y^2} + \left( \frac{2}{\Delta x^2} + \frac{2}{\Delta y^2} \right) \phi_P \quad TM$$

The discretized eigenvalues problems (2.3.10), (2.4.5) have the form:

$$Ax = \lambda x$$

where A is a matrix (n,n) , obtained collecting equations (3.2.9),(3.2.10) for TE case, and equations (3.2.9),(3.2.11) for TM case. The discretized eigenvalues problem obtained must be solved by a numerical routine. As a matter of fact, an highly sparse matrix us obtained, so the sparse matrix routines of Matlab has been used.

### 3.3) FINITE DIFFERENCE SINGLE GRID TE EVALUATION OF TE AND TM MODES IN METALLIC WAVEGUIDES

In order to use a single grid we need to enforce both BC on a single grid. We describe here in detail the use of TE grid [26] (fig 3.2.3a) for TM modes.

Only the inclusion of BC into the eigenvalue matrix problems is modified, so let us consider again the external point P on the TE grid (fig 3.2.4 a). Since the BC (3.2.3) require  $\phi_D = 0$ , we can express the potential in B and D through a Taylor approximation:

$$\begin{aligned}
 3.3.1.) \quad \phi_B &= \phi_P + \left. \frac{\partial \phi}{\partial y} \right|_P \cdot (-\Delta y) + \frac{1}{2} \left. \frac{\partial^2 \phi}{\partial y^2} \right|_P \cdot (-\Delta y)^2 \\
 \phi_D &= \phi_P + \left. \frac{\partial \phi}{\partial y} \right|_P \cdot \left( \frac{\Delta y}{2} \right) + \frac{1}{2} \left. \frac{\partial^2 \phi}{\partial y^2} \right|_P \cdot \left( \frac{\Delta y}{2} \right)^2
 \end{aligned}$$

Adding  $\phi_B + 2 \cdot \phi_D$  we get:  $\left. \frac{\partial^2 \phi}{\partial y^2} \right|_P = \frac{4}{3 \cdot (\Delta y)^2} \cdot (\phi_B + 2\phi_D - 3\phi_P)$

and recalling that the BC prescribes  $\phi_D = 0$ , we get:

$$3.3.2.) \quad \left. \frac{\partial^2 \phi}{\partial y^2} \right|_P = \frac{4}{3 \cdot (\Delta y)^2} \cdot (\phi_B - 3\phi_P)$$

which, together with (3.2.7) gives the discretized form of the laplacian

$$3.3.3.) \quad \nabla_t^2 \phi_P = \frac{\phi_A}{(\Delta x)^2} + \frac{\phi_C}{(\Delta x)^2} + \frac{4}{3 \cdot (\Delta y)^2} \phi_B + \left( \frac{2}{(\Delta x)^2} + \frac{4}{(\Delta y)^2} \right) \phi_P$$

as a replacement of (3.2.11) for external points in TM modes.

Let us now consider, the dual case use of the TM grid [27] for TE modes. The geometry for an edge point P, is shown in Fig.3.3.1 We express the potential in B, P, D and H through a third order polynomial approximation:

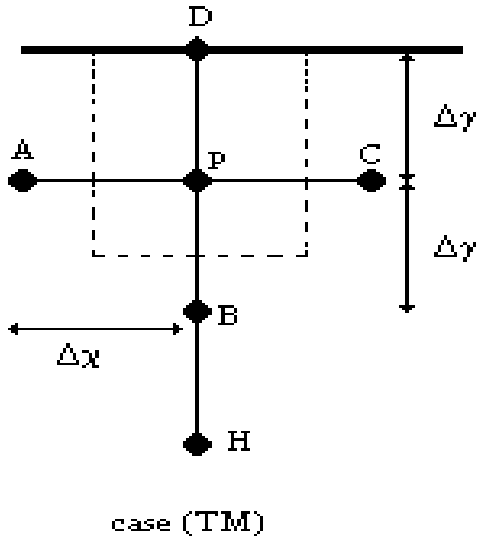


Fig. 3.3.1. Boundary point TM case

$$3.3.4.) \quad \phi = \frac{1}{3}ay^3 + \frac{1}{2}by^2 + cy + d$$

Forcing both the BC in D and the potential sample values:

$$3.3.5.) \quad \left\{ \begin{array}{l} \frac{\partial \phi}{\partial y} \Big|_D = a\Delta y^2 + b\Delta y + c = 0 \\ \phi_P = d \\ \phi_B = -\frac{1}{3}a\Delta y^3 + \frac{1}{2}b\Delta y^2 - c\Delta y + \phi_P \\ \phi_H = -\frac{8}{3}a\Delta y^3 + \frac{4}{2}b\Delta y^2 - 2c\Delta y + \phi_P \end{array} \right.$$

The linear system (3.3.5) can be easily solved obtaining:

$$\begin{aligned}
3.3.6.) \quad & \left. \frac{\partial^2 \phi}{\partial y^2} \right|_P = 2ay + b \quad y = 0 \\
& b = \frac{2}{11\Delta y^2} \cdot (\phi_H + \phi_B - 2\phi_P)
\end{aligned}$$

(3.3.7), together with (3.2.8) gives the discretized form of the laplacian in P

$$3.3.7.) \quad \nabla_t^2 \phi_P = \frac{\phi_A}{\Delta x^2} + \frac{\phi_C}{\Delta x^2} + \frac{2\phi_B}{11\Delta y^2} + \frac{2\phi_H}{11\Delta y^2} - \left( \frac{2}{\Delta x^2} + \frac{4}{11\Delta y^2} \right) \phi_P$$

which is the replacement of (3.2.10) for external points in TE modes.

### 3.4) VECTOR FINITE DIFFERENCE APPROACH: TE MODES

Up to now, we have computed the waveguide modes through the Hertz-Debye (scalar) potentials. The mode vectors must therefore be computed using numerical derivatives. An alternative approach is to compute directly the mode vector [28].

Let us consider a waveguide. The TE mode vector  $\vec{e}$  is an eigenfunction of Laplace operator, with suitable conditions:

$$3.4.1.) \quad \begin{cases} \nabla_t^2 \vec{e} + k_t^2 \vec{e} = 0 \\ \nabla_t \cdot \vec{e} = 0 \\ \left. \vec{e} \times \vec{i}_n \right|_C = 0 \end{cases}$$

where C is the contour of the waveguide (see Fig.3.4.1).

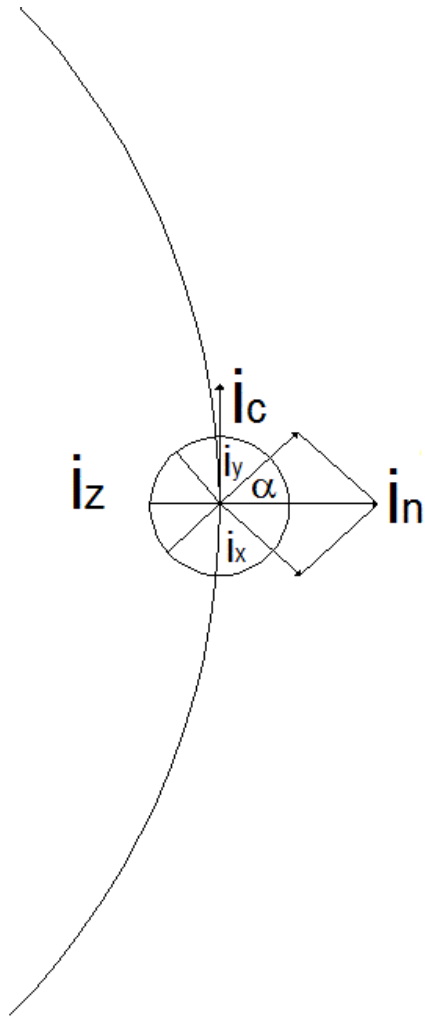


Fig. 3.4.1. Vectors geometry with respect to the contour of the conductor.

If we introduce the (two-dimensional) magnetic current  $\vec{M}$  equivalent to the transverse field  $\vec{e} = \vec{i}_z \times \vec{M}$  we get from (3.4.1)

$$3.4.2.) \quad \nabla_t^2 \vec{e} = -\nabla_t \times \nabla_t \times \vec{e} = -\nabla_t \times [\vec{i}_z \nabla_t \cdot \vec{M}] = [-\nabla_t \times \nabla_t \times \vec{M} + \nabla_t^2 \vec{M}] \times \vec{i}_z$$

$$3.4.3.) \quad \nabla_t \cdot \vec{e} = \nabla_t \cdot [\vec{i}_z \times \vec{M}] = -\vec{i}_z \cdot [\nabla_t \times \vec{M}] = 0$$

By (3.4.3), it follows that  $\nabla_t \times \vec{M} = 0$ . When substituted in (3.35), after replacing and collecting terms we get:

$$\begin{aligned}
 3.4.4.) \quad \nabla_t^2 \vec{e} + k_t^2 \vec{e} &= \left[ -\nabla_t \times \nabla_t \times \vec{M} + \nabla_t^2 \vec{M} \right] \times \vec{i}_z + k_t^2 \left( \vec{i}_z \times \vec{M} \right) = \\
 &= \vec{i}_z \times \left[ -\left( \nabla_t^2 \vec{M} + k_t^2 \vec{M} \right) \right]
 \end{aligned}$$

the TE eigenvalue problem can therefore be rewritten in this form:

$$3.4.5.) \quad \begin{cases} \nabla_t^2 \vec{M} + k_t^2 \vec{M} = 0 \\ \nabla_t \times \vec{M} = 0 \\ \vec{M} \cdot \vec{i}_n|_C = 0 \end{cases}$$

and in (x,y) components, as:

$$3.4.6.) \quad \begin{cases} \nabla_t^2 \vec{M} = -k_t^2 \vec{M} \\ \frac{\partial M_y}{\partial x} - \frac{\partial M_x}{\partial y} = 0 \\ M_x \cos(\alpha) + M_y \sin(\alpha) = 0 \end{cases}$$

where the third of (3.4.6) is the boundary condition (BC) on the contour C. FD approach to the solution of this problem is based on the replacement of problem (3.4.6) with a discretized version. The main difference with the previous paragraphs is that only the BC are inserted into the approximation of the Laplace operator. The second of (3.4.6) is dealt with as a constrain on the eigenvectors. In this way (3.4.6) becomes a constrained matrix eigenvalue problem.

For an internal point P as in Fig.3.2.1 we can use a second-order Taylor expression as :

$$\begin{aligned}
3.4.7.) \quad \vec{M}_B &= \vec{M}_P + \left. \frac{\partial \vec{M}}{\partial y} \right|_P \cdot (-\Delta y) + \frac{1}{2} \left. \frac{\partial^2 \vec{M}}{\partial y^2} \right|_P \cdot (-\Delta y)^2 \\
\vec{M}_D &= \vec{M}_P + \left. \frac{\partial \vec{M}}{\partial y} \right|_P \cdot (+\Delta y) + \frac{1}{2} \left. \frac{\partial^2 \vec{M}}{\partial y^2} \right|_P \cdot (+\Delta y)^2
\end{aligned}$$

Adding to these equation and we find:

$$3.4.8.) \quad \left. \frac{\partial^2 \vec{M}}{\partial y^2} \right|_P = \frac{1}{\Delta y^2} \cdot (\vec{M}_B + \vec{M}_D - 2\vec{M}_P)$$

Likely in x direction:

$$3.4.9.) \quad \left. \frac{\partial^2 \vec{M}}{\partial x^2} \right|_P = \frac{1}{\Delta x^2} \cdot (\vec{M}_A + \vec{M}_C - 2\vec{M}_P)$$

Summing (3.4.8) and (3.4.9) we obtain :

$$3.4.10.) \quad \nabla_t^2 \vec{M}_P = \frac{\vec{M}_A}{\Delta x^2} + \frac{\vec{M}_C}{\Delta x^2} + \frac{\vec{M}_B}{\Delta y^2} + \frac{\vec{M}_D}{\Delta y^2} - \left( \frac{2}{\Delta x^2} + \frac{2}{\Delta y^2} \right) \vec{M}_P$$

To discretize the second condition of (3.4.6) we can use a first -order Taylor expression. Starting from (3.4.7) without the second-order term we can easily get:

$$3.4.11.) \quad \left( \frac{\partial M_y}{\partial x} - \frac{\partial M_x}{\partial y} \right) = \frac{M_{C,y}}{2\Delta x} - \frac{M_{A,y}}{2\Delta x} - \frac{M_{D,x}}{2\Delta y} + \frac{M_{B,x}}{2\Delta y} = 0$$



For a boundary point P, such as P in Fig.3.4.2, we need a different approach, since D is not a sampling point for the current. The BC is now  $M_{D,y} = 0$  and this condition can be incorporated into the FD matrix. Adding the Taylor expansion of  $M_{D,y}$

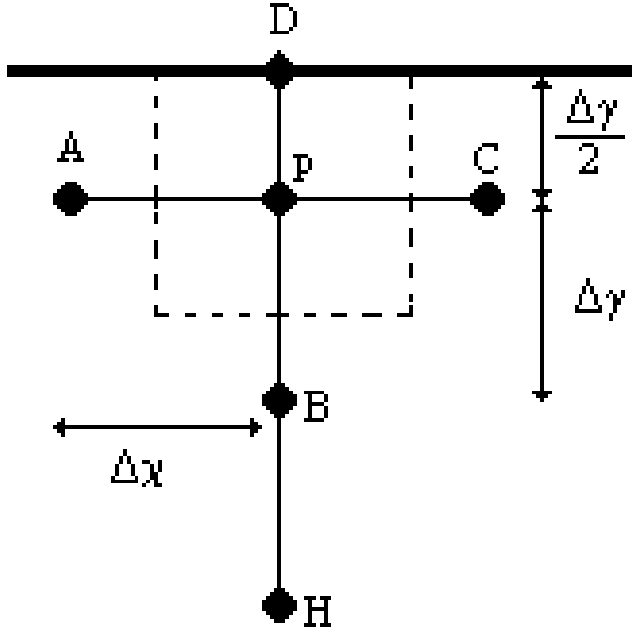


Fig. 3.4.2. Boundary point of TE grids

$$3.4.12.) \quad M_{D,y} = M_{P,y} + \frac{\partial M_y}{\partial y} \bigg|_P \cdot \left( +\frac{\Delta y}{2} \right) + \frac{1}{2} \frac{\partial^2 M_y}{\partial y^2} \bigg|_P \cdot \left( +\frac{\Delta y}{2} \right)^2 = 0$$

with  $\frac{1}{2} M_{B,y} = 0$  given by (3.4.7) and using  $M_{D,y} = 0$  we get:

$$3.4.13.) \quad \frac{\partial^2 M_y}{\partial y^2} \bigg|_P = \frac{4}{3\Delta y^2} \cdot (M_{B,y} - 3M_{P,y})$$

so

$$3.4.14.) \quad \nabla_t^2 M_{P,y} = \frac{M_{A,y}}{\Delta x^2} + \frac{M_{C,y}}{\Delta x^2} + \frac{3M_{B,y}}{4\Delta y^2} - \left( \frac{2}{\Delta x^2} + \frac{4}{\Delta y^2} \right) M_{P,y}$$

Also the x component of (3.4.10) relevant to P needs to be modified, for the same reason. To do this we need another point H (see Fig.3.4.1) . Summing the Taylor expansion :

$$3.4.15.) \quad M_{H,x} = M_{P,x} + \frac{\partial M_x}{\partial y} \Big|_P \cdot (2\Delta y) + \frac{1}{2} \frac{\partial^2 M_x}{\partial y^2} \Big|_P \cdot (2\Delta y)^2$$

with  $M_{B,x}$  given by (3.4.7) we get:

$$3.4.16.) \quad \frac{\partial^2 M_x}{\partial y^2} \Big|_P = \frac{1}{\Delta y^2} \cdot (M_{H,x} - 2M_{B,x} + M_{P,x})$$

and the x-components of (3.4.10) is replaced by:

$$3.4.17.) \quad \nabla_t^2 M_{P,x} = \frac{M_{A,x}}{\Delta x^2} + \frac{M_{C,x}}{\Delta x^2} + \frac{M_{H,x}}{\Delta y^2} - 2\frac{M_{B,x}}{\Delta y^2} - \left( \frac{2}{\Delta x^2} + \frac{1}{\Delta y^2} \right) M_{P,x}$$

At the same time, the condition (3.4.11) becomes analogously:

$$3.4.18.) \quad \frac{M_{C,y}}{2\Delta x} - \frac{M_{A,y}}{2\Delta x} - \frac{M_{H,x}}{2\Delta y} + 4\frac{M_{B,x}}{2\Delta y} - 3\frac{M_{P,x}}{2\Delta y} = 0$$

The discretized version of (3.4.6) is obtained collecting (3.4.10) and the constraint (3.4.11) to get the constrained eigenvalue problems:

3.4.19.)

$$\begin{cases} Ax = \lambda x \\ C^T x = 0 \end{cases}$$

where A is a (2n,2n) matrix, and C is (2n,m) with n>m and  $\lambda = -k_t^2$ . Of course, for all boundary points the equations (3.4.10) (3.4.11) are replaced by the modified ones (such as (3.4.14),(3.4.17) and (3.4.18) ).

### 3.5) VECTOR FINITE DIFFERENCE APPROACH: TM MODES

The TM mode vectors  $\vec{h}$  are eigenfunction of the Helmholtz equation:

$$3.5.1.) \quad \begin{cases} \nabla_t^2 \vec{h} + k_t^2 \vec{h} = 0 \\ \nabla_t \cdot \vec{h} = 0 \\ \vec{e} \times \vec{i}_n \Big|_C = \frac{1}{A} \cdot (\vec{h} \times \vec{i}_z) \times \vec{i}_n \Big|_C = \frac{1}{A} \cdot (\vec{h} \times \vec{i}_n) \Big|_C \times \vec{i}_z = 0 \end{cases}$$

where C is the contour of the waveguide (see Fig.3.4.1).

If we introduce the (two-dimensional) magnetic current  $\vec{M}$  equivalent to the transverse field  $\vec{M} = \frac{1}{A} \vec{h}$  and replacing in equation (3.5.1), the

TM eigenvalue problem [29] can therefore be rewritten as:

$$3.5.2.) \quad \begin{cases} \nabla_t^2 \vec{M} + k_t^2 \vec{M} = 0 \\ \nabla_t \cdot \vec{M} = 0 \\ \vec{M} \cdot \vec{i}_n \Big|_C = 0 \end{cases}$$

and in (x,y) components, as:

$$3.5.3.) \quad \begin{cases} \nabla_t^2 \vec{M} = -k_t^2 \vec{M} \\ \frac{\partial M_x}{\partial x} + \frac{\partial M_y}{\partial y} = 0 \\ M_x \cos(\alpha) + M_y \sin(\alpha) = 0 \end{cases}$$

The main difference is the constrain given by the second of (3.5.3.) To discretize it we can use a first-order Taylor expression. Starting from equation (3.4.7) without the second-order term we can easily get:

$$3.5.4.) \quad \left( \frac{\partial M_x}{\partial x} + \frac{\partial M_y}{\partial y} \right) = \frac{M_{C,x}}{2\Delta x} - \frac{M_{A,x}}{2\Delta x} + \frac{M_{D,y}}{2\Delta y} - \frac{M_{B,y}}{2\Delta y} = 0$$

For a boundary points (see Fig.3.3.1) the equation (3.4.14) change respect to the TM case, because the boundary condition on the TM grids are different . For the laplacian we have:

$$3.5.5.) \quad \nabla_t^2 M_{P,y} = \frac{M_{A,y}}{\Delta x^2} + \frac{M_{C,y}}{\Delta x^2} + \frac{M_{B,y}}{\Delta y^2} - \left( \frac{2}{\Delta x^2} + \frac{2}{\Delta y^2} \right) M_{P,y}$$

At the same time, the condition (3.5.4) becomes analogously:

$$3.5.6.) \quad \frac{M_{C,x}}{2\Delta x} - \frac{M_{A,x}}{2\Delta x} + \frac{M_{H,y}}{2\Delta y} - 4 \frac{M_{B,y}}{2\Delta y} + 3 \frac{M_{P,y}}{2\Delta y} = 0$$

In this case the constrained eigenvalue problems (3.4.19) is obtained collecting (3.4.10) and the constraint (3.5.4). For all boundary points the equations (3.4.10) (3.5.4) are replaced by the modified ones (such as (3.5.5),(3.4.17) and (3.5.6) ).

### 3.6) EXTENSION TO 3D PROBLEM

The extension of F approach described in the previous sections can be devised also for the evaluation of modes in cavities to assess the feasibility of such extension in the cavity cases, we describe here the computation of scalar eigenfunction on a single grid, irrespective of the boundary condition (Dirichlet or Newmann). Let us consider a rectangular cavities. The modes can be found from a suitable scalar eigenfunction  $\phi$ , solution of the Helmothz equation:

$$3.6.1.) \quad \nabla_t^2 \phi + k_t^2 \phi = \frac{\partial^2 \phi}{\partial x^2} + \frac{\partial^2 \phi}{\partial y^2} + \frac{\partial^2 \phi}{\partial z^2} + k_t^2 \phi = 0$$

with the boundary condition (BC)

$$3.6.2.) \quad \phi = 0 \quad \text{Dirichlet}$$

$$3.6.3.) \quad \frac{\partial \phi}{\partial n} = 0. \quad \text{Newmann}$$

at the boundary of the resonant cavities.

The FD approach follows the one described in 3.2 and 3.3. The chosen sampling grid is shown in Fig.3.6.1 (and is the standard one for Fig.3.6.1 Dirichlet, Newmann boundary condition).

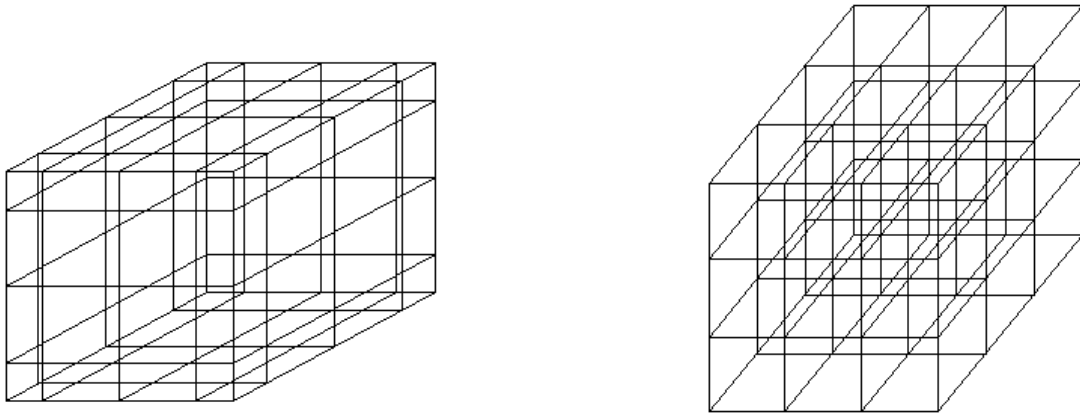


Fig. 3.6.1. Standard Newmann and Dirichlet grid, as suggested from BC

For an internal point  $P$  see (Fig 3.6.2) we can use a second-order Taylor expression as in (3.2.4-3.2.8). The final expression of Laplacian is :

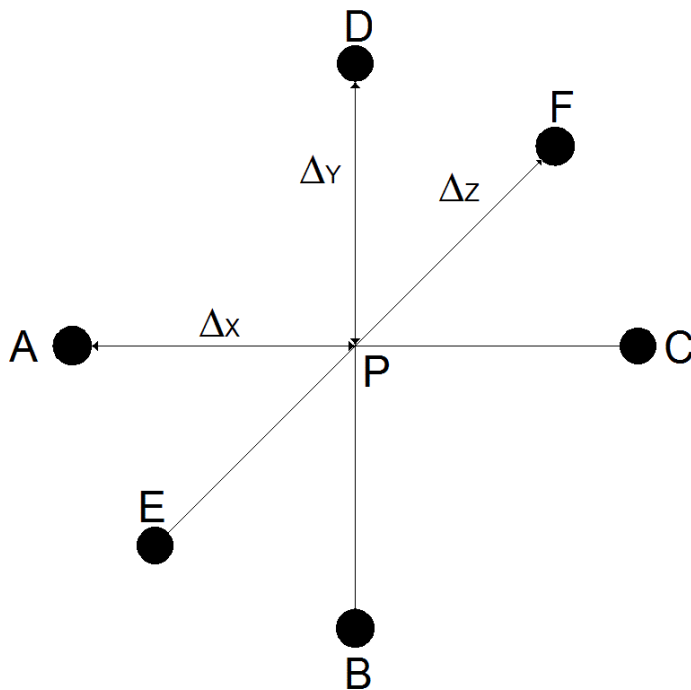


Fig. 3.6.2. Internal point of 3D Newmann grid

$$3.6.4.) \nabla_t^2 \phi_P = \frac{\phi_A}{\Delta x^2} + \frac{\phi_C}{\Delta x^2} + \frac{\phi_B}{\Delta y^2} + \frac{\phi_D}{\Delta y^2} + \frac{\phi_E}{\Delta z^2} + \frac{\phi_F}{\Delta z^2} - \left( \frac{2}{\Delta x^2} + \frac{2}{\Delta y^2} + \frac{2}{\Delta z^2} \right) \phi_P$$

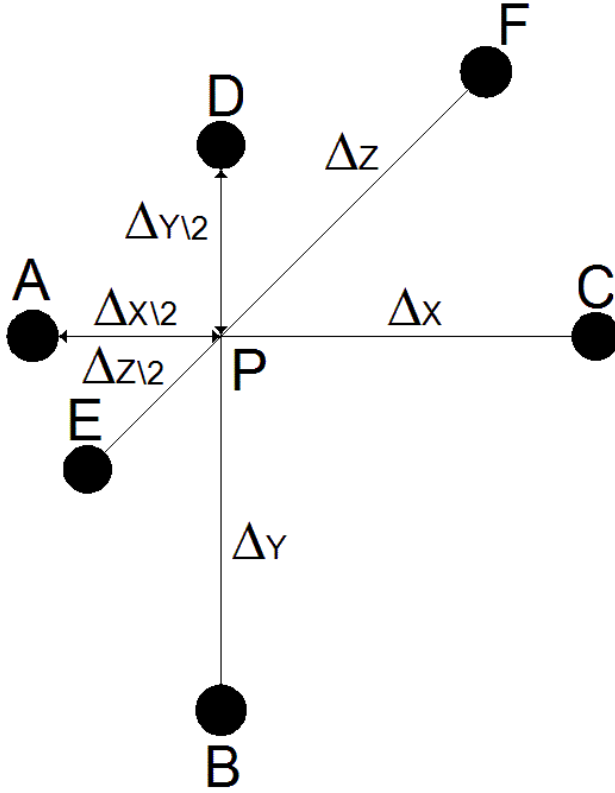


Fig. 3.6.3. Boundary point of 3D Newmann grid

For a boundary point see (fig.3.6.3) the expression (3.6.4) becomes, for the boundary condition (3.6.2):

$$3.6.5.) \nabla_t^2 \phi_P = \frac{\phi_C}{\Delta x^2} + \frac{\phi_B}{\Delta y^2} + \frac{\phi_F}{\Delta z^2} - \left( \frac{1}{\Delta x^2} + \frac{1}{\Delta y^2} + \frac{1}{\Delta z^2} \right) \phi_P$$

since the development is the same as the one leading to 3.2.10. For the Dirichlet BC we can follow:

$$3.6.6.) \nabla_t^2 \phi_P = \frac{4\phi_C}{3\Delta x^2} + \frac{4\phi_D}{3\Delta y^2} + \frac{4\phi_F}{3\Delta z^2} - \left( \frac{4}{\Delta x^2} + \frac{4}{\Delta y^2} + \frac{4}{\Delta z^2} \right) \phi_P$$



## Chapter IV

### FINITE DIFFERENCE IN POLAR AND ELLIPTICAL GRID

#### INTRODUCTION

In this chapter we discuss the numerical computation of the eigenvalue of the Laplace operator using a curvilinear finite difference method. This allows to analyze the circular and elliptical waveguide modes using a finite difference approach.

#### 4.1) POLAR FINITE DIFFERENCE

In FD approach both the equation (3.2.1) and the BC (3.2.2),(3.2.3) are replaced by a discretized version. If the waveguide boundary consists of straight lines, parallel to the coordinate axes, the FD method can be applied on a cartesian grid [21]. This grid defines also a partition of the waveguide surface into rectangular cells, which completely fill the waveguide section. For every other waveguide, the section cannot be exactly partitioned using rectangular cells and this leads to numerical errors (since the eigenvalue problem is quite ill – conditioned [32] )

In order to obtain high accuracy, the waveguide surface must be discretized maintaining also the correct geometry of the boundary. So a different discretization scheme should be used, which matches exactly the waveguide boundary. Therefore the discretization nodes must be at the intersections of a suitable framework, of which the waveguide boundary is a coordinate curve. In this way the waveguide section is exactly partitioned into discretization cell.

The discretized equations can be obtained in two ways. The standard approach is to sum the Taylor expansion of the potentials [20], as in chapter III. Alternatively we can integrate (3.2.1) over a discretization cell [21]

$$4.1.1.) \quad \int \nabla_t^2 \phi \cdot dS = -k_t^2 \int \phi \cdot dS$$

Use of Gauss Theorem then gives:

$$4.1.2.) \quad \int_{\Gamma_F} \nabla_t \phi \cdot i_n dl$$

i.e

$$4.1.3.) \quad \int_{\Gamma_F} \frac{\partial \phi}{\partial n} \cdot dl = -k_t^2 \int_{S_F} \phi \cdot dS$$

where  $\Gamma_F$  is the cell boundary,  $S_F$  is the cell surface in the r.h.s. The Integral in the l.h.s can be numerical evaluated, replacing  $\frac{\partial \phi}{\partial n}$  with its FD approximation, while the integral in the r.h.s in the spirit of FD approach, is evaluated as:

$$4.1.4.) \quad \int_{S_F} \phi \cdot dS = \phi \cdot S$$

wherein  $\phi$  is evaluated at the discretization point of cell  $S_F$ , and  $S$  is the cell area. So equation (4.1.3) becomes:

$$4.1.5.) \quad \frac{1}{S} \int_{\Gamma_F} \frac{\partial \phi}{\partial n} \cdot dl = -k_t^2 \phi$$

where the l.h.s is expressed in discretized form.

The l.h.s of (4.1.3) is then divided into four (or more) sides, along the coordinate curves, and the normal derivative is evaluated in finite terms.

The two approaches apply in non-overlapping sets of cases, but, when both can be used, the results is the same, as we will show later.

Since both discretizations (either the standard FD and that based on (4.3) ) can easily include the BC (3.2.2),(3.2.3), the resulting FD formulation is equivalent to the complete eigenvalue problem (3.2.1),(3.2.2),(3.2.3).

In order to explain the difference with the standard grid FD, and to assess our approach, we start considering a circular waveguide [22,23] (see Fig. 4.1.1), using as grid lines the coordinate lines of a polar framework.

We assume a regular spacing on the coordinate lines, with step  $\Delta r$  ,  $\Delta\vartheta$ , and let  $\phi_{nq} = \phi(n\Delta r, q\Delta\vartheta)$ .

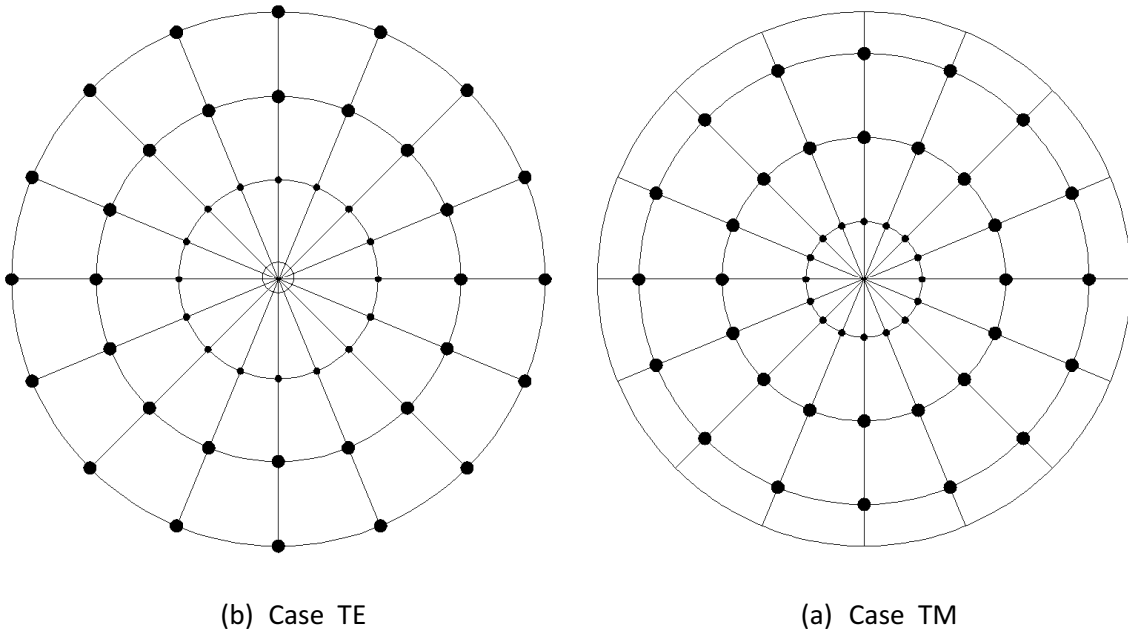


Fig. 4.1.1. Standard TE and TM grid, as suggested from BC

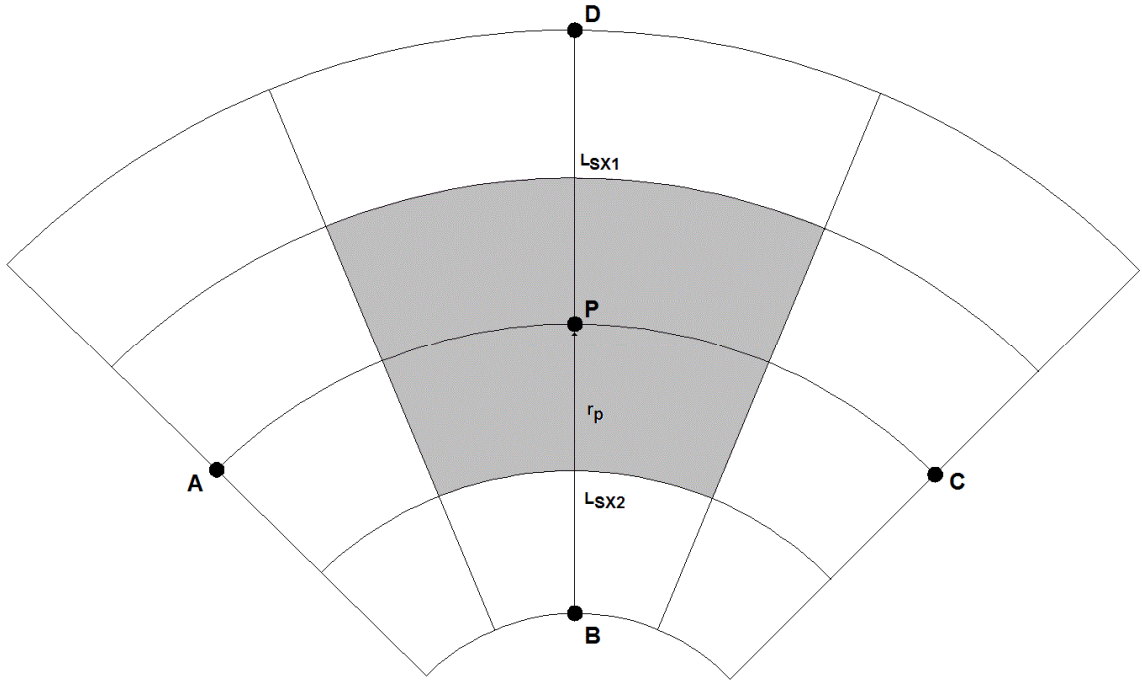


Fig. 4.1.2. Internal point of grid TE and TM

Let P the point of coordinates  $(n\Delta r, q\Delta\vartheta)$ , and consider the four nearby points A, B, C and D, as shown in Fig. 4.1.2. We get, for the l.h.s of (4.1.3)

$$4.1.6.) \frac{1}{S_F} \cdot \left[ \frac{(\phi_D - \phi_P)}{\Delta r} \cdot L_{SX1} + \frac{(\phi_B - \phi_P)}{\Delta r} \cdot L_{SX2} + \frac{(\phi_A - \phi_P)}{\Delta\vartheta \cdot r_p} \cdot \Delta r + \frac{(\phi_C - \phi_P)}{\Delta\vartheta \cdot r_p} \cdot \Delta r \right]$$

where  $S_F = r_p \cdot \Delta r \cdot \Delta\vartheta$ ,  $L_{SX1} = \left(r_p + \frac{\Delta r}{2}\right) \cdot \Delta\vartheta$  and  $L_{SX2} = \left(r_p - \frac{\Delta r}{2}\right) \cdot \Delta\vartheta$

Replacing and collecting term we get the discretized form of (3.2.1) as:

$$\begin{aligned}
4.1.7.) \quad & \frac{1}{r_p^2 (\Delta \vartheta)^2} \cdot \phi_A + \left( \frac{1}{2r_p \Delta r} + \frac{1}{(\Delta r)^2} \right) \cdot \phi_D + \frac{1}{r_p^2 (\Delta \vartheta)^2} \cdot \phi_C + \left( \frac{1}{(\Delta r)^2} - \frac{1}{2r_p \Delta r} \right) \cdot \phi_B + \\
& - \left( \frac{2}{(\Delta r)^2} + \frac{2}{r_p^2 (\Delta \vartheta)^2} \right) \cdot \phi_P \cong -k_t^2 \phi_P^2
\end{aligned}$$

This expression can be used for all internal point, except the circle center. It is worth noting that (4.1.8) can be obtained also starting from the laplacian operator in polar coordinates:

$$4.1.8.) \quad \left[ \frac{1}{r_p^2} \cdot \frac{\partial^2 \phi}{\partial \vartheta^2} + \frac{1}{r_p} \cdot \frac{\partial \phi}{\partial r} + \frac{\partial^2 \phi}{\partial r^2} \right] = -k_t^2 \phi$$

and using a Taylor approximation

$$4.1.9.) \quad \phi_B = \phi_P + \frac{\partial \phi}{\partial r} \Big|_P \cdot (-\Delta r) + \frac{1}{2} \frac{\partial^2 \phi}{\partial r^2} \Big|_P \cdot (-\Delta r)^2$$

$$4.1.10.) \quad \phi_D = \phi_P + \frac{\partial \phi}{\partial r} \Big|_P \cdot (+\Delta r) + \frac{1}{2} \frac{\partial^2 \phi}{\partial r^2} \Big|_P \cdot (+\Delta r)^2$$

Adding and subtracting the last two equations we find:

$$4.1.11.) \quad \frac{\partial^2 \phi}{\partial r^2} \Big|_P = \frac{1}{(\Delta r)^2} \cdot (\phi_B + \phi_D - 2\phi_P)$$

and:

$$4.1.12.) \quad \left. \frac{\partial \phi}{\partial r} \right|_P = \frac{\phi_D - \phi_B}{2 \cdot \Delta r}$$

Likely in  $\vartheta$  direction

$$4.1.13.) \quad \left. \frac{\partial^2 \phi}{\partial \vartheta^2} \right|_P = \frac{1}{(\Delta \vartheta)^2} \cdot (\phi_A + \phi_C - 2\phi_P)$$

Collecting all those equation in (4.1.8) we get (4.1.7).

Equation (4.1.7) cannot be used for the center of the circle, since it is a point of singularity for the polar frame. As a consequence, Taylor expression cannot be used there. So we use (4.1.5) instead. Its l.h.s is divided into  $N = \frac{2\pi}{\Delta \vartheta}$  sides, along the coordinate curves, and the normal derivative is evaluated in finite terms using (4.1.11) and (4.1.12).

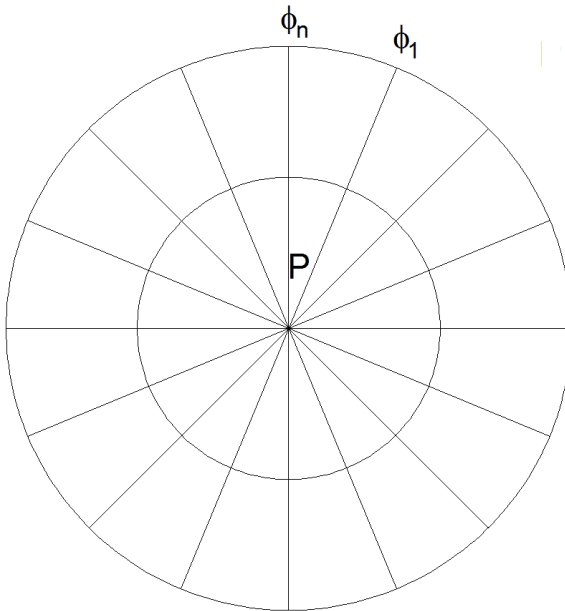


Fig. 4.1.3. Center of circle

Therefore the discretized form of the Laplace operator at the circle center is:

$$\begin{aligned}
 4.1.14.) \quad & \left( \frac{1}{\pi \cdot \left( \frac{\Delta r}{2} \right)^2} \right) \cdot \sum_{q=1}^N \frac{(\phi_q - \phi_P)}{\Delta r} \cdot \frac{\Delta r}{2} \cdot \Delta \vartheta = \\
 & = \left( \frac{4}{\pi \cdot \Delta r^2} \right) \cdot \left( \sum_{q=1}^N \phi_q \frac{\Delta \vartheta}{2} - N \frac{\Delta \vartheta}{2} \phi_P \right) \cong -k_t^2 \phi_P
 \end{aligned}$$

Boundary points, where BC (3.2.1),(3.2.2) must be enforced required a modification of (4.1.7). As a matter of fact, BC (3.2.1),(3.2.2) needs to be included in the algebraic eigenvalue problem. The standard solution, widely used for the rectangular grid case, makes use of different grids for TE and TM, as in Fig.4.1.1. Let us consider an edge point, and consider the three nearby points A,B,C ad shown in Fig.4.1.4.

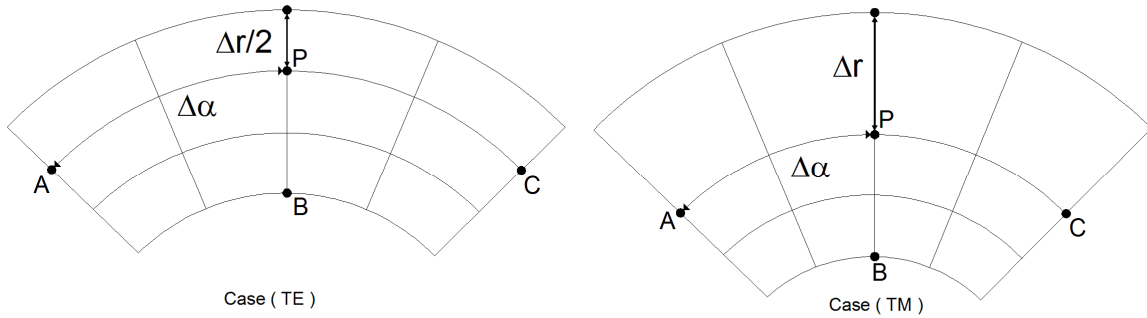


Fig. 4.1.4. Boundary point of circular waveguide

For Te modes, we can evaluate  $\phi_x$  by a first-order approximation (compare (4.1.10))

$$4.1.15.) \quad \phi_P = \phi_X + \left. \frac{\partial \phi}{\partial r} \right|_X \cdot \left( \frac{\Delta r}{2} \right)$$

since the BC require  $\left. \frac{\partial \phi}{\partial r} \right|_D = 0$ , we get:

$$4.1.16.) \quad \phi_P = \phi_D.$$

As a consequence (4.1.11) and (4.1.12) becomes :

$$4.1.17.) \quad \begin{aligned} \left. \frac{\partial^2 \phi}{\partial r^2} \right|_P &= \frac{1}{\Delta r^2} \cdot (\phi_B - \phi_P) \\ \left. \frac{\partial \phi}{\partial r} \right|_P &= -\frac{1}{2r_p \Delta r} \cdot (\phi_B - \phi_P) \end{aligned}$$

and (4.1.7) by:

$$4.1.18.) \quad \begin{aligned} &\frac{1}{r_p^2 \Delta \vartheta^2} \cdot \phi_A + \frac{1}{r_p^2 \Delta \vartheta^2} \cdot \phi_C + \left( \frac{1}{\Delta r^2} - \frac{1}{2r_p \Delta r} \right) \cdot \phi_B + \\ & - \left( \frac{1}{\Delta r^2} - \frac{1}{2r_p \Delta r} + \frac{2}{r_p^2 \Delta \vartheta^2} \right) \cdot \phi_P \cong -k_t^2 \phi_P \end{aligned}$$

For TM case, on the other hand, the standard approach requires each boundary point X to be a sampling point, so that  $\phi_X = 0$  (see Fig.4.1.1.b), which can be directly put in to (4.1.11) and (4.1.12) to get, instead of (4.1.7) the equation:

$$4.1.19.) \quad \begin{aligned} &\frac{1}{r_p^2 \Delta \vartheta^2} \cdot \phi_A + \frac{1}{r_p^2 \Delta \vartheta^2} \cdot \phi_C + \left( \frac{1}{\Delta r^2} - \frac{1}{r_p \Delta r} \right) \cdot \phi_B + \\ & - \left( -\frac{1}{r_p \Delta r} + \frac{2}{\Delta r^2} + \frac{2}{r_p^2 \Delta \vartheta^2} \right) \cdot \phi_P \cong -k_t^2 \phi_P^2 \end{aligned}$$



Since TE and TM modes need to be considered together in many applications, e.g., mode matching or FDTD (using[5]), use of a single grid for all modes will be considered here. This requires to rephrase the FD of BC (3.2.1),(3.2.2) to match the other grid.

We describe here in detail the use of TE grid [26] (Fig.4.1.1a) for TM modes. Let us consider again the external point P on the TE grid (Fig.4.1.4a ). Since the BC (3.2.1),(3.2.2) require  $\phi_x = 0$ , we can express the potential in B and X through a Taylor approximation:

$$\begin{aligned}
 4.1.20.) \quad \phi_B &= \phi_P + \left. \frac{\partial \phi}{\partial r} \right|_P \cdot (-\Delta r) + \frac{1}{2} \left. \frac{\partial^2 \phi}{\partial r^2} \right|_P \cdot (-\Delta r)^2 \\
 \phi_X = 0 &= \phi_P + \left. \frac{\partial \phi}{\partial r} \right|_P \cdot \left( \frac{\Delta r}{2} \right) + \frac{1}{2} \left. \frac{\partial^2 \phi}{\partial r^2} \right|_P \cdot \left( \frac{\Delta r}{2} \right)^2
 \end{aligned}$$

recalling the BC for TM  $\phi_x = 0$ . Adding these equation and solving for the second derivative we get:

$$4.1.21.) \quad \left. \frac{\partial^2 \phi}{\partial r^2} \right|_P = \frac{4}{3 \cdot (\Delta r)^2} \cdot (\phi_B - 3\phi_P)$$

which, together with (4.1.13) gives the discretized form of eigen function equation for point P:

$$\begin{aligned}
 4.1.22.) \quad \nabla_t^2 \phi_P &= \frac{1}{r_p^2 \Delta \alpha^2} \cdot \phi_A + \frac{1}{r_p^2 \Delta \alpha^2} \cdot \phi_C + \left( \frac{4}{3 \Delta r^2} - \frac{1}{3 r_p \Delta r} \right) \cdot \phi_B + \\
 &- \left( \frac{4}{\Delta r^2} + \frac{1}{r_p \Delta r} + \frac{2}{r_p^2 \Delta \alpha^2} \right) \cdot \phi_P \equiv -k_t^2 \phi_P^2
 \end{aligned}$$

as a replacement of (4.1.7) for this point in TM modes. To use the TM grids [27]

for TE modes, we apply the procedure leading to (3.3.4) replacing the y axis with an r axis pointing toward the circle center. The results are:

$$4.1.23.) \quad \begin{aligned} \left. \frac{\partial \phi}{\partial r} \right|_P &= -\frac{1}{2\Delta r} \cdot (\phi_H - 4\phi_B + 3\phi_P) \\ \left. \frac{\partial^2 \phi}{\partial r^2} \right|_P &= \frac{2}{11\Delta r^2} \cdot (\phi_H + \phi_B - 2\phi_P) \end{aligned}$$

and (4.1.22) is replaced by:

$$4.1.24.) \quad \begin{aligned} &\frac{\phi_A}{r_p^2 \Delta \vartheta^2} + \frac{\phi_C}{r_p^2 \Delta \vartheta^2} + \left( \frac{2}{11\Delta r^2} + \frac{1}{2r_p \Delta r} \right) \phi_H + \left( \frac{2}{11r_p \Delta r} - \frac{2}{r_p \Delta r} \right) \phi_B + \\ &- \left( -\frac{3}{2r_p \Delta r} + \frac{4}{11\Delta r^2} + \frac{2}{r_p^2 \Delta \vartheta^2} \right) \phi_P = -k_t^2 \phi \end{aligned}$$

## 4.2) FINITE DIFFERENCE IN ELLIPTICAL WAVEGUIDE

Aim of this paragraph is to develop a FD technique for the calculation of modes and eigenvalues of an elliptical waveguide, taking exactly into account the curved boundary of the waveguide. To do this we build up the discretization grid using the coordinate lines of an elliptic cylindrical framework [22] (Fig. 4.2.1).

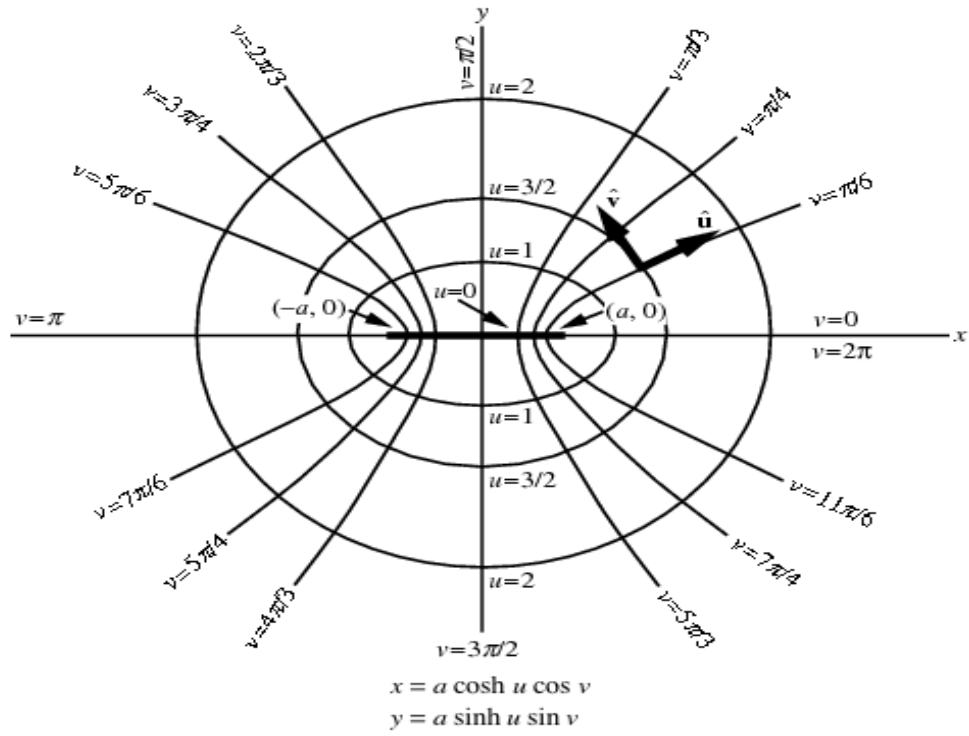


Fig. 4.2.1. Geometry of the elliptic cylindrical coordinates.

Assuming a regular spacing on the coordinate lines, with step  $\Delta u, \Delta v$ , and letting the standard set of grid points for TE and TM modes are shown in Fig.4.2.2. Letting  $\phi_{pq} = \phi(p\Delta u, q\Delta v)$  the eigenvalues equation (3.2.1) can be expressed us:

$$4.2.1.) \quad \frac{1}{a^2 (\sinh^2 p\Delta u + \sin^2 q\Delta v)} \cdot \left[ \frac{\partial^2 \phi}{\partial u^2} + \frac{\partial^2 \phi}{\partial v^2} \right]_{pq} = -k_t^2 \phi_{pq}$$

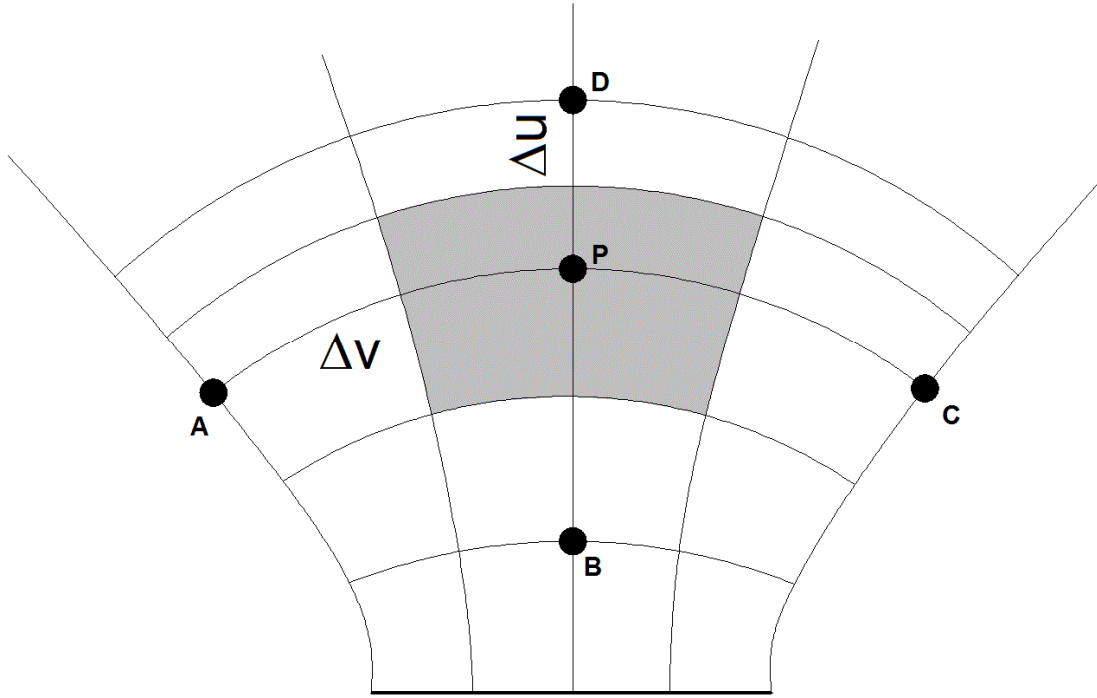


Fig. 4.2.2. Internal point of the elliptic cylindrical coordinates grid TE and TM

In this case it is simpler to discretize (4.2.1) using a Taylor expansion, for each internal point P since the term in brackets expanded exactly as in a rectangular grid:

$$4.2.2.) \quad \left[ \frac{\partial^2 \phi}{\partial u^2} + \frac{\partial^2 \phi}{\partial v^2} \right] = \frac{1}{\Delta v^2} \cdot \phi_A + \frac{1}{\Delta u^2} \cdot \phi_D + \frac{1}{\Delta v^2} \cdot \phi_C + \frac{1}{\Delta u^2} \cdot \phi_B - \left( \frac{2}{(\Delta u)^2} + \frac{2}{(\Delta v)^2} \right) \cdot \phi_P$$

Equation (4.2.2) cannot be used for the two foci, for points between them and for external points. For a point P lying on the segment joining the two foci (see Fig.4.2.3,  $u=0$ ). Since P is a singular point we use (4.1.5) and we write:

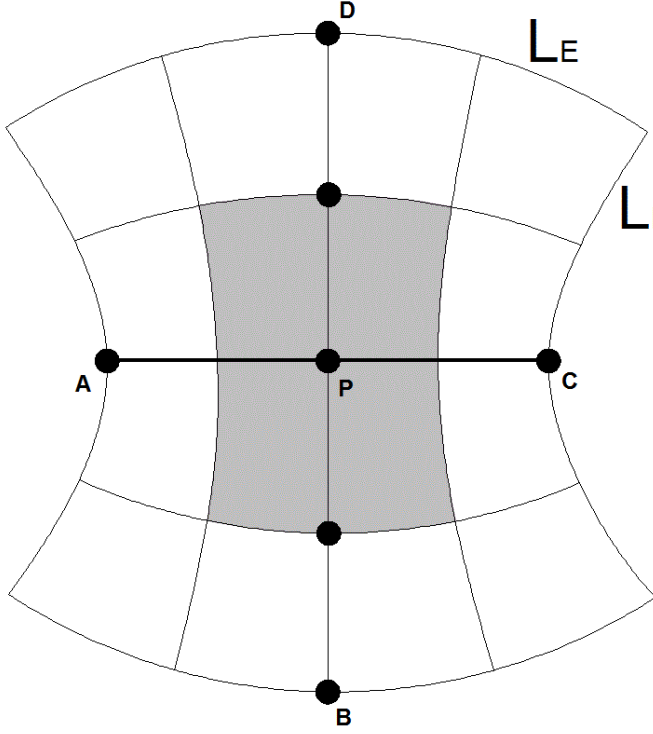


Fig. 4.2.3. point between foci

$$4.2.3.) \quad \frac{1}{S_A} \left[ \frac{(\phi_C - \phi_P)}{h_v \Delta v} \cdot L_I + \frac{(\phi_A - \phi_P)}{h_v \Delta v} \cdot L_I + \frac{(\phi_B - \phi_P)}{h_u \Delta u} \cdot L_E + \frac{(\phi_D - \phi_P)}{h_u \Delta u} \cdot L_E \right] = -k_t^2 \phi_P$$

where  $h = h_u(u, v) = h_v(u, v) = \frac{1}{a \sqrt{\sinh^2 u + \sin^2 v}}$  are scale factor of the elliptic

cylindrical coordinate system,  $S_A = h_u^2 \Delta u \Delta v$  is the area of the cell and  $L_I = h_v \Delta v$ ,

$L_E = h_u \Delta u$  are the length sides of cell. Reordering we get the final expression:

$$4.2.4.) \quad \frac{1}{h^2 \Delta v^2} \cdot \phi_A + \frac{1}{h^2 \Delta u^2} \cdot \phi_D + \frac{1}{h^2 \Delta v^2} \cdot \phi_C + \frac{1}{h^2 \Delta u^2} \cdot \phi_B + \left( \frac{2}{(h \Delta u)^2} + \frac{2}{(h \Delta v)^2} \right) \cdot \phi_P = -k_t^2 \phi_P$$

For the foci, we use (4.1.5) on the cell shown in Fig.4.2.4. This cell is bounded by the ellipse at  $u = \Delta u / 2$ , and by the branch of the hyperbola at  $v = \Delta v / 2$  (intersecting in B and D). If  $S_F$  is the area of the cell, we get:

$$4.2.5.) \quad \frac{1}{S_F} [(\phi_C - \phi_P) \cdot 2L_e + (\phi_A - \phi_P) \cdot 2L_i] = -k_t^2 \phi_P$$

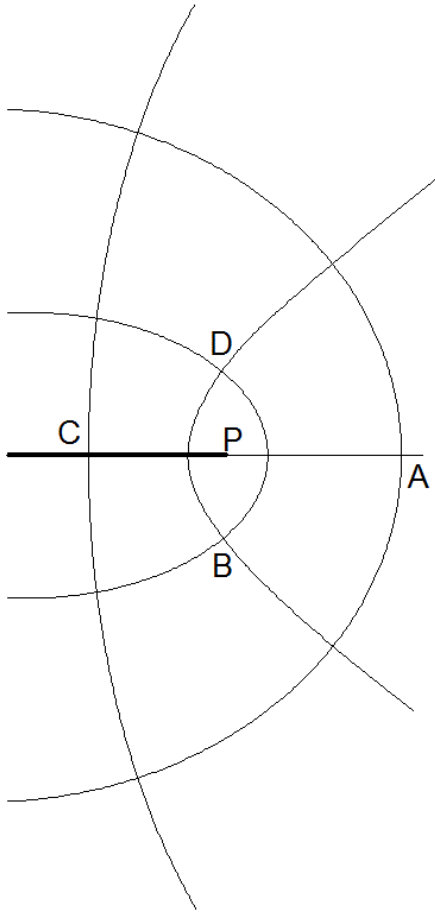


Fig. 4.2.4. Focus (P) of the ellipse

$L_e$  and  $L_i$  are half the length of the arc of the ellipse and of the arc of the hyperbola respectively. These can be computed from the scale factor of the elliptic cylindrical coordinate system:

$$4.2.6.) \quad h_u(u, v) = h_v(u, v) = \frac{1}{a\sqrt{\sinh^2 u + \sin^2 v}}$$

As

$$4.2.7.) \quad L_e = \int_0^{\frac{\Delta v}{2}} h_u\left(\frac{\Delta u}{2}, v\right) dv \cong \frac{\Delta v}{4} \left( h_u\left(\frac{\Delta u}{2}, 0\right) + h_u\left(\frac{\Delta u}{2}, \frac{\Delta v}{2}\right) \right)$$

and

$$4.2.8.) \quad L_i = \int_0^{\frac{\Delta u}{2}} h_v\left(u, \frac{\Delta v}{2}\right) du \cong \frac{\Delta u}{4} \left( h_v\left(\frac{\Delta v}{2}, 0\right) + h_v\left(\frac{\Delta v}{2}, \frac{\Delta u}{2}\right) \right)$$

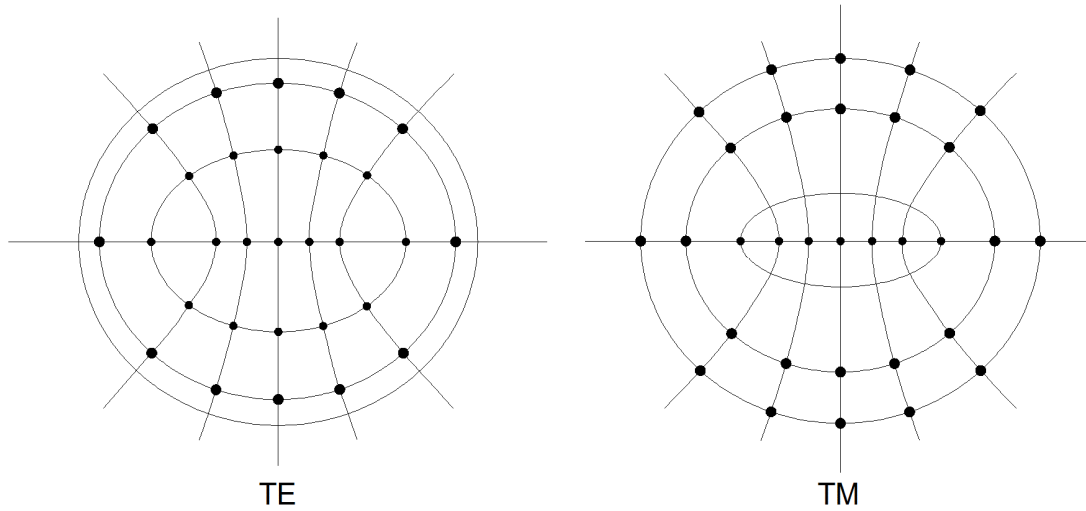


Fig. 4.2.5. Standard TE and TM grid, as suggested from BC

Finally, for a boundary point, the approach is close to the one used for a circular waveguide. For an external point in the TE grid, P in Fig.4.2.6, the BC is equivalent to  $\phi_P = \phi_D$ . For the TM grid, the potential in the external point D is  $\phi_D = 0$ .

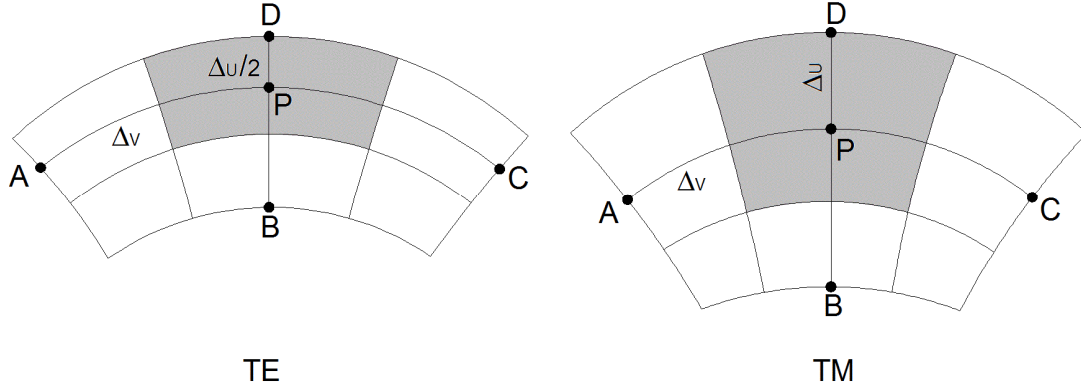


Fig. 4.2.6. Boundary point for TE case and TM case

The two discretized expression for  $\nabla^2\phi$  in P are, in TE case:

$$\begin{aligned}
 4.2.9.) \quad & \frac{1}{a^2 (\sinh^2 p \Delta u + \sin^2 q \Delta v)} \cdot \left[ \frac{\partial^2 \phi}{\partial u^2} + \frac{\partial^2 \phi}{\partial v^2} \right] = \\
 & = \frac{1}{\Delta v^2} \cdot \phi_A + \frac{1}{\Delta v^2} \cdot \phi_C + \frac{1}{\Delta u^2} \cdot \phi_B - \left( \frac{1}{(\Delta u)^2} + \frac{2}{(\Delta v)^2} \right) \cdot \phi_P
 \end{aligned}$$

and in TM case

$$\begin{aligned}
 4.2.10.) \quad & \frac{1}{a^2 (\sinh^2 p \Delta u + \sin^2 q \Delta v)} \cdot \left[ \frac{\partial^2 \phi}{\partial u^2} + \frac{\partial^2 \phi}{\partial v^2} \right] = \\
 & = \frac{1}{\Delta v^2} \cdot \phi_A + \frac{1}{\Delta v^2} \cdot \phi_C + \frac{1}{\Delta u^2} \cdot \phi_B - \left( \frac{2}{(\Delta u)^2} + \frac{2}{(\Delta v)^2} \right) \cdot \phi_P
 \end{aligned}$$

In order to use a single grid we must force the BC  $\phi = 0$  on the TE grid. We can express the potential D through a Taylor approximation:



$$4.2.11.) \quad \phi_D = \phi_P + \left. \frac{\partial \phi}{\partial u} \right|_P \cdot \frac{\Delta u}{2} + \frac{1}{2} \left. \frac{\partial^2 \phi}{\partial u^2} \right|_P \cdot \left( \frac{\Delta u}{2} \right)^2$$

and insert the BC for TM  $\phi_D = 0$  . Since

$$4.2.12.) \quad \phi_B = \phi_P + \left. \frac{\partial \phi}{\partial u} \right|_P \cdot (-\Delta u) + \frac{1}{2} \left. \frac{\partial^2 \phi}{\partial u^2} \right|_P \cdot (-\Delta u)^2$$

We can compute  $\phi_B + 2 \cdot \phi_D = \phi_B$  and therefore:

$$4.2.13.) \quad \left. \frac{\partial^2 \phi}{\partial u^2} \right|_P = \frac{4}{3\Delta u^2} \cdot (\phi_B - 3\phi_P)$$

The final expression is therefore:

$$4.2.14.) \quad \frac{1}{a^2 (\sinh^2 p \Delta u + \sin^2 q \Delta v)} \cdot \left[ \frac{\partial^2 \phi}{\partial u^2} + \frac{\partial^2 \phi}{\partial v^2} \right] =$$

$$\frac{1}{\Delta v^2} \cdot \phi_A + \frac{1}{\Delta v^2} \cdot \phi_C + \frac{4}{3 \cdot \Delta u^2} \cdot \phi_B - \left( \frac{4}{\Delta u^2} + \frac{2}{\Delta v^2} \right) \cdot \phi_P$$

### 4.3) VECTOR POLAR FINITE DIFFERENCE

We consider the TE eigenvalue problem [24] which as shown in ct 3.4 can be written as:

$$4.3.1.) \quad \nabla_t^2 \vec{M} + k_t^2 \vec{M} = 0$$

with additional conditions:

$$4.3.2.) \quad \begin{cases} \nabla_t \times \vec{M} = 0 \\ \vec{M} \cdot \vec{i}_n \Big|_C = 0 \end{cases}$$

Of course  $\vec{M}$  is evaluated only on the points of a polar grid (see Fig.4.1.1 a) with spacing  $\Delta r, \Delta \vartheta$ , and the equations are replaced by difference equations. For each internal grid point (see Fig.4.1.2), a second order Taylor approximation allows to evaluate the surface magnetic current in terms of the current samples at the neighboring points. Taking into account the expansion of the vector Laplace operator in polar coordinates:

$$4.3.3.) \quad \nabla_t^2 \vec{M} = \left[ \frac{\partial^2 M_r}{\partial r^2} + \frac{1}{r} \cdot \frac{\partial M_r}{\partial r} - \frac{M_r}{r^2} + \frac{1}{r^2} \cdot \frac{\partial^2 M_r}{\partial \vartheta^2} - \frac{2}{r^2} \cdot \frac{\partial M_\vartheta}{\partial \vartheta} \right] \vec{u}_r + \left[ \frac{\partial^2 M_\vartheta}{\partial r^2} + \frac{1}{r} \cdot \frac{\partial M_\vartheta}{\partial r} - \frac{M_\vartheta}{r^2} + \frac{1}{r^2} \cdot \frac{\partial^2 M_\vartheta}{\partial \vartheta^2} + \frac{2}{r^2} \cdot \frac{\partial M_r}{\partial \vartheta} \right] \vec{u}_\vartheta$$

the terms in the brackets are obtained as:

$$\begin{aligned}
\frac{\partial^2 M_{\vartheta}}{\partial \vartheta^2} &= \frac{M_{A,\vartheta} + M_{C,\vartheta} - 2M_{P,\vartheta}}{\Delta \vartheta^2} \\
\frac{\partial M_{\vartheta}}{\partial \vartheta} &= \frac{M_{C,\vartheta} - M_{A,\vartheta}}{2\Delta \vartheta} \\
\frac{\partial^2 M_{\vartheta}}{\partial r^2} &= \frac{M_{B,\vartheta} + M_{D,\vartheta} - 2M_{P,\vartheta}}{\Delta r^2} \\
\frac{\partial M_{\vartheta}}{\partial r} &= \frac{M_{D,\vartheta} - M_{B,\vartheta}}{2\Delta r} \\
\frac{\partial^2 M_r}{\partial r^2} &= \frac{M_{B,r} + M_{D,r} - 2M_{P,r}}{\Delta r^2} \\
\frac{\partial M_r}{\partial r} &= \frac{M_{D,r} - M_{B,r}}{2\Delta r} \\
\frac{\partial^2 M_r}{\partial \vartheta^2} &= \frac{M_{A,r} + M_{C,r} - 2M_{P,r}}{\Delta \vartheta^2} \\
\frac{\partial M_r}{\partial \vartheta} &= \frac{M_{C,r} - M_{A,r}}{2\Delta \vartheta}
\end{aligned}$$

the expression for an internal point P as in Fig.4.1.2 is :

$$\begin{aligned}
4.3.4.) \quad \nabla_t^2 \vec{M}_P &= \left[ M_{B,r} K_1 + M_{D,r} K_2 + M_{A,r} K_3 + M_{C,r} K_3 - M_{P,r} K_4 M_{A,\alpha} K_5 - M_{C,\alpha} K_5 \right] \cdot \vec{u}_r + \\
&+ \left[ M_{B,\alpha} K_1 + M_{D,\alpha} K_2 + M_{A,\alpha} K_3 + M_{C,\alpha} K_3 - M_{P,\alpha} K_4 - M_{A,r} K_5 + M_{C,r} K_5 \right] \cdot \vec{u}_{\vartheta}
\end{aligned}$$

where

$$\begin{aligned}
K_1 &= \frac{1}{\Delta r^2} - \frac{1}{2r_p \Delta r} & K_2 &= \frac{1}{\Delta r^2} + \frac{1}{2r_p \Delta r} \\
K_3 &= \frac{1}{r_p^2 \Delta \vartheta^2} & K_4 &= K_1 + K_2 + 2K_3 + \frac{1}{r_p^2} \\
K_5 &= \frac{1}{2r_p^2 \Delta \vartheta}
\end{aligned}$$

To discretize the first of the (4.32) we can use a first-order Taylor expression. Since (4.32) is:

$$4.3.5.) \quad \nabla \times \vec{M} = \frac{1}{r} \cdot \frac{\partial(r \cdot M_{\vartheta})}{\partial r} - \frac{1}{r} \cdot \frac{\partial M_r}{\partial \vartheta} = \frac{1}{r} \cdot M_{\vartheta} + \frac{\partial M_{\vartheta}}{\partial r} - \frac{1}{r} \cdot \frac{\partial M_r}{\partial \vartheta} = 0$$

then

$$4.3.6.) \quad \left( \frac{1}{r_p} \cdot M_{P,\vartheta} + \frac{M_{D,\vartheta} - M_{B,\vartheta}}{2\Delta r} - \frac{1}{r_p} \cdot \frac{M_{C,r} - M_{A,r}}{2\Delta \vartheta} \right) = 0$$

For a boundary point, such as P in Fig.4.3.1, using the same method apply rectangular waveguide. The BC is  $M_{D',r} = 0$  and this condition can be incorporated into the FD matrix.

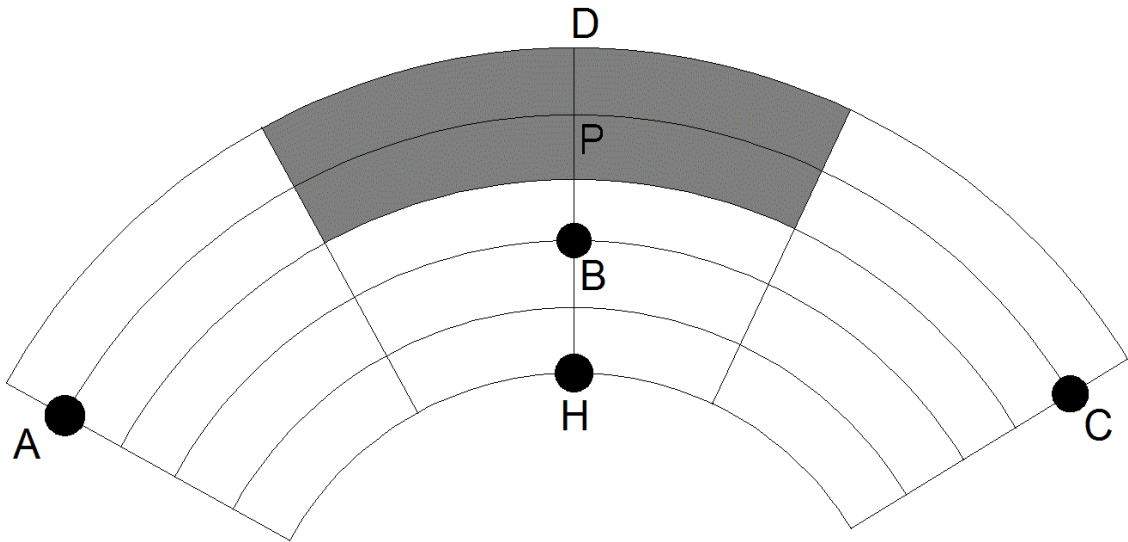


Fig.4.3.1 - Boundary point of polar framework

Also the  $\vec{u}_\vartheta$  component of (4.3.6) relevant to P needs to be modified, for the same reason. To do this we need another point H. Equation (4.3.6) is then replaced by:

$$4.3.7.) \quad \nabla_t^2 \vec{M}_P = \left[ M_{B,r} H_1 + M_{A,r} K_3 + M_{C,r} K_3 - M_{P,r} H_4 + M_{A,\vartheta} K_5 - M_{C,\vartheta} K_5 \right] \cdot \vec{u}_r + \\ + \left[ M_{H,\vartheta} K_1 - M_{B,\vartheta} H_2 + M_{A,\vartheta} K_3 + M_{C,\vartheta} K_3 - M_{P,\vartheta} H_5 - M_{A,r} K_5 + M_{C,r} K_5 \right] \cdot \vec{u}_\vartheta$$

where  $H_1 = \frac{4}{3\Delta r^2} - \frac{1}{3r_p \Delta r}$ ,  $H_2 = \frac{2}{\Delta r^2} + \frac{4}{2r_p \Delta r}$ ,  $H_3 = \frac{1}{r_p \Delta r} + \frac{2}{r_p \Delta \vartheta^2}$  and

$$H_4 = 3H_1 + H_3 + 2K_3, \quad H_5 = \frac{1}{r_p \Delta r} + \frac{3}{2r_p \Delta r} - \frac{1}{r_p^2} - 2K_3.$$

At the same time, the condition (4.3.6) becomes analogously:

$$4.3.8.) \quad \left( \left( \frac{1}{r_p} + \frac{3}{2\Delta r} \right) M_{P,\vartheta} + \frac{M_{H,\vartheta}}{2\Delta r} - \frac{4M_{B,\vartheta}}{2\Delta r} - \frac{1}{r_p} \cdot \frac{M_{C,r} - M_{A,r}}{2\Delta \vartheta} \right) = 0$$

It remains to consider the center of the circle. In this point it is not possible to use a Taylor expression since it is a point of singularity for the polar framework. Therefore we integrate (4.3.2), as in the scalar case, (4.1.1) and obtain:

$$4.3.9.) \quad \int_S \nabla_t^2 \vec{M} \cdot d\vec{S} = -k_t^2 \int_S \vec{M} \cdot d\vec{S}$$

Because of (4.3.3) the Laplace operator becomes :

$$4.3.10.) \quad \nabla_t^2 \vec{M} = \nabla_t \left( \nabla_t \vec{M} \right) - \nabla_t \times \nabla_t \times \vec{M} = \nabla_t \left( \nabla_t \vec{M} \right)$$

we replace (4.3.10) in (4.3.9) becomes:

$$4.3.11.) \quad \int_S \nabla_t (\nabla_t \cdot \vec{M}) \cdot d\vec{S} = -k_t^2 \int \vec{M} \cdot d\vec{S}$$

We apply the theorem of the gradient [33] to the l.h.s of (4.3.10)

$$4.3.12.) \quad \int_S \nabla_t (\nabla_t \cdot \vec{M}) \cdot d\vec{S} = \int_C \nabla_t \vec{M} \cdot \vec{i}_n \cdot d\vec{l} = \int_C \nabla_t \vec{M} \cdot \vec{i}_n \cdot \frac{\Delta r}{2} \cdot d\vartheta$$

since  $d\vec{l} = \frac{\Delta r}{2} \cdot d\vartheta \cdot \vec{i}_n$ . Using the divergence of  $\vec{M}$  in polar coordinate we get for the r.h.s of (4.3.11):

$$4.3.13.) \quad \int_C \frac{\partial(r \cdot M_r)}{\partial r} \cdot \vec{i}_n \cdot \frac{\Delta r}{2} \cdot d\vartheta + \int_C \frac{\partial M_\vartheta}{\partial \vartheta} \cdot \vec{i}_n \cdot d\vartheta$$

Since  $\vec{i}_n = \vec{i}_x \cos(\vartheta) + \vec{i}_y \sin(\vartheta)$ . We decompose (4.3.12) in an x component:

$$4.3.14.) \quad \int_C \frac{\partial(r \cdot M_r)}{\partial r} \cdot \vec{i}_x \cos(\vartheta) \cdot \frac{\Delta r}{2} \cdot d\vartheta + \int_C \frac{\partial M_\vartheta}{\partial \vartheta} \cdot \vec{i}_x \cos(\vartheta) \cdot d\vartheta$$

and a y component:

$$4.3.15.) \quad \int_C \frac{\partial(r \cdot M_r)}{\partial r} \cdot \vec{i}_y \sin(\vartheta) \cdot \frac{\Delta r}{2} \cdot d\vartheta + \int_C \frac{\partial M_\vartheta}{\partial \vartheta} \cdot \vec{i}_y \sin(\vartheta) \cdot d\vartheta$$

compute by parts the second integral of (4.3.14) and (4.3.15)

$$4.3.16.) \quad \int_C \frac{\partial M_\vartheta}{\partial \vartheta} \cdot \vec{i}_x \cos(\vartheta) \cdot d\vartheta = \left| M_\vartheta \cos(\vartheta) \right|_{-\pi}^{+\pi} - \int_{-\pi}^{+\pi} -M_\vartheta \sin(\vartheta) \cdot d\vartheta = \int_{-\pi}^{+\pi} M_\vartheta \sin(\vartheta) \cdot d\vartheta$$

$$4.3.17.) \quad \int_C \frac{\partial M_\vartheta}{\partial \vartheta} \cdot \vec{i}_y \sin(\vartheta) \cdot d\vartheta = - \int_{-\pi}^{+\pi} M_\vartheta \cos(\vartheta) \cdot d\vartheta$$

we insert (4.3.16) with (4.3.17), (4.3.14) and (4.3.15) into (4.3.12) to get:

$$4.3.18.) \quad \int_C \frac{\partial(r \cdot M_r)}{\partial r} \cdot \vec{i}_x \cos(\vartheta) \cdot \frac{\Delta r}{2} \cdot d\vartheta + \int_{-\pi}^{+\pi} M_\vartheta \sin(\vartheta) \cdot d\vartheta \cdot \vec{i}_x + \\ + \int_C \frac{\partial(r \cdot M_r)}{\partial r} \cdot \vec{i}_y \sin(\vartheta) \cdot \frac{\Delta r}{2} \cdot d\vartheta + \int_{-\pi}^{+\pi} M_\vartheta \cos(\vartheta) \cdot d\vartheta \cdot \vec{i}_y = -k_t^2 A_t$$

where  $A_r = 4 / \pi \cdot \Delta r^2$ . In (4.3.16) and (4.3.17)  $\vec{M}_0$  must be evaluated in Cartesian coordinates:  $\vec{M}_0 = M_{0x} \cdot \vec{i}_x - M_{0y} \cdot \vec{i}_y$

To evaluate (4.3.15) we need  $M_\vartheta\left(\frac{\Delta r}{2}, \vartheta\right)$ ,  $\left. \frac{\partial(r \cdot M_r)}{\partial r} \right|_{r=\frac{\Delta r}{2}}$  along C, and therefore

outside of the discretization grid. In order to include (4.3.16) and (4.3.17) into the

FD matrix, we must express the  $M_\vartheta\left(\frac{\Delta r}{2}, \vartheta\right)$  in terms of  $\vec{M}$  at the discretization

points, as averages. Since  $\vec{M}_0$  does not have polar components, such averages must be computed as (compare Fig.4.3.2)

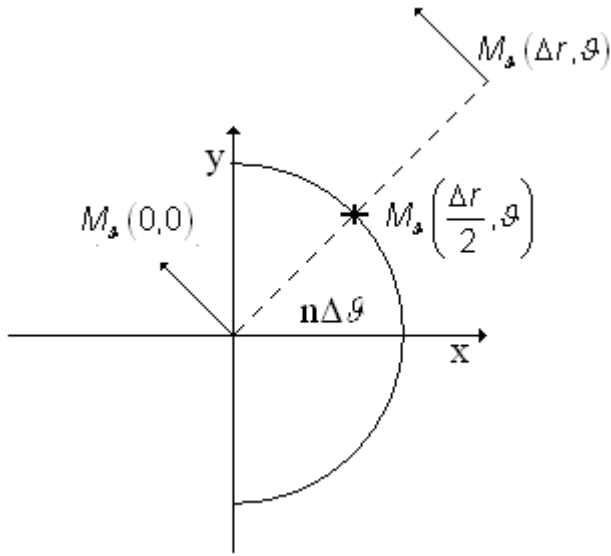


Fig.4.3.2 – component of  $\bar{M}$  between center and next point.

$$M_{\vartheta}\left(\frac{\Delta r}{2}, \vartheta\right) = \frac{1}{2} \cdot \left[ M_{\vartheta}(\Delta r, \vartheta) + \lim_{\varepsilon \rightarrow 0} M_{\vartheta}(\varepsilon, \vartheta) \right] =$$

$$= \frac{1}{2} \cdot \left[ M_{\vartheta}(\Delta r, \vartheta) + (M_{0,y} \cos(\vartheta) - M_{0,x} \sin(\vartheta)) \right]$$

4.3.19.)

$$\left. \frac{\partial(r \cdot M_r)}{\partial r} \right|_{\frac{\Delta r}{2}, \vartheta} = \left[ \frac{(r \cdot M_r)|_{\Delta r} - \lim_{\varepsilon \rightarrow 0} (r \cdot M_r)|_{\varepsilon}}{\Delta r} \right] =$$

$$= \left[ \frac{\Delta r \cdot M_r(\Delta r, \vartheta) - 0}{\Delta r} \right] = M_r(\Delta r, \vartheta)$$

Now solving the first integral of (4.3.14) and (4.3.15)

$$4.3.20.) \quad \int_c \left. \frac{\partial(r \cdot M_r)}{\partial r} \right|_{\frac{\Delta r}{2}, \vartheta} \cdot \cos(\vartheta) \cdot \frac{\Delta r}{2} \cdot d\vartheta = \sum_{q=1}^N M_{r,q} \cdot \cos(\vartheta_q) \cdot \Delta \vartheta$$



$$4.3.21.) \quad \int_C \left. \frac{\partial(r \cdot M_r)}{\partial r} \right|_{\frac{\Delta r}{2}, \vartheta} \cdot \sin(\vartheta) \cdot \frac{\Delta r}{2} \cdot d\vartheta = \sum_{q=1}^N M_{r,q} \cdot \sin(\vartheta_q) \cdot \Delta \vartheta$$

where  $M_{r,q} = M_r(\Delta r, q\Delta \vartheta)$ ; now solving (4.3.16) and (4.3.17):

$$4.3.22.) \quad \begin{aligned} \int_C \frac{\partial M_{\vartheta}}{\partial \vartheta} \cdot \cos(\vartheta) \cdot d\vartheta &= \int_{-\pi}^{+\pi} M_{\vartheta} \sin(\vartheta) \cdot d\vartheta = \\ &= \sum_{q=1}^N \left[ \frac{M_{\vartheta,q} \cdot \sin(\vartheta_q) + (M_{0,y}^q \sin(\vartheta_q) \cos(\vartheta_q) - M_{0,x}^q \sin^2(\vartheta_q))}{2} \right] \end{aligned}$$

$$4.3.23.) \quad \begin{aligned} \int_C \frac{\partial M_{\vartheta}}{\partial \vartheta} \cdot \sin(\vartheta) \cdot d\vartheta &= - \int_{-\pi}^{+\pi} M_{\vartheta} \cos(\vartheta) \cdot d\vartheta = \\ &= - \sum_{q=1}^N \left[ \frac{M_{\vartheta,q} \cdot \cos(\vartheta_q) + (M_{0,y}^q \cos^2(\vartheta_q) - M_{0,x}^q \sin(\vartheta_q) \cos(\vartheta_q))}{2} \right] \end{aligned}$$

where  $M_{\vartheta,q} = M_{\vartheta}(\Delta r, q\Delta \vartheta)$ ; we sum (4.3.21) and (4.3.23) and we get , for the x component:

$$4.3.24.) \quad \begin{aligned} \int_C \left. \frac{\partial(r \cdot M_r)}{\partial r} \right|_{\frac{\Delta r}{2}, \vartheta} \cdot \cos(\vartheta) \cdot \frac{\Delta r}{2} \cdot d\vartheta + \int_{-\pi}^{+\pi} M_{\vartheta} \sin(\vartheta) \cdot d\vartheta &= \\ &= \sum_{q=1}^N M_{r,q} \cdot \cos(\vartheta_q) \cdot \Delta \vartheta + \\ &+ \sum_{q=1}^N \left[ \frac{M_{\vartheta,q} \cdot \sin(\vartheta_q) + (M_{0,y}^q \sin(\vartheta_q) \cos(\vartheta_q) - M_{0,x}^q \sin^2(\vartheta_q))}{2} \right] = \\ &= \sum_{q=1}^N \left[ \frac{M_{r,q} \cdot \cos(\vartheta_q) \cdot \Delta \vartheta + M_{\vartheta,q} \cdot \sin(\vartheta_q) + (M_{0,y}^q \sin(\vartheta_q) \cos(\vartheta_q) - M_{0,x}^q \sin^2(\vartheta_q))}{2} \right] \end{aligned}$$

we sum (4.3.20) and (4.3.22) and we get , for the y component:

$$\begin{aligned}
 & \int_C \left. \frac{\partial(r \cdot M_r)}{\partial r} \right|_{\frac{\Delta r}{2}, \vartheta} \cdot \sin(\vartheta) \cdot \frac{\Delta r}{2} \cdot d\vartheta - \int_{-\pi}^{+\pi} M_{\vartheta} \cos(\vartheta) \cdot d\vartheta = \\
 & = \sum_{q=1}^N M_{r,q} \cdot \sin(\vartheta_q) \cdot \Delta\vartheta + \\
 4.3.25.) & - \sum_{q=1}^N \left[ \frac{M_{\vartheta,q} \cdot \cos(\vartheta_q) + (M_{0,y}^q \cos^2(\vartheta_q) - M_{0,x}^q \sin(\vartheta_q) \cos(\vartheta_q))}{2} \right] \\
 & = \sum_{q=1}^N \left[ \frac{M_{r,q} \cdot \sin(\vartheta_q) \cdot \Delta\vartheta + M_{\vartheta,q} \cdot \cos(\vartheta_q) + (M_{0,y}^q \cos^2(\vartheta_q) - M_{0,x}^q \sin(\vartheta_q) \cos(\vartheta_q))}{2} \right]
 \end{aligned}$$

#### 4.4) VECTOR ELLIPTIC FINITE DIFFERENCE

In the same way as the circular case, in an elliptic waveguide,  $\vec{M}$  is evaluated only on the points of a elliptic grid (see Fig.4.2.1) with spacing  $(\Delta u, \Delta v)$ .

The expression of the Laplace vector operator in elliptic coordinates can be simplified if we let  $\vec{A} = h\vec{M}$ , where

$$4.4.1.) \quad h = \frac{1}{a_f \sqrt{\sinh^2 u + \sin^2 v}}$$

is the common value of the scale factor,  $2a_f$  being the inter-focal distance. The

$u$  component of  $\nabla_t^2 \vec{M}$  is

$$4.4.2.) \quad \begin{aligned} & -\frac{1}{h^5} \cdot \frac{\partial h^2}{\partial u} \cdot \frac{\partial(A_u)}{\partial u} + \frac{1}{h^3} \frac{\partial^2(A_u)}{\partial u^2} - \frac{1}{h^5} \cdot \frac{\partial h^2}{\partial u} \cdot \frac{\partial(A_v)}{\partial v} - \frac{\partial h}{\partial v} \cdot \frac{1}{h^3} \cdot \frac{\partial(A_v)}{\partial u} + \\ & \frac{\partial h}{\partial v} \cdot \frac{1}{h^3} \cdot \frac{\partial(A_u)}{\partial v} + \frac{1}{h^5} \cdot \frac{\partial h^2}{\partial v} \cdot \frac{\partial(A_v)}{\partial u} - \frac{1}{h^5} \cdot \frac{\partial h^2}{\partial v} \cdot \frac{\partial(A_u)}{\partial v} + \frac{1}{h^3} \cdot \frac{\partial^2(A_u)}{\partial v^2} \end{aligned}$$

and the  $v$  components is:

$$4.4.3.) \quad \begin{aligned} & -\frac{1}{h^5} \cdot \frac{\partial h^2}{\partial v} \cdot \frac{\partial(A_u)}{\partial u} - \frac{1}{h^5} \cdot \frac{\partial h^2}{\partial v} \cdot \frac{\partial(A_v)}{\partial v} + \frac{1}{h^3} \frac{\partial^2(A_v)}{\partial v^2} + \frac{1}{h^3} \cdot \frac{\partial^2(A_v)}{\partial u^2} - \\ & \frac{1}{h^5} \cdot \frac{\partial h^2}{\partial u} \cdot \frac{\partial(A_v)}{\partial u} + \frac{1}{h^5} \cdot \frac{\partial h^2}{\partial u} \cdot \frac{\partial(A_u)}{\partial v} \end{aligned}$$

For each internal grid point, as in Fig.4.2.2, a second order Taylor approximation allows to discretize the Laplace operator (4.4.2,4.4.3) in terms of the current samples at the neighboring points. The resulting derivatives are as follows:

$$\begin{aligned}
\frac{\partial(A_u)}{\partial u} &= \frac{A_{D,u} - A_{B,u}}{2\Delta u} \\
\frac{\partial(A_u)}{\partial v} &= \frac{A_{C,u} - A_{A,u}}{2\Delta v} \\
\frac{\partial(A_v)}{\partial v} &= \frac{A_{C,v} - A_{A,v}}{2\Delta v} \\
\frac{\partial(A_v)}{\partial u} &= \frac{A_{D,v} - A_{B,v}}{2\Delta u} \\
\frac{\partial^2(A_u)}{\partial u^2} &= \frac{1}{(\Delta u)^2} \cdot (A_{D,u} + A_{B,u} - 2A_{P,u}) \\
\frac{\partial^2(A_v)}{\partial v^2} &= \frac{1}{(\Delta v)^2} \cdot (A_{C,v} + A_{A,v} - 2A_{P,v}) \\
\frac{1}{h^3} &= a_f^3 \cdot (\sinh^2 u + \sin^2 v)^{\frac{3}{2}} \\
\frac{1}{h^5} &= a_f^5 \cdot (\sinh^2 u + \sin^2 v)^{\frac{5}{2}} \\
4.4.4.) \quad \frac{1}{h^5} \cdot \frac{\partial h^2}{\partial u} &= -2a_f^3 \cdot (\sinh^2 u + \sin^2 v)^{\frac{3}{2}} \cdot \sinh u \cdot \cosh u \\
\frac{1}{h^5} \cdot \frac{\partial h^2}{\partial v} &= -2a_f^3 \cdot (\sinh^2 u + \sin^2 v)^{\frac{3}{2}} \cdot \sin v \cdot \cos v
\end{aligned}$$

The same simplification is obtained for the first equation 4.3.2 for elliptic case, since letting  $\vec{A} = h\vec{M}$  makes this equation almost identical to the rectangular case:

$$4.4.5.) \quad \frac{1}{h^2} \left( \frac{\partial A_v}{\partial u} - \frac{\partial A_u}{\partial v} \right) = \frac{1}{h^2} \left( \frac{A_{C,u} - A_{A,u}}{2\Delta u} - \frac{A_{D,v} - A_{B,v}}{2\Delta v} \right) = 0$$

The singular points of the elliptical framework, either the foci, or the points on the inter--focal segment, require a different treatment. For a focus of the ellipse, Fig.4.2.4, as in the circular case we use the integral form of the eigenvalue equation, as in (4.3.11-4.3.13). The central term of (4.3.12) becomes

$$4.4.6.) \int_C \nabla_t \vec{M} \cdot \vec{i}_n \cdot dl = \int_C \frac{1}{h^2} \cdot \frac{\partial M_u}{\partial u} \cdot \vec{i}_n \cdot dl + \int_C \frac{1}{h^2} \cdot \frac{\partial M_v}{\partial v} \cdot \vec{i}_n \cdot dl$$

The integrals are divided in 4 parts. We describe here in details only the evaluation of the part over  $C_1$ . Letting  $Q = \left(a, \frac{\Delta v}{2}\right)$  and  $R = \left(\frac{\Delta u}{2}, 0\right)$ , we have

$$4.4.7.) \int_{C_1} \frac{1}{h^2} \cdot \frac{\partial M_u}{\partial u} \cdot \vec{i}_n \cdot dl = \int_0^{\frac{\Delta u}{2}} \frac{1}{h^2} \cdot \frac{\partial M_u}{\partial u} \cdot \vec{i}_n \cdot h \cdot du = \frac{1}{h} \cdot \vec{i}_n \Big|_{x_p}^{\frac{\Delta u}{2}} \cdot \int_0^{\frac{\Delta u}{2}} \frac{\partial M_u}{\partial u} \cdot du =$$

$$\frac{-\vec{i}_x}{h(Q)} \cdot \left[ \frac{M_u(A) + M_u(B) + M_u(C) + M_u(D)}{4} - \frac{M_u(A) + M_u(B)}{2} \right]$$

and

$$4.4.8.) \int_{C_1} \frac{1}{h^2} \cdot \frac{\partial M_v}{\partial v} \cdot \vec{i}_n \cdot dl = \frac{1}{h} \cdot \vec{i}_n \cdot \frac{\partial M_v}{\partial v} \Big|_Q \int_0^{\frac{\Delta u}{2}} du = \frac{1}{h(Q)} \cdot (-\vec{i}_x) \cdot \left( \frac{M_v(B) - M_v(A)}{\Delta v} \right) \frac{\Delta u}{2}$$

The same approach can be used for points on the inter-focal segment, such as the one in Fig.4.2.3.

## Chapter V

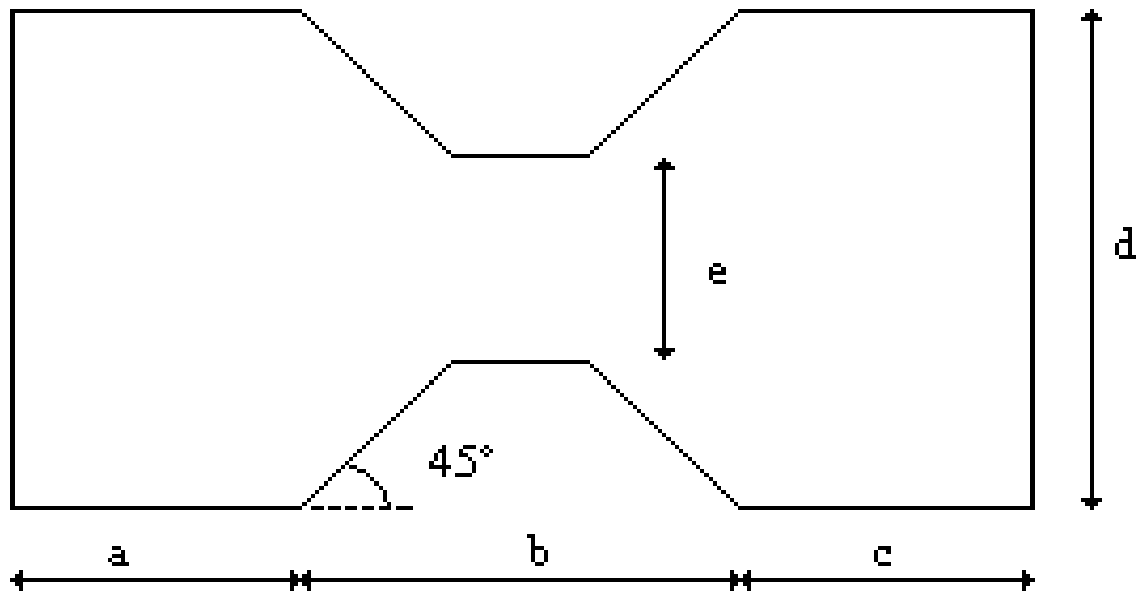
### INTRODUCTION

In this chapter we extended the FD approach to waveguides (and apertures) with irregular boundaries, and therefore non-regular discretization grids. We show that a suitable FD approximation of the Laplace operator is still possible. We consider in detail a ridged-waveguide, with trapezoidal ridges, and a rounded-ended waveguide.

#### 5.1) FINITE DIFFERENCE IN RIDGED WAVEGUIDE

In this paragraph we develop a general scheme for the FD approximation of the Laplace operator, based on a non-regular discretization [35].

In order to describe the details of the method we consider a ridge waveguide with trapezoidal ridge shape, with edge of 45 degrees (see Fig. 5.1.1).



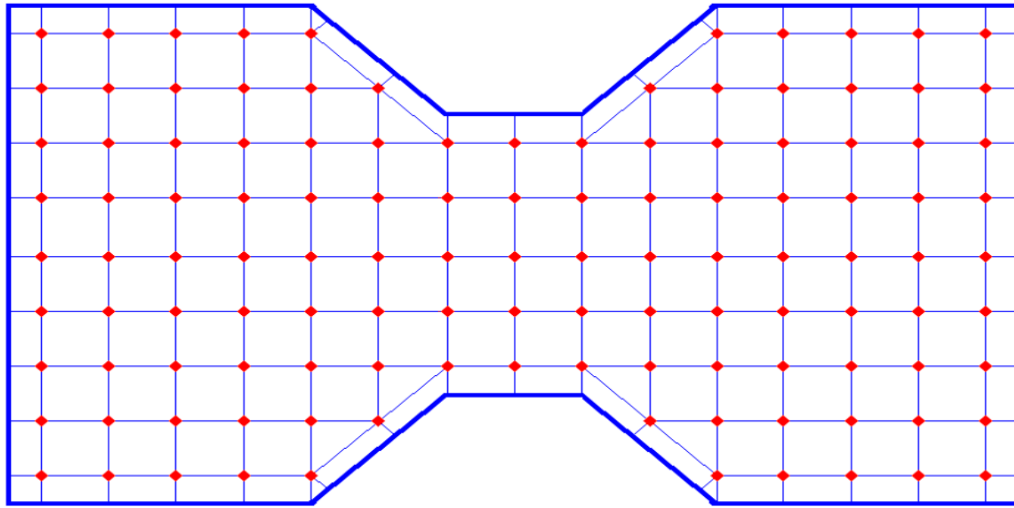


Fig. 5.1.1. Waveguides section with trapezoidal ridge, and FD corner mesh grids

We consider a “TE” grid, as in of Fig.5.1.1b. For a consider a generic point 0 of coordinates  $(x_0, y_0)$  we use the five nearby points 1, 2, 3, 4 and 5, as shown in Fig. 5.1.2 .

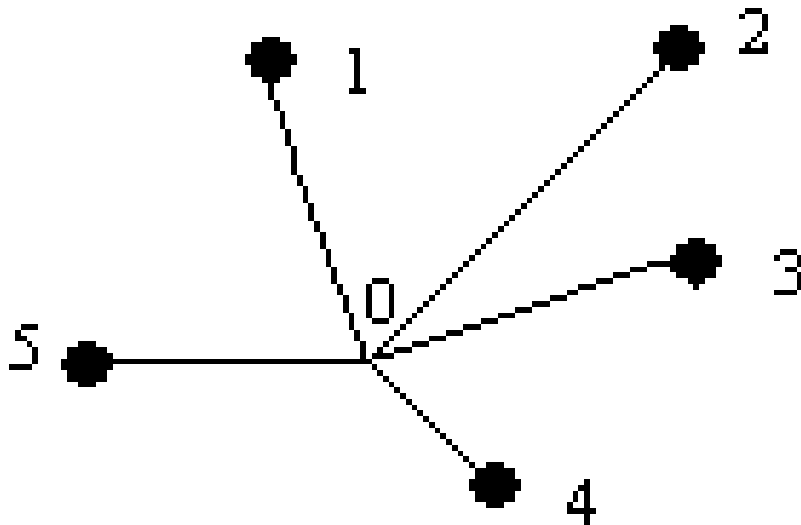


Fig. 5.1.2. Generic internal case of five points used to develop FD scheme

Let us number with 0 the sampling point, and with  $i$  ( $i = 1, \dots, 5$ ) its neighboring points. Using a second order Taylor approximation we can write for each internal grid point.

$$\begin{aligned}
 \phi_i - \phi_0 = \\
 5.1.1.) \quad & \left. \frac{\partial \phi}{\partial x} \right|_0 \cdot \Delta x_i + \left. \frac{\partial \phi}{\partial y} \right|_0 \cdot \Delta y_i + \frac{1}{2} \left. \frac{\partial^2 \phi}{\partial x^2} \right|_0 \cdot \Delta x_i^2 + \\
 & + \frac{1}{2} \left. \frac{\partial^2 \phi}{\partial y^2} \right|_0 \cdot \Delta y_i^2 + \left. \frac{\partial^2 \phi}{\partial x \partial y} \right|_0 \cdot \Delta x_i \cdot \Delta y_i
 \end{aligned}$$

where all derivatives of  $\phi$  are computed at the central sampling point, and  $(\Delta x_i, \Delta y_i)$  is the position of the  $i$ -th point w.r.t point 0.

A suitable linear combination of these expansions is the sought FD approximation to the Laplace operator, up to the second order:

$$5.1.2.) \quad \nabla_t^2 \phi = \frac{\partial^2 \phi}{\partial x^2} + \frac{\partial^2 \phi}{\partial y^2} \cong \sum_i A_i (\phi_i - \phi_0)$$

The coefficient can be easily obtained by the solution of a set of 5 linear equations. (5.1.2) can be rewritten, using (5.1.1), as

$$5.1.3.) \quad B_1 \frac{\partial \phi}{\partial x} + B_2 \frac{\partial \phi}{\partial y} + B_3 \frac{\partial^2 \phi}{\partial x^2} + B_4 \frac{\partial^2 \phi}{\partial y^2} + B_5 \frac{\partial^2 \phi}{\partial x \partial y}$$

The  $B_i$  in (5.1.3) are linear combination of the unknown coefficient  $A_i$ .



$$\begin{aligned}
B_1 &= A_1 \Delta x_1 + A_2 \Delta x_2 + A_3 \Delta x_3 + A_4 \Delta x_4 + A_5 \Delta x_5 \\
B_2 &= A_1 \Delta y_1 + A_2 \Delta y_2 + A_3 \Delta y_3 + A_4 \Delta y_4 + A_5 \Delta y_5 \\
5.1.4.) \quad B_3 &= A_1 \Delta x_1^2 + A_2 \Delta x_2^2 + A_3 \Delta x_3^2 + A_4 \Delta x_4^2 + A_5 \Delta x_5^2 \\
B_4 &= A_1 \Delta y_1^2 + A_2 \Delta y_2^2 + A_3 \Delta y_3^2 + A_4 \Delta y_4^2 + A_5 \Delta y_5^2 \\
B_5 &= A_1 \Delta x_1 \Delta y_1 + A_2 \Delta x_2 \Delta y_2 + A_3 \Delta x_3 \Delta y_3 + A_4 \Delta x_4 \Delta y_4 + A_5 \Delta x_5 \Delta y_5
\end{aligned}$$

Eq. (5.1.2) can approximate, to the second order, the Laplace operator if

$$5.1.5.) \quad B_1 = B_2 = B_5 = 0 \quad B_3 = B_4 = 1$$

which is a linear system in the  $A_i$ . Its solution gives the required coefficient of (5.1.4).

Note that use of only four points lead to an impossible system, unless the grid is rectangular, since in this case  $B_5 = 0$  identically. Therefore, for each internal point of Fig.5.1.1 internal point this approach is equal to use the standard FD approximation (3.2.9).

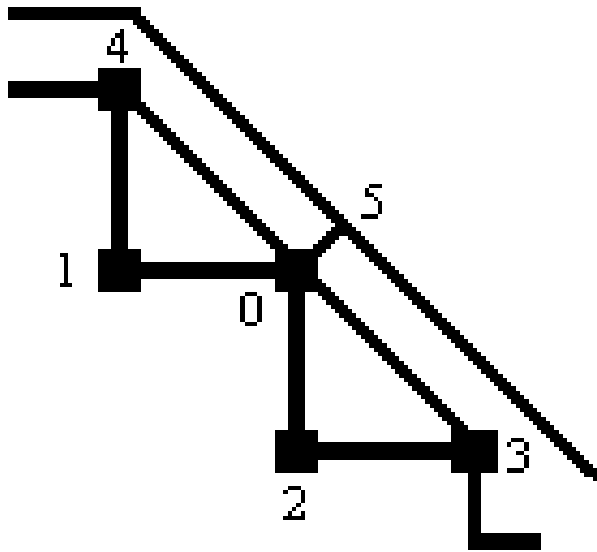


Fig. 5.1.3. Boundary Point of trapezoidal ridge

For external sampling points (see Fig.5.1.3 and Fig.5.1.4), we require, as usual in standard FD, that the normal derivative must be equal to zero at the sampling point itself and can be expressed as:

$$5.1.6.) \quad \left. \frac{\partial \phi}{\partial n} \right|_0 = \alpha_x \left. \frac{\partial \phi}{\partial x} \right|_0 + \alpha_y \left. \frac{\partial \phi}{\partial y} \right|_0 = 0$$

where  $\alpha_x, \alpha_y$  are the component of a vector normal to the boundary. Eq. (5.5) .

can be used to replace equations  $B_1=0, B_2=0$  with a single one, to compensate for the absence of one unknown (see Fig. 5.1.4) In this way we approximate the Laplace operator, and the TE boundary condition, using 4 sapling point.

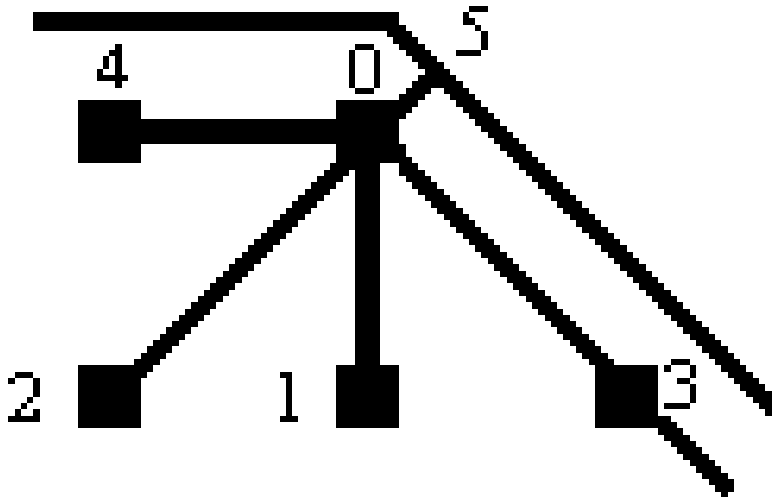


Fig. 5.1.4. Boundary Point of trapezoidal ridge

For a boundary point as in Fig. 5.3, the coefficients are given, assuming  $\Delta x_i = \Delta y_i$ , by the linear system (and its solution)

$$5.1.7.) \quad \begin{cases} -A_1 + A_2 - 2A_3 + 2A_4 = 0 \\ A_1 + A_3 + A_4 = \frac{2}{\Delta x^2} \\ A_2 + A_3 + A_4 = \frac{2}{\Delta x^2} \\ -A_3 - A_4 = 0 \end{cases}$$

where

$$5.1.8.) \quad \begin{cases} A_1 = \frac{2}{\Delta x^2} \\ A_2 = \frac{2}{\Delta x^2} \\ A_3 = 0 \\ A_4 = 0 \end{cases}$$

The corresponding FD approximation of the Laplace operator is therefore

$$5.1.9.) \quad (\phi_1 + \phi_2) \frac{2}{\Delta x^2} - \phi_0 \frac{4}{\Delta x^2} = \frac{\partial^2 \phi}{\partial x^2} + \frac{\partial^2 \phi}{\partial y^2}$$

In the same way, for a boundary point as in Fig. 5.1.4, i.e., a point in the concave vertex of the boundary, we get:

$$5.1.10.) \quad (\phi_1 + \phi_4) \frac{1}{\Delta x^2} + (\phi_2 + \phi_3) \frac{1}{2\Delta x^2} - \phi_0 \frac{3}{\Delta x^2} = \frac{\partial^2 \phi}{\partial x^2} + \frac{\partial^2 \phi}{\partial y^2}$$

The proposed scheme could be used on the whole WG section, but usually it is needed only close to the boundaries, where the actual geometry cannot match the rectangular standard grid.

Eqs. (3.2.9),(3.2.10),(5.1.9),5.1.10) are used to fill the matrix equivalent of the Laplace operator, so that the continuous eigenvalue problem (3.2.1) is replaced by a matrix one.

## **5.2) ROUNDED-END WAVEGUIDE**

In this paragraph we present a FD technique for the computation of modes and eigenvalues of a waveguide whose boundary consists of segments and arcs, taking exactly into account the curved boundary of the waveguide and therefore with no loss of accuracy. Among those waveguides, rounded-end waveguides (Fig.5.2.1) are the most interesting and therefore will be considered here.

The border of the structure border is not coincide with the coordinate curves of any know framework, so a different approach is needed. From the edge structure, it follows that a polar grid is the better choice on the rounded part, and a Cartesian one on the horizontal parts. So we divide the whole section into three parts, as in Fig.5.2.1. In the external ones we use a polar framework, while in the central one we can use the standard Cartesian framework. The proposed approach is to use a polar grid for the curved region and a rectangular grid for the straight ones.

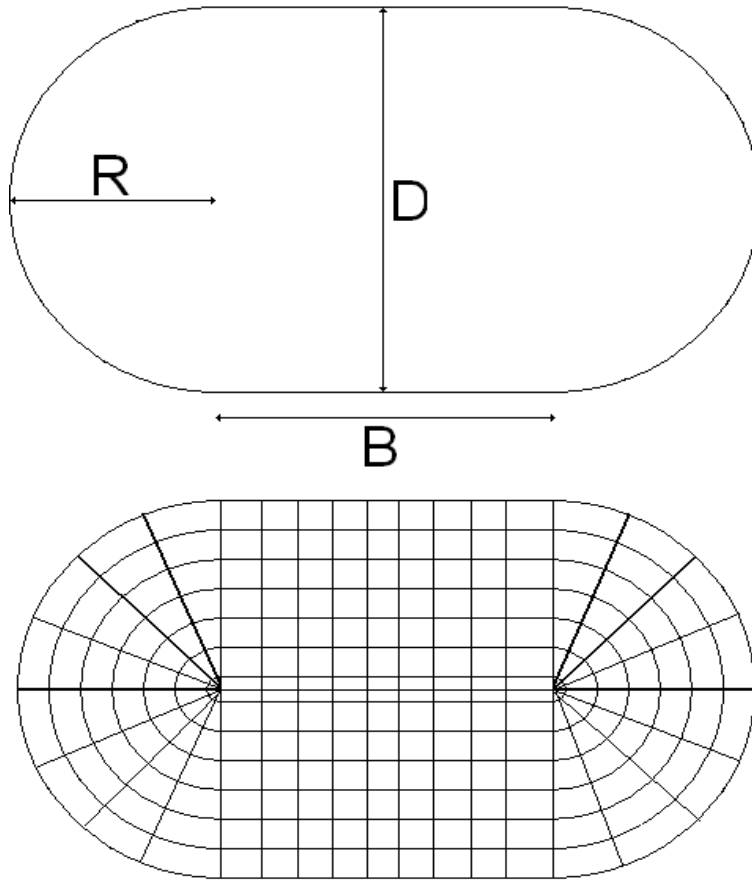


Fig. 5.2.1 A mixed mesh (cartesian-polar) of non standard waveguide and its dimension

In cartesian framework we assume a regular spacing on the coordinate lines, with steps  $\Delta x, \Delta y$ .

For each internal points we can use the standard expression of the Laplacian (3.2.8) and the discretized form (3.2.9). Equation (3.2.9) cannot be used for boundary points, where BC (3.2.2), (3.2.3) must be enforced. For a boundary point, using 3 nearby points, A, B, C, in Fig.3.2.4a, we can use the expression (3.2.10).

In the polar regions we use the expressions (4.1.7) and (4.1.18), so it remains to analyze the border between the polar and the cartesian regions, Fig.5.2.2. Since the grid geometry here is not a regular one, a new approximation of the laplacian

operator must be used, tailored to the geometry at hand. For this points we use the expressions (5.1.2), (5.1.3), (5.1.4), (5.1.5), (5.1.6).

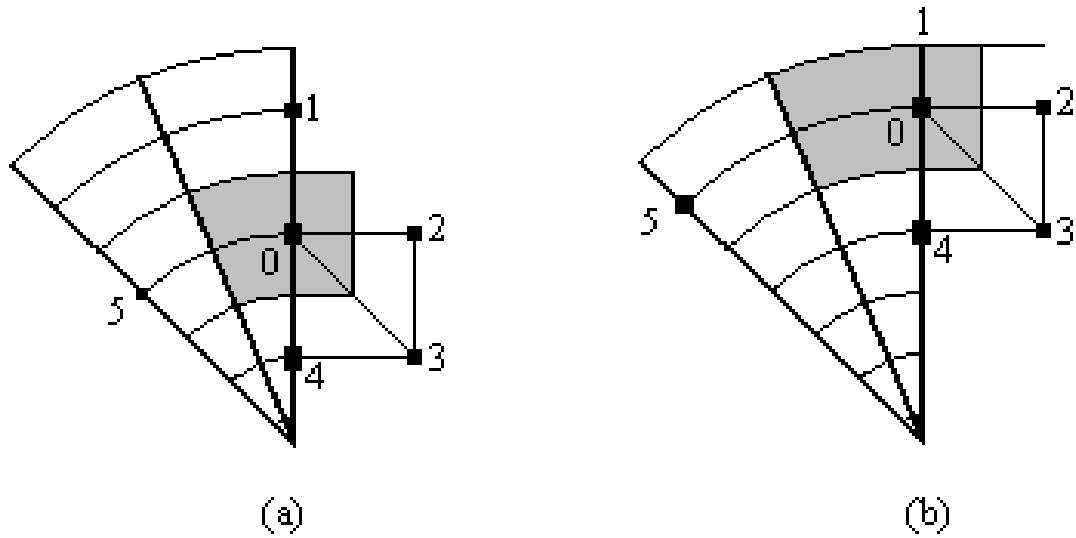


Fig. 5.2.2. (a) Point between Polar and Cartesian framework (b) Boundary point between Polar and Cartesian framework

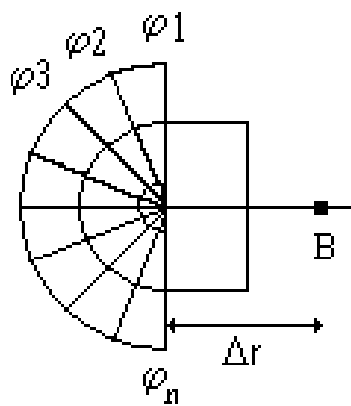


Fig. 5.2.3. Center Point between Polar and Cartesian framework

For the center of the circle, see Fig.5.2.3, we still use (4.1.5) to get:

$$5.1.11.) \quad \left( \frac{8}{\pi \Delta r^2} \right) \cdot \sum_{q=1}^N \frac{(\phi_q - \phi_P)}{\Delta r} \cdot \frac{\Delta r}{2} \cdot \Delta \vartheta + \left( \frac{2}{\Delta r^2} \right) \cdot \left( \frac{(\phi_1 + \phi_N)}{2} + \phi_B - \phi_P \right) = -k_t^2 \phi_P$$

## Chapter VI

### NUMERICAL RESULTS

#### INTRODUCTION

In this chapter we report and discuss the numerical results about the procedures and structures, discussed in the chapter III, IV and V

#### 6.1) FD IN SQUARE AND RECTANGULAR WAVEGUIDE

In this paragraph we will show the results of techniques presented in the paragraph 3.3. It is easy to see that  $k_t^2$  is the eigenvalue of an highly sparse matrix, since, for each row of it, no more than 5 elements can be different from zero. Therefore, very effective routines can be used to compute the smallest eigenvalues (the only ones of interest) and the corresponding eigenvectors, i.e., the field distribution of the modes inside the waveguide. To assess the proposed technique we will analyze both square and rectangular waveguide and compare the eigenvalues of the first few TE and TM modes with their exact values.

In the table 6.1.1 you can see the  $k_t$  of TE and TM modes calculated on the TE grids. Data of the square waveguide:

$a=10, b=10 \quad \Delta x=\Delta y=0.1$

$k_{ta}=k_t$  analytical

$k_{tp}=k_t$  of the program

ep= percentage (relative) error

Total points of the grid: 10000

In the table 6.1.2 you can see the  $k_t$  of TE and TM modes calculated on the TM grids. Data of the square waveguide:



a=10, b=10  $\Delta x=\Delta y=0.1$

kta=kt analytical ktp=kt of the program

ep= percentage (relative) error ; Total points of the grid: 9801

Table 6.1.1: comparison between our FD code and analytic results for TE and TM modes on TE grid in a square waveguide

| TE MODES | kta(TE)  | ktp(TE)  | ep(TE)% |
|----------|----------|----------|---------|
| 01       | 0,314159 | 0,314146 | 0,0041  |
| 10       | 0,314159 | 0,314146 | 0,0041  |
| 11       | 0,444288 | 0,444270 | 0,0041  |
| 02       | 0,628319 | 0,628215 | 0,0164  |
| 20       | 0,628319 | 0,628215 | 0,0164  |
| 12       | 0,702482 | 0,702383 | 0,0140  |
| 21       | 0,702482 | 0,702383 | 0,0140  |
| 22       | 0,888577 | 0,888430 | 0,0164  |
| 03       | 0,942478 | 0,942129 | 0,0370  |
| 30       | 0,942478 | 0,942129 | 0,0370  |
| 13       | 0,993459 | 0,993124 | 0,0337  |
| 31       | 0,993459 | 0,993124 | 0,0337  |
| 23       | 1,132717 | 1,132370 | 0,0307  |
| 32       | 1,132717 | 1,132370 | 0,0307  |
| 04       | 1,256637 | 1,255810 | 0,0658  |
| 40       | 1,256637 | 1,255810 | 0,0658  |
| 14       | 1,295312 | 1,294507 | 0,0622  |
| 41       | 1,295312 | 1,294507 | 0,0622  |
| 33       | 1,332865 | 1,332372 | 0,0370  |
| 24       | 1,404963 | 1,404177 | 0,0559  |
| 42       | 1,404963 | 1,404177 | 0,0559  |
| 05       | 1,570796 | 1,569182 | 0,1028  |
| 50       | 1,570796 | 1,569182 | 0,1028  |
| 34       | 1,570796 | 1,569926 | 0,0554  |
| 43       | 1,570796 | 1,569926 | 0,0554  |
| 15       | 1,601904 | 1,600319 | 0,0990  |
| 51       | 1,601904 | 1,600319 | 0,0990  |
| 25       | 1,691799 | 1,690262 | 0,0909  |
| 52       | 1,691799 | 1,690262 | 0,0909  |
| 44       | 1,777153 | 1,775984 | 0,0658  |

| TM MODES | kta(TM)  | ktp(TM)  | ep(TM)% |
|----------|----------|----------|---------|
| 11       | 0,444288 | 0,444271 | 0,0040  |
| 12       | 0,702482 | 0,702386 | 0,0136  |
| 21       | 0,702482 | 0,702386 | 0,0136  |
| 22       | 0,888577 | 0,888435 | 0,0160  |
| 13       | 0,993459 | 0,993134 | 0,0327  |
| 31       | 0,993459 | 0,993134 | 0,0327  |
| 23       | 1,132717 | 1,132380 | 0,0298  |
| 32       | 1,132717 | 1,132380 | 0,0298  |
| 14       | 1,295312 | 1,294531 | 0,0603  |
| 41       | 1,295312 | 1,294531 | 0,0603  |
| 33       | 1,332865 | 1,332386 | 0,0359  |
| 24       | 1,404963 | 1,404201 | 0,0542  |
| 42       | 1,404963 | 1,404201 | 0,0542  |
| 34       | 1,570796 | 1,569952 | 0,0538  |
| 43       | 1,570796 | 1,569952 | 0,0538  |
| 15       | 1,601904 | 1,600366 | 0,0960  |
| 51       | 1,601904 | 1,600366 | 0,0960  |
| 25       | 1,691799 | 1,690308 | 0,0882  |
| 52       | 1,691799 | 1,690308 | 0,0882  |
| 44       | 1,777153 | 1,776019 | 0,0638  |
| 35       | 1,831848 | 1,830331 | 0,0828  |
| 53       | 1,831848 | 1,830331 | 0,0828  |
| 16       | 1,910956 | 1,908285 | 0,1398  |
| 61       | 1,910956 | 1,908285 | 0,1398  |
| 26       | 1,986918 | 1,984319 | 0,1308  |
| 62       | 1,986918 | 1,984319 | 0,1308  |
| 45       | 2,011601 | 2,009877 | 0,0857  |
| 54       | 2,011601 | 2,009877 | 0,0857  |
| 36       | 2,107444 | 2,104873 | 0,1220  |
| 63       | 2,107444 | 2,104873 | 0,1220  |

Table 6.1.2: comparison between our FD code and analytic results for TE and TM modes on TM grid in a square waveguide

| TE MODES | k <sub>ta</sub> (TE) | k <sub>tp</sub> (TE) | ep(TE)% |
|----------|----------------------|----------------------|---------|
| 01       | 0,314159             | 0,314145             | 0,0046  |
| 10       | 0,314159             | 0,314145             | 0,0046  |
| 11       | 0,444288             | 0,444268             | 0,0046  |
| 02       | 0,628319             | 0,628203             | 0,0184  |
| 20       | 0,628319             | 0,628203             | 0,0184  |
| 12       | 0,702482             | 0,702372             | 0,0157  |
| 21       | 0,702482             | 0,702372             | 0,0157  |
| 22       | 0,888577             | 0,888413             | 0,0184  |
| 03       | 0,942478             | 0,942088             | 0,0414  |
| 30       | 0,942478             | 0,942088             | 0,0414  |
| 13       | 0,993459             | 0,993084             | 0,0377  |
| 31       | 0,993459             | 0,993084             | 0,0377  |
| 23       | 1,132717             | 1,132328             | 0,0343  |
| 32       | 1,132717             | 1,132328             | 0,0343  |
| 04       | 1,256637             | 1,255713             | 0,0736  |
| 40       | 1,256637             | 1,255713             | 0,0736  |
| 14       | 1,295312             | 1,294412             | 0,0695  |
| 41       | 1,295312             | 1,294412             | 0,0695  |
| 33       | 1,332865             | 1,332313             | 0,0414  |
| 24       | 1,404963             | 1,404084             | 0,0625  |
| 42       | 1,404963             | 1,404084             | 0,0625  |
| 05       | 1,570796             | 1,568993             | 0,1148  |
| 50       | 1,570796             | 1,568993             | 0,1148  |
| 34       | 1,570796             | 1,569823             | 0,0620  |
| 43       | 1,570796             | 1,569823             | 0,0620  |
| 15       | 1,601904             | 1,600133             | 0,1106  |
| 51       | 1,601904             | 1,600133             | 0,1106  |
| 25       | 1,691799             | 1,690082             | 0,1015  |
| 52       | 1,691799             | 1,690082             | 0,1015  |
| 44       | 1,777153             | 1,775846             | 0,0736  |

| TM MODES | k <sub>ta</sub> (TM) | k <sub>tp</sub> (TM) | ep(TM)% |
|----------|----------------------|----------------------|---------|
| 11       | 0,444288             | 0,444270             | 0,0041  |
| 12       | 0,702482             | 0,702383             | 0,0140  |
| 21       | 0,702482             | 0,702383             | 0,0140  |
| 22       | 0,888577             | 0,888430             | 0,0164  |
| 13       | 0,993459             | 0,993124             | 0,0337  |
| 31       | 0,993459             | 0,993124             | 0,0337  |
| 23       | 1,132717             | 1,132370             | 0,0307  |
| 32       | 1,132717             | 1,132370             | 0,0307  |
| 14       | 1,295312             | 1,294507             | 0,0622  |
| 41       | 1,295312             | 1,294507             | 0,0622  |
| 33       | 1,332865             | 1,332372             | 0,0370  |
| 24       | 1,404963             | 1,404177             | 0,0559  |
| 42       | 1,404963             | 1,404177             | 0,0559  |
| 34       | 1,570796             | 1,569926             | 0,0554  |
| 43       | 1,570796             | 1,569926             | 0,0554  |
| 15       | 1,601904             | 1,600319             | 0,0990  |
| 51       | 1,601904             | 1,600319             | 0,0990  |
| 25       | 1,691799             | 1,690262             | 0,0909  |
| 52       | 1,691799             | 1,690262             | 0,0909  |
| 44       | 1,777153             | 1,775984             | 0,0658  |
| 35       | 1,831848             | 1,830284             | 0,0854  |
| 53       | 1,831848             | 1,830284             | 0,0854  |
| 16       | 1,910956             | 1,908203             | 0,1441  |
| 61       | 1,910956             | 1,908203             | 0,1441  |
| 26       | 1,986918             | 1,984239             | 0,1348  |
| 62       | 1,986918             | 1,984239             | 0,1348  |
| 45       | 2,011601             | 2,009824             | 0,0883  |
| 54       | 2,011601             | 2,009824             | 0,0883  |
| 36       | 2,107444             | 2,104794             | 0,1258  |
| 63       | 2,107444             | 2,104794             | 0,1258  |

In the table 6.1.3 you can see the  $k_t$  of TE and TM modes calculated on the TE grids. Data of the rectangular waveguide:

$$a=10, b=5 \quad \Delta x=\Delta y=0.1$$

$k_{ta}=k_t$  analytical

$k_{tp}=k_t$  of the program

ep= percentage (relative) error

Total points of the grid: 5000

In the table 6.1.4 you can see the  $k_t$  of TE and TM modes calculated on the TM grids. Data of the square waveguide:

$$a=10, b=5 \quad \Delta x=\Delta y=0.1$$

$k_{ta}=k_t$  analytical

$k_{tp}=k_t$  of the program

ep= percentage (relative) error

Total points of the grid: 4851

In the table 6.1.5 you can see the  $k_t$  of TE and TM modes calculated on the TE grids. Data of the square waveguide:

$$a=2 \quad b=10 \quad \Delta x=\Delta y=0.1$$

$k_{ta}=k_t$  analytical

$k_{tp}=k_t$  of the program

ep= percentage (relative) error

Total points of the grid: 2000

In the table 6.1.6 you can see the  $k_t$  of TE and TM modes calculated on the TE grids. Data of the square waveguide:

$$a=2 \quad b=10 \quad \Delta x=\Delta y=0.1$$

$k_{ta}=k_t$  analytical

$k_{tp}=k_t$  of the program

ep= percentage (relative) error      Total points of the grid: 1881

Table 6.1.3: comparison between our FD code and analytic results for TE and TM modes on TE grid in a rectangular waveguide

| TE MODES | kta(TE)  | ktp(TE)  | ep(TE)% |
|----------|----------|----------|---------|
| 10       | 0,314159 | 0,314146 | 0,0041  |
| 01       | 0,628319 | 0,628215 | 0,0164  |
| 20       | 0,628319 | 0,628215 | 0,0164  |
| 11       | 0,702482 | 0,702383 | 0,0140  |
| 21       | 0,888577 | 0,888430 | 0,0164  |
| 30       | 0,942478 | 0,942129 | 0,0370  |
| 31       | 1,132717 | 1,132370 | 0,0307  |
| 02       | 1,256637 | 1,255810 | 0,0658  |
| 40       | 1,256637 | 1,255810 | 0,0658  |
| 12       | 1,295312 | 1,294507 | 0,0622  |
| 22       | 1,404963 | 1,404177 | 0,0559  |
| 41       | 1,404963 | 1,404177 | 0,0559  |
| 50       | 1,570796 | 1,569182 | 0,1028  |
| 32       | 1,570796 | 1,569926 | 0,0554  |
| 51       | 1,691799 | 1,690262 | 0,0909  |
| 42       | 1,777153 | 1,775984 | 0,0658  |
| 03       | 1,884956 | 1,882166 | 0,1480  |
| 60       | 1,884956 | 1,882166 | 0,1480  |
| 13       | 1,910956 | 1,908203 | 0,1441  |
| 23       | 1,986918 | 1,984239 | 0,1348  |
| 61       | 1,986918 | 1,984239 | 0,1348  |
| 52       | 2,011601 | 2,009824 | 0,0883  |
| 33       | 2,107444 | 2,104794 | 0,1258  |
| 70       | 2,199115 | 2,194686 | 0,2014  |
| 43       | 2,265435 | 2,262655 | 0,1227  |
| 62       | 2,265435 | 2,262655 | 0,1227  |
| 71       | 2,287114 | 2,282828 | 0,1874  |
| 53       | 2,453662 | 2,450486 | 0,1295  |
| 04       | 2,513274 | 2,506665 | 0,2630  |
| 80       | 2,513274 | 2,506665 | 0,2630  |

| TM MODES | kta(TM)  | ktp(TM)  | ep(TM)% |
|----------|----------|----------|---------|
| 11       | 0,702482 | 0,702389 | 0,0132  |
| 21       | 0,888577 | 0,888437 | 0,0157  |
| 31       | 1,132717 | 1,132382 | 0,0296  |
| 12       | 1,295312 | 1,294555 | 0,0584  |
| 22       | 1,404963 | 1,404202 | 0,0541  |
| 41       | 1,404963 | 1,404223 | 0,0527  |
| 32       | 1,570796 | 1,569972 | 0,0525  |
| 51       | 1,691799 | 1,690309 | 0,0881  |
| 42       | 1,777153 | 1,776037 | 0,0628  |
| 13       | 1,910956 | 1,908367 | 0,1355  |
| 23       | 1,986918 | 1,984320 | 0,1308  |
| 61       | 1,986918 | 1,984397 | 0,1268  |
| 52       | 2,011601 | 2,009892 | 0,0849  |
| 33       | 2,107444 | 2,104947 | 0,1185  |
| 43       | 2,265435 | 2,262752 | 0,1184  |
| 62       | 2,265435 | 2,262807 | 0,1160  |
| 71       | 2,287114 | 2,282956 | 0,1818  |
| 53       | 2,453662 | 2,450644 | 0,1230  |
| 14       | 2,532833 | 2,526661 | 0,2437  |
| 72       | 2,532833 | 2,528717 | 0,1625  |
| 24       | 2,590624 | 2,584378 | 0,2411  |
| 81       | 2,590624 | 2,584567 | 0,2338  |
| 63       | 2,665730 | 2,661961 | 0,1414  |
| 34       | 2,684178 | 2,678237 | 0,2213  |
| 44       | 2,809926 | 2,803842 | 0,2165  |
| 82       | 2,809926 | 2,804006 | 0,2107  |
| 73       | 2,896405 | 2,887471 | 0,3085  |
| 91       | 2,896405 | 2,891435 | 0,1716  |
| 54       | 2,963773 | 2,957670 | 0,2059  |
| 92       | 3,094110 | 3,085451 | 0,2798  |

Table 6.1.4: comparison between our FD code and analytic results for TE and TM modes on TM grid in a rectangular waveguide.

| TE MODES | kta(TE)  | ktp(TE)  | ep(TE)% | TM MODES | kta(TM)  | ktp(TM)  | ep(TM)% |
|----------|----------|----------|---------|----------|----------|----------|---------|
| 10       | 0,314159 | 0,314145 | 0,0046  | 11       | 0,702482 | 0,702383 | 0,0140  |
| 01       | 0,628319 | 0,628190 | 0,0204  | 21       | 0,888577 | 0,888430 | 0,0164  |
| 20       | 0,628319 | 0,628203 | 0,0184  | 31       | 1,132717 | 1,132370 | 0,0307  |
| 11       | 0,702482 | 0,702360 | 0,0172  | 12       | 1,295312 | 1,294507 | 0,0622  |
| 21       | 0,888577 | 0,888404 | 0,0194  | 22       | 1,404963 | 1,404177 | 0,0559  |
| 30       | 0,942478 | 0,942088 | 0,0414  | 41       | 1,404963 | 1,404177 | 0,0559  |
| 31       | 1,132717 | 1,132322 | 0,0349  | 32       | 1,570796 | 1,569926 | 0,0554  |
| 02       | 1,256637 | 1,255615 | 0,0813  | 51       | 1,691799 | 1,690262 | 0,0909  |
| 40       | 1,256637 | 1,255713 | 0,0736  | 42       | 1,777153 | 1,775984 | 0,0658  |
| 12       | 1,295312 | 1,294317 | 0,0768  | 13       | 1,910956 | 1,908203 | 0,1441  |
| 22       | 1,404963 | 1,403997 | 0,0687  | 23       | 1,986918 | 1,984239 | 0,1348  |
| 41       | 1,404963 | 1,404079 | 0,0629  | 61       | 1,986918 | 1,984239 | 0,1348  |
| 50       | 1,570796 | 1,568993 | 0,1148  | 52       | 2,011601 | 2,009824 | 0,0883  |
| 32       | 1,570796 | 1,569745 | 0,0670  | 33       | 2,107444 | 2,104794 | 0,1258  |
| 51       | 1,691799 | 1,690077 | 0,1018  | 43       | 2,265435 | 2,262655 | 0,1227  |
| 42       | 1,777153 | 1,775777 | 0,0774  | 62       | 2,265435 | 2,262655 | 0,1227  |
| 03       | 1,884956 | 1,881520 | 0,1823  | 71       | 2,287114 | 2,282828 | 0,1874  |
| 60       | 1,884956 | 1,881843 | 0,1651  | 53       | 2,453662 | 2,450486 | 0,1295  |
| 13       | 1,910956 | 1,907565 | 0,1775  | 14       | 2,532833 | 2,526273 | 0,2590  |
| 23       | 1,986918 | 1,983622 | 0,1659  | 72       | 2,532833 | 2,528578 | 0,1680  |
| 61       | 1,986918 | 1,983924 | 0,1506  | 24       | 2,590624 | 2,584187 | 0,2485  |
| 52       | 2,011601 | 2,009554 | 0,1017  | 81       | 2,590624 | 2,584187 | 0,2485  |
| 33       | 2,107444 | 2,104197 | 0,1541  | 63       | 2,665730 | 2,661785 | 0,1480  |
| 70       | 2,199115 | 2,194179 | 0,2244  | 34       | 2,684178 | 2,677868 | 0,2351  |
| 43       | 2,265435 | 2,262064 | 0,1488  | 44       | 2,809926 | 2,803645 | 0,2235  |
| 62       | 2,265435 | 2,262278 | 0,1393  | 82       | 2,809926 | 2,803645 | 0,2235  |
| 71       | 2,287114 | 2,282334 | 0,2090  | 73       | 2,896405 | 2,887199 | 0,3179  |
| 53       | 2,453662 | 2,449869 | 0,1546  | 91       | 2,896405 | 2,891228 | 0,1788  |
| 04       | 2,513274 | 2,505176 | 0,3222  | 54       | 2,963773 | 2,957313 | 0,2180  |
| 80       | 2,513274 | 2,505920 | 0,2926  | 92       | 3,094110 | 3,085178 | 0,2887  |

Table 6.1.5: comparison between our FD code and analytic results for TE and TM modes on TE grid in a rectangular waveguide

| TE MODES | k <sub>ta</sub> (TE) | k <sub>tp</sub> (TE) | ep(TE)% |
|----------|----------------------|----------------------|---------|
| 0 1      | 0,314159             | 0,314146             | 0,0041  |
| 0 2      | 0,628319             | 0,628215             | 0,0164  |
| 0 3      | 0,942478             | 0,942129             | 0,0370  |
| 0 4      | 1,256637             | 1,255810             | 0,0658  |
| 0 5      | 1,570796             | 1,569182             | 0,1028  |
| 1 0      | 1,570796             | 1,569182             | 0,1028  |
| 1 1      | 1,601904             | 1,600319             | 0,0990  |
| 1 2      | 1,691799             | 1,690262             | 0,0909  |
| 1 3      | 1,831848             | 1,830284             | 0,0854  |
| 0 6      | 1,884956             | 1,882166             | 0,1480  |
| 1 4      | 2,011601             | 2,009824             | 0,0883  |
| 0 7      | 2,199115             | 2,194686             | 0,2014  |
| 1 5      | 2,221442             | 2,219158             | 0,1028  |
| 1 6      | 2,453662             | 2,450486             | 0,1295  |
| 0 8      | 2,513274             | 2,506665             | 0,2630  |
| 1 7      | 2,702500             | 2,697958             | 0,1681  |
| 0 9      | 2,827433             | 2,818025             | 0,3328  |
| 1 8      | 2,963773             | 2,957313             | 0,2180  |
| 010      | 3,141593             | 3,128689             | 0,4107  |
| 2 0      | 3,141593             | 3,128689             | 0,4107  |
| 2 1      | 3,157262             | 3,144421             | 0,4067  |
| 2 2      | 3,203808             | 3,191136             | 0,3955  |
| 1 9      | 3,234468             | 3,225460             | 0,2785  |
| 2 3      | 3,279919             | 3,267461             | 0,3798  |
| 2 4      | 3,383599             | 3,371314             | 0,3631  |
| 011      | 3,455752             | 3,438582             | 0,4968  |
| 110      | 3,512407             | 3,500147             | 0,3491  |
| 2 5      | 3,512407             | 3,500147             | 0,3491  |
| 2 6      | 3,663695             | 3,651198             | 0,3411  |
| 012      | 3,769911             | 3,747626             | 0,5911  |

| TM MODES | k <sub>ta</sub> (TM) | k <sub>tp</sub> (TM) | ep(TM)% |
|----------|----------------------|----------------------|---------|
| 1 1      | 1,601904             | 1,600555             | 0,0842  |
| 1 2      | 1,691799             | 1,690487             | 0,0776  |
| 1 3      | 1,831848             | 1,830496             | 0,0738  |
| 1 4      | 2,011601             | 2,010027             | 0,0782  |
| 1 5      | 2,221442             | 2,219363             | 0,0936  |
| 1 6      | 2,453662             | 2,450704             | 0,1206  |
| 1 7      | 2,702500             | 2,698205             | 0,1589  |
| 1 8      | 2,963773             | 2,957606             | 0,2081  |
| 2 1      | 3,157262             | 3,146306             | 0,3470  |
| 2 2      | 3,203808             | 3,192994             | 0,3375  |
| 1 9      | 3,234468             | 3,225820             | 0,2674  |
| 2 3      | 3,279919             | 3,269278             | 0,3244  |
| 2 4      | 3,383599             | 3,373081             | 0,3108  |
| 110      | 3,512407             | 3,500593             | 0,3364  |
| 2 5      | 3,512407             | 3,501862             | 0,3002  |
| 2 6      | 3,663695             | 3,652864             | 0,2956  |
| 111      | 3,796001             | 3,780262             | 0,4146  |
| 2 7      | 3,834803             | 3,823320             | 0,2994  |
| 2 8      | 4,023202             | 4,010599             | 0,3133  |
| 112      | 4,084070             | 4,063575             | 0,5018  |
| 2 9      | 4,226581             | 4,212289             | 0,3381  |
| 113      | 4,375732             | 4,349574             | 0,5978  |
| 210      | 4,442883             | 4,426242             | 0,3746  |
| 114      | 4,670313             | 4,637514             | 0,7023  |
| 211      | 4,670313             | 4,650575             | 0,4226  |
| 3 1      | 4,722849             | 4,685667             | 0,7873  |
| 3 2      | 4,754092             | 4,717144             | 0,7772  |
| 3 3      | 4,805713             | 4,769110             | 0,7616  |
| 3 4      | 4,877063             | 4,840858             | 0,7424  |
| 212      | 4,907325             | 4,883657             | 0,4823  |

Table 6.1.6: comparison between our FD code and analytic results for TE and TM modes on TM grid in a rectangular waveguide

| TE MODES | k <sub>ta</sub> (TE) | k <sub>tp</sub> (TE) | ep(TE)% |
|----------|----------------------|----------------------|---------|
| 01       | 0,314159             | 0,314145             | 0,0046  |
| 02       | 0,628319             | 0,628203             | 0,0184  |
| 03       | 0,942478             | 0,942088             | 0,0414  |
| 04       | 1,256637             | 1,255713             | 0,0736  |
| 05       | 1,570796             | 1,568238             | 0,1629  |
| 10       | 1,570796             | 1,568993             | 0,1148  |
| 11       | 1,601904             | 1,599392             | 0,1568  |
| 12       | 1,691799             | 1,689381             | 0,1430  |
| 13       | 1,831848             | 1,829453             | 0,1307  |
| 06       | 1,884956             | 1,881843             | 0,1651  |
| 14       | 2,011601             | 2,009025             | 0,1280  |
| 07       | 2,199115             | 2,194179             | 0,2244  |
| 15       | 2,221442             | 2,218357             | 0,1389  |
| 16       | 2,453662             | 2,449633             | 0,1642  |
| 08       | 2,513274             | 2,505920             | 0,2926  |
| 17       | 2,702500             | 2,696997             | 0,2036  |
| 09       | 2,827433             | 2,816982             | 0,3696  |
| 18       | 2,963773             | 2,956180             | 0,2562  |
| 0 10     | 3,141593             | 3,121714             | 0,6328  |
| 20       | 3,141593             | 3,127287             | 0,4554  |
| 21       | 3,157262             | 3,137480             | 0,6265  |
| 22       | 3,203808             | 3,184295             | 0,6091  |
| 19       | 3,234468             | 3,224090             | 0,3208  |
| 23       | 3,279919             | 3,260771             | 0,5838  |
| 24       | 3,383599             | 3,364805             | 0,5554  |
| 0 11     | 3,455752             | 3,436757             | 0,5497  |
| 11 0     | 3,512407             | 3,493828             | 0,5290  |
| 25       | 3,512407             | 3,498470             | 0,3968  |
| 26       | 3,663695             | 3,645056             | 0,5088  |
| 0 12     | 3,769911             | 3,745314             | 0,6524  |

| TM MODES | k <sub>ta</sub> (TM) | k <sub>tp</sub> (TM) | ep(TM)% |
|----------|----------------------|----------------------|---------|
| 11       | 1,601904             | 1,600319             | 0,0990  |
| 12       | 1,691799             | 1,690262             | 0,0909  |
| 13       | 1,831848             | 1,830284             | 0,0854  |
| 14       | 2,011601             | 2,009824             | 0,0883  |
| 15       | 2,221442             | 2,219158             | 0,1028  |
| 16       | 2,453662             | 2,450486             | 0,1295  |
| 17       | 2,702500             | 2,697958             | 0,1681  |
| 18       | 2,963773             | 2,957313             | 0,2180  |
| 21       | 3,157262             | 3,144421             | 0,4067  |
| 22       | 3,203808             | 3,191136             | 0,3955  |
| 19       | 3,234468             | 3,225460             | 0,2785  |
| 23       | 3,279919             | 3,267461             | 0,3798  |
| 24       | 3,383599             | 3,371314             | 0,3631  |
| 110      | 3,512407             | 3,500147             | 0,3491  |
| 25       | 3,512407             | 3,500147             | 0,3491  |
| 26       | 3,663695             | 3,651198             | 0,3411  |
| 111      | 3,796001             | 3,779706             | 0,4293  |
| 27       | 3,834803             | 3,821694             | 0,3418  |
| 28       | 4,023202             | 4,008998             | 0,3530  |
| 112      | 4,084070             | 4,062885             | 0,5187  |
| 29       | 4,226581             | 4,210696             | 0,3758  |
| 1 13     | 4,375732             | 4,348725             | 0,6172  |
| 2 10     | 4,442883             | 4,424635             | 0,4107  |
| 1 14     | 4,670313             | 4,636477             | 0,7245  |
| 2 11     | 4,670313             | 4,648929             | 0,4579  |
| 31       | 4,722849             | 4,679464             | 0,9186  |
| 32       | 4,754092             | 4,710982             | 0,9068  |
| 33       | 4,805713             | 4,763014             | 0,8885  |
| 34       | 4,877063             | 4,834848             | 0,8656  |
| 2 12     | 4,907325             | 4,881946             | 0,5172  |

In the tables 6.1.7,6.1.8 you can see the  $k_t$  of TE and TM modes calculated on the TE grids where varying  $\Delta x = \Delta y$ . Data of the square waveguide:

$a=10, b=5$

$k_{ta}=k_t$  analytical

$k_{tp}=k_t$  of the program

$ep$ = percentage (relative) error

In the tables 6.1.9,6.1.10 you can see the  $k_t$  of TE and TM modes calculated on the TM grids where varying  $\Delta x = \Delta y$ . Data of the square waveguide:

$a=10, b=5$

$k_{ta}=k_t$  analytical

$k_{tp}=k_t$  of the program

$ep$ = percentage (relative) error

In the tables 6.1.11,6.1.12 you can see the  $k_t$  of TE and TM modes calculated on the TM grids where varying  $\Delta x \neq \Delta y$ . Data of the square waveguide:

$a=10, b=5$

$k_{ta}=k_t$  analytical

$k_{tp}=k_t$  of the program

$ep$ = percentage (relative) error

In the tables 6.1.13,6.1.14 you can see the  $k_t$  of TE and TM modes calculated on the TM grids where varying  $\Delta x \neq \Delta y$ . Data of the square waveguide:

$a=10, b=5$

$k_{ta}=k_t$  analytical

$k_{tp}=k_t$  of the program

$ep$ = percentage (relative) error



Table 6.1.7: comparison between our FD code and analytic results for TE on TE grid in rectangular waveguide, when varying  $\Delta x = \Delta y$

|          |          | $\Delta y = \Delta x = 0,2$ |         | $\Delta y = \Delta x = 0,1$ |         | $\Delta y = \Delta x = 0,05$ |         |
|----------|----------|-----------------------------|---------|-----------------------------|---------|------------------------------|---------|
| TE MODES | kta(TE)  | ktp(TE)                     | ep(TE)% | ktp(TE)                     | ep(TE)% | ktp(TE)                      | ep(TE)% |
| 10       | 0,314159 | 0,314108                    | 0,0165  | 0,314146                    | 0,0041  | 0,314156                     | 0,0010  |
| 01       | 0,628319 | 0,627905                    | 0,0658  | 0,628215                    | 0,0164  | 0,628293                     | 0,0041  |
| 20       | 0,628319 | 0,627905                    | 0,0658  | 0,628215                    | 0,0164  | 0,628293                     | 0,0041  |
| 11       | 0,702482 | 0,702089                    | 0,0559  | 0,702383                    | 0,0140  | 0,702457                     | 0,0035  |
| 21       | 0,888577 | 0,887992                    | 0,0658  | 0,888430                    | 0,0164  | 0,888540                     | 0,0041  |
| 30       | 0,942478 | 0,941083                    | 0,1480  | 0,942129                    | 0,0370  | 0,942391                     | 0,0093  |
| 31       | 1,132717 | 1,131328                    | 0,1227  | 1,132370                    | 0,0307  | 1,132630                     | 0,0077  |
| 02       | 1,256637 | 1,253332                    | 0,2630  | 1,255810                    | 0,0658  | 1,256430                     | 0,0165  |
| 40       | 1,256637 | 1,253332                    | 0,2630  | 1,255810                    | 0,0658  | 1,256430                     | 0,0165  |
| 12       | 1,295312 | 1,292093                    | 0,2485  | 1,294507                    | 0,0622  | 1,295111                     | 0,0155  |
| 22       | 1,404963 | 1,401823                    | 0,2235  | 1,404177                    | 0,0559  | 1,404767                     | 0,0140  |
| 41       | 1,404963 | 1,401823                    | 0,2235  | 1,404177                    | 0,0559  | 1,404767                     | 0,0140  |
| 50       | 1,570796 | 1,564345                    | 0,4107  | 1,569182                    | 0,1028  | 1,570393                     | 0,0257  |
| 32       | 1,570796 | 1,567316                    | 0,2216  | 1,569926                    | 0,0554  | 1,570579                     | 0,0139  |
| 51       | 1,691799 | 1,685657                    | 0,3631  | 1,690262                    | 0,0909  | 1,691415                     | 0,0227  |
| 42       | 1,777153 | 1,772480                    | 0,2630  | 1,775984                    | 0,0658  | 1,776861                     | 0,0164  |
| 03       | 1,884956 | 1,873813                    | 0,5911  | 1,882166                    | 0,1480  | 1,884258                     | 0,0370  |
| 60       | 1,884956 | 1,873813                    | 0,5911  | 1,882166                    | 0,1480  | 1,884258                     | 0,0370  |
| 13       | 1,910956 | 1,899958                    | 0,5755  | 1,908203                    | 0,1441  | 1,910268                     | 0,0360  |
| 23       | 1,986918 | 1,976219                    | 0,5385  | 1,984239                    | 0,1348  | 1,986248                     | 0,0337  |
| 61       | 1,986918 | 1,976219                    | 0,5385  | 1,984239                    | 0,1348  | 1,986248                     | 0,0337  |
| 52       | 2,011601 | 2,004499                    | 0,3530  | 2,009824                    | 0,0883  | 2,011156                     | 0,0221  |
| 33       | 2,107444 | 2,096858                    | 0,5023  | 2,104794                    | 0,1258  | 2,106782                     | 0,0315  |
| 70       | 2,199115 | 2,181432                    | 0,8041  | 2,194686                    | 0,2014  | 2,198007                     | 0,0504  |
| 43       | 2,265435 | 2,254333                    | 0,4900  | 2,262655                    | 0,1227  | 2,264740                     | 0,0307  |
| 62       | 2,265435 | 2,254333                    | 0,4900  | 2,262655                    | 0,1227  | 2,264740                     | 0,0307  |
| 71       | 2,287114 | 2,270003                    | 0,7482  | 2,282828                    | 0,1874  | 2,286042                     | 0,0469  |
| 53       | 2,453662 | 2,440973                    | 0,5172  | 2,450486                    | 0,1295  | 2,452868                     | 0,0324  |
| 04       | 2,513274 | 2,486899                    | 1,0494  | 2,506665                    | 0,2630  | 2,511621                     | 0,0658  |
| 80       | 2,513274 | 2,486899                    | 1,0494  | 2,506665                    | 0,2630  | 2,511621                     | 0,0658  |

Table 6.1.8: comparison between our FD code and analytic results for TM on TE grid in rectangular waveguide, when varying  $\Delta x = \Delta y$ .

|          |          | $\Delta y = \Delta x = 0,2$ |         | $\Delta y = \Delta x = 0,1$ |         | $\Delta y = \Delta x = 0,05$ |         |
|----------|----------|-----------------------------|---------|-----------------------------|---------|------------------------------|---------|
| TM MODES | kta(TM)  | ktp(TM)                     | ep(TM)% | ktp(TM)                     | ep(TM)% | ktp(TM)                      | ep(TM)% |
| 11       | 0,702482 | 0,702134                    | 0,0494  | 0,702389                    | 0,0132  | 0,702458                     | 0,0034  |
| 21       | 0,888577 | 0,888044                    | 0,0599  | 0,888437                    | 0,0157  | 0,888541                     | 0,0040  |
| 31       | 1,132717 | 1,131424                    | 0,1142  | 1,132382                    | 0,0296  | 1,132632                     | 0,0075  |
| 12       | 1,295312 | 1,292474                    | 0,2191  | 1,294555                    | 0,0584  | 1,295117                     | 0,0151  |
| 22       | 1,404963 | 1,402020                    | 0,2095  | 1,404202                    | 0,0541  | 1,404770                     | 0,0138  |
| 41       | 1,404963 | 1,402183                    | 0,1978  | 1,404223                    | 0,0527  | 1,404772                     | 0,0136  |
| 32       | 1,570796 | 1,567679                    | 0,1985  | 1,569972                    | 0,0525  | 1,570584                     | 0,0135  |
| 51       | 1,691799 | 1,686027                    | 0,3412  | 1,690309                    | 0,0881  | 1,691421                     | 0,0224  |
| 42       | 1,777153 | 1,772894                    | 0,2396  | 1,776037                    | 0,0628  | 1,776867                     | 0,0161  |
| 13       | 1,910956 | 1,901236                    | 0,5086  | 1,908367                    | 0,1355  | 1,910288                     | 0,0350  |
| 23       | 1,986918 | 1,976848                    | 0,5068  | 1,984320                    | 0,1308  | 1,986258                     | 0,0332  |
| 61       | 1,986918 | 1,977455                    | 0,4762  | 1,984397                    | 0,1268  | 1,986268                     | 0,0327  |
| 52       | 2,011601 | 2,005039                    | 0,3262  | 2,009892                    | 0,0849  | 2,011165                     | 0,0217  |
| 33       | 2,107444 | 2,098053                    | 0,4456  | 2,104947                    | 0,1185  | 2,106801                     | 0,0305  |
| 43       | 2,265435 | 2,255088                    | 0,4567  | 2,262752                    | 0,1184  | 2,264752                     | 0,0301  |
| 62       | 2,265435 | 2,255519                    | 0,4377  | 2,262807                    | 0,1160  | 2,264759                     | 0,0298  |
| 71       | 2,287114 | 2,270992                    | 0,7049  | 2,282956                    | 0,1818  | 2,286058                     | 0,0462  |
| 53       | 2,453662 | 2,442210                    | 0,4667  | 2,450644                    | 0,1230  | 2,452888                     | 0,0316  |
| 14       | 2,532833 | 2,509628                    | 0,9162  | 2,526661                    | 0,2437  | 2,531241                     | 0,0629  |
| 72       | 2,532833 | 2,516923                    | 0,6282  | 2,528717                    | 0,1625  | 2,531786                     | 0,0413  |
| 24       | 2,590624 | 2,566404                    | 0,9349  | 2,584378                    | 0,2411  | 2,589038                     | 0,0612  |
| 81       | 2,590624 | 2,567852                    | 0,8790  | 2,584567                    | 0,2338  | 2,589061                     | 0,0603  |
| 63       | 2,665730 | 2,651346                    | 0,5396  | 2,661961                    | 0,1414  | 2,664765                     | 0,0362  |
| 34       | 2,684178 | 2,661834                    | 0,8324  | 2,678237                    | 0,2213  | 2,682646                     | 0,0571  |
| 44       | 2,809926 | 2,786382                    | 0,8379  | 2,803842                    | 0,2165  | 2,808380                     | 0,0550  |
| 82       | 2,809926 | 2,787634                    | 0,7933  | 2,804006                    | 0,2107  | 2,808400                     | 0,0543  |
| 73       | 2,896405 | 2,861752                    | 1,1964  | 2,887471                    | 0,3085  | 2,894136                     | 0,0783  |
| 91       | 2,896405 | 2,877345                    | 0,6581  | 2,891435                    | 0,1716  | 2,895137                     | 0,0438  |
| 54       | 2,963773 | 2,940736                    | 0,7773  | 2,957670                    | 0,2059  | 2,962202                     | 0,0530  |
| 92       | 3,094110 | 3,060575                    | 1,0838  | 3,085451                    | 0,2798  | 3,091910                     | 0,0711  |

Table 6.1.9: comparison between our FD code and analytic results for TE on TM grid in rectangular waveguide, when varying  $\Delta x = \Delta y$ .

|          |          | $\Delta y = \Delta x = 0,2$ |         | $\Delta y = \Delta x = 0,1$ |         | $\Delta y = \Delta x = 0,05$ |         |
|----------|----------|-----------------------------|---------|-----------------------------|---------|------------------------------|---------|
| TE MODES | kta(TE)  | ktp(TE)                     | ep(TE)% | ktp(TE)                     | ep(TE)% | ktp(TE)                      | ep(TE)% |
| 10       | 0,314159 | 0,314095                    | 0,0204  | 0,314145                    | 0,0046  | 0,314156                     | 0,0011  |
| 01       | 0,628319 | 0,627710                    | 0,0969  | 0,628190                    | 0,0204  | 0,628290                     | 0,0046  |
| 20       | 0,628319 | 0,627808                    | 0,0813  | 0,628203                    | 0,0184  | 0,628291                     | 0,0044  |
| 11       | 0,702482 | 0,701909                    | 0,0816  | 0,702360                    | 0,0172  | 0,702454                     | 0,0039  |
| 21       | 0,888577 | 0,887785                    | 0,0891  | 0,888404                    | 0,0194  | 0,888537                     | 0,0045  |
| 30       | 0,942478 | 0,940760                    | 0,1823  | 0,942088                    | 0,0414  | 0,942385                     | 0,0098  |
| 31       | 1,132717 | 1,130951                    | 0,1560  | 1,132322                    | 0,0349  | 1,132624                     | 0,0082  |
| 02       | 1,256637 | 1,251846                    | 0,3813  | 1,255615                    | 0,0813  | 1,256406                     | 0,0184  |
| 40       | 1,256637 | 1,252588                    | 0,3222  | 1,255713                    | 0,0736  | 1,256418                     | 0,0174  |
| 12       | 1,295312 | 1,290649                    | 0,3600  | 1,294317                    | 0,0768  | 1,295087                     | 0,0174  |
| 22       | 1,404963 | 1,400450                    | 0,3212  | 1,403997                    | 0,0687  | 1,404744                     | 0,0156  |
| 41       | 1,404963 | 1,401070                    | 0,2771  | 1,404079                    | 0,0629  | 1,404754                     | 0,0149  |
| 50       | 1,570796 | 1,562944                    | 0,4999  | 1,568993                    | 0,1148  | 1,570369                     | 0,0272  |
| 32       | 1,570796 | 1,565934                    | 0,3096  | 1,569745                    | 0,0670  | 1,570556                     | 0,0153  |
| 51       | 1,691799 | 1,684285                    | 0,4442  | 1,690077                    | 0,1018  | 1,691392                     | 0,0241  |
| 42       | 1,777153 | 1,770902                    | 0,3517  | 1,775777                    | 0,0774  | 1,776835                     | 0,0179  |
| 03       | 1,884956 | 1,869213                    | 0,8352  | 1,881520                    | 0,1823  | 1,884175                     | 0,0414  |
| 60       | 1,884956 | 1,871505                    | 0,7136  | 1,881843                    | 0,1651  | 1,884217                     | 0,0392  |
| 13       | 1,910956 | 1,895419                    | 0,8131  | 1,907565                    | 0,1775  | 1,910186                     | 0,0403  |
| 23       | 1,986918 | 1,971826                    | 0,7595  | 1,983622                    | 0,1659  | 1,986169                     | 0,0377  |
| 61       | 1,986918 | 1,973968                    | 0,6517  | 1,983924                    | 0,1506  | 1,986207                     | 0,0357  |
| 52       | 2,011601 | 2,002477                    | 0,4536  | 2,009554                    | 0,1017  | 2,011122                     | 0,0238  |
| 33       | 2,107444 | 2,092603                    | 0,7043  | 2,104197                    | 0,1541  | 2,106705                     | 0,0351  |
| 70       | 2,199115 | 2,177974                    | 0,9613  | 2,194179                    | 0,2244  | 2,197942                     | 0,0534  |
| 43       | 2,265435 | 2,250096                    | 0,6771  | 2,262064                    | 0,1488  | 2,264664                     | 0,0340  |
| 62       | 2,265435 | 2,251588                    | 0,6112  | 2,262278                    | 0,1393  | 2,264691                     | 0,0328  |
| 71       | 2,287114 | 2,266625                    | 0,8958  | 2,282334                    | 0,2090  | 2,285978                     | 0,0497  |
| 53       | 2,453662 | 2,436545                    | 0,6976  | 2,449869                    | 0,1546  | 2,452789                     | 0,0356  |
| 04       | 2,513274 | 2,477315                    | 1,4308  | 2,505176                    | 0,3222  | 2,511425                     | 0,0736  |
| 80       | 2,513274 | 2,482084                    | 1,2410  | 2,505920                    | 0,2926  | 2,511523                     | 0,0697  |

Table 6.1.10: comparison between our FD code and analytic results for TE on TM grid in rectangular waveguide when varying  $\Delta x = \Delta y$

| TM MODES | kta(TM)  | $\Delta y = \Delta x = 0,2$ |         | $\Delta y = \Delta x = 0,1$ |         | $\Delta y = \Delta x = 0,05$ |         |
|----------|----------|-----------------------------|---------|-----------------------------|---------|------------------------------|---------|
|          |          | ktp(TM)                     | ep(TM)% | ktp(TM)                     | ep(TM)% | ktp(TM)                      | ep(TM)% |
| 11       | 0,702482 | 0,702089                    | 0,0559  | 0,702383                    | 0,0140  | 0,702457                     | 0,0035  |
| 21       | 0,888577 | 0,887992                    | 0,0658  | 0,888430                    | 0,0164  | 0,888540                     | 0,0041  |
| 31       | 1,132717 | 1,131328                    | 0,1227  | 1,132370                    | 0,0307  | 1,132630                     | 0,0077  |
| 12       | 1,295312 | 1,292093                    | 0,2485  | 1,294507                    | 0,0622  | 1,295111                     | 0,0155  |
| 22       | 1,404963 | 1,401823                    | 0,2235  | 1,404177                    | 0,0559  | 1,404767                     | 0,0140  |
| 41       | 1,404963 | 1,401823                    | 0,2235  | 1,404177                    | 0,0559  | 1,404767                     | 0,0140  |
| 32       | 1,570796 | 1,567316                    | 0,2216  | 1,569926                    | 0,0554  | 1,570579                     | 0,0139  |
| 51       | 1,691799 | 1,685657                    | 0,3631  | 1,690262                    | 0,0909  | 1,691415                     | 0,0227  |
| 42       | 1,777153 | 1,772480                    | 0,2630  | 1,775984                    | 0,0658  | 1,776861                     | 0,0164  |
| 13       | 1,910956 | 1,899958                    | 0,5755  | 1,908203                    | 0,1441  | 1,910268                     | 0,0360  |
| 23       | 1,986918 | 1,976219                    | 0,5385  | 1,984239                    | 0,1348  | 1,986248                     | 0,0337  |
| 61       | 1,986918 | 1,976219                    | 0,5385  | 1,984239                    | 0,1348  | 1,986248                     | 0,0337  |
| 52       | 2,011601 | 2,004499                    | 0,3530  | 2,009824                    | 0,0883  | 2,011156                     | 0,0221  |
| 33       | 2,107444 | 2,096858                    | 0,5023  | 2,104794                    | 0,1258  | 2,106782                     | 0,0315  |
| 43       | 2,265435 | 2,254333                    | 0,4900  | 2,262655                    | 0,1227  | 2,264740                     | 0,0307  |
| 62       | 2,265435 | 2,254333                    | 0,4900  | 2,262655                    | 0,1227  | 2,264740                     | 0,0307  |
| 71       | 2,287114 | 2,270003                    | 0,7482  | 2,282828                    | 0,1874  | 2,286042                     | 0,0469  |
| 53       | 2,453662 | 2,440973                    | 0,5172  | 2,450486                    | 0,1295  | 2,452868                     | 0,0324  |
| 14       | 2,532833 | 2,506657                    | 1,0335  | 2,526273                    | 0,2590  | 2,531192                     | 0,0648  |
| 72       | 2,532833 | 2,515848                    | 0,6706  | 2,528578                    | 0,1680  | 2,531769                     | 0,0420  |
| 24       | 2,590624 | 2,564943                    | 0,9913  | 2,584187                    | 0,2485  | 2,589013                     | 0,0622  |
| 81       | 2,590624 | 2,564943                    | 0,9913  | 2,584187                    | 0,2485  | 2,589013                     | 0,0622  |
| 63       | 2,665730 | 2,649972                    | 0,5911  | 2,661785                    | 0,1480  | 2,664743                     | 0,0370  |
| 34       | 2,684178 | 2,659004                    | 0,9379  | 2,677868                    | 0,2351  | 2,682599                     | 0,0588  |
| 44       | 2,809926 | 2,784871                    | 0,8916  | 2,803645                    | 0,2235  | 2,808355                     | 0,0559  |
| 82       | 2,809926 | 2,784871                    | 0,8916  | 2,803645                    | 0,2235  | 2,808355                     | 0,0559  |
| 73       | 2,896405 | 2,859697                    | 1,2674  | 2,887199                    | 0,3179  | 2,894102                     | 0,0795  |
| 91       | 2,896405 | 2,875730                    | 0,7138  | 2,891228                    | 0,1788  | 2,895110                     | 0,0447  |
| 54       | 2,963773 | 2,937999                    | 0,8696  | 2,957313                    | 0,2180  | 2,962157                     | 0,0545  |

Table 6.1.11: comparison between our FD code and analytic results for TE on TE grid in rectangular waveguide, when varying  $\Delta x \neq \Delta y$ .

|          |                      | $\Delta x=0.01 ; \Delta y=0,05$ |         | $\Delta x=0.01 ; \Delta y=0,025$ |         |
|----------|----------------------|---------------------------------|---------|----------------------------------|---------|
| TE MODES | k <sub>ta</sub> (TE) | k <sub>tp</sub> (TE)            | ep(TE)% | k <sub>tp</sub> (TE)             | ep(TE)% |
| 10       | 0,314159             | 0,314146                        | 0,0041  | 0,314146                         | 0,0041  |
| 01       | 0,628319             | 0,628215                        | 0,0164  | 0,628215                         | 0,0164  |
| 20       | 0,628319             | 0,628293                        | 0,0041  | 0,628312                         | 0,0010  |
| 11       | 0,702482             | 0,702453                        | 0,0041  | 0,702470                         | 0,0016  |
| 21       | 0,888577             | 0,888485                        | 0,0103  | 0,888499                         | 0,0087  |
| 30       | 0,942478             | 0,942129                        | 0,0370  | 0,942129                         | 0,0370  |
| 31       | 1,132717             | 1,132413                        | 0,0269  | 1,132424                         | 0,0259  |
| 02       | 1,256637             | 1,255810                        | 0,0658  | 1,255810                         | 0,0658  |
| 40       | 1,256637             | 1,256430                        | 0,0165  | 1,256585                         | 0,0041  |
| 12       | 1,295312             | 1,295108                        | 0,0157  | 1,295259                         | 0,0041  |
| 22       | 1,404963             | 1,404212                        | 0,0534  | 1,404221                         | 0,0528  |
| 41       | 1,404963             | 1,404732                        | 0,0164  | 1,404871                         | 0,0066  |
| 50       | 1,570796             | 1,569182                        | 0,1028  | 1,569182                         | 0,1028  |
| 32       | 1,570796             | 1,570422                        | 0,0238  | 1,570546                         | 0,0160  |
| 51       | 1,691799             | 1,690291                        | 0,0892  | 1,690298                         | 0,0887  |
| 42       | 1,777153             | 1,776423                        | 0,0411  | 1,776532                         | 0,0349  |
| 03       | 1,884956             | 1,882166                        | 0,1480  | 1,882166                         | 0,1480  |
| 60       | 1,884956             | 1,884258                        | 0,0370  | 1,884781                         | 0,0093  |
| 13       | 1,910956             | 1,910266                        | 0,0361  | 1,910782                         | 0,0091  |
| 23       | 1,986918             | 1,984263                        | 0,1336  | 1,984270                         | 0,1333  |
| 61       | 1,986918             | 1,986223                        | 0,0350  | 1,986720                         | 0,0100  |
| 52       | 2,011601             | 2,010211                        | 0,0691  | 2,010308                         | 0,0643  |
| 33       | 2,107444             | 2,106665                        | 0,0370  | 2,107132                         | 0,0148  |
| 70       | 2,199115             | 2,194686                        | 0,2014  | 2,194686                         | 0,2014  |
| 43       | 2,265435             | 2,263000                        | 0,1075  | 2,263086                         | 0,1037  |
| 62       | 2,265435             | 2,264396                        | 0,0459  | 2,264831                         | 0,0266  |
| 71       | 2,287114             | 2,282849                        | 0,1865  | 2,282854                         | 0,1862  |
| 53       | 2,453662             | 2,452093                        | 0,0640  | 2,452495                         | 0,0476  |
| 04       | 2,513274             | 2,506665                        | 0,2630  | 2,506665                         | 0,2630  |
| 80       | 2,513274             | 2,511621                        | 0,0658  | 2,512861                         | 0,0164  |

Table 6.1.12: comparison between our FD code and analytic results for TM on TE grid in rectangular waveguide, when varying  $\Delta x \neq \Delta y$ .

|          |                      | $\Delta x=0.01 ; \Delta y=0.05$ |         | $\Delta x=0.01 ; \Delta y=0.025$ |         |
|----------|----------------------|---------------------------------|---------|----------------------------------|---------|
| TM MODES | k <sub>ta</sub> (TM) | k <sub>tp</sub> (TM)            | ep(TM)% | k <sub>tp</sub> (TM)             | ep(TM)% |
| 11       | 0,702482             | 0,702453                        | 0,0040  | 0,702470                         | 0,0016  |
| 21       | 0,888577             | 0,888488                        | 0,0100  | 0,888501                         | 0,0085  |
| 31       | 1,132717             | 1,132422                        | 0,0261  | 1,132432                         | 0,0252  |
| 12       | 1,295312             | 1,295114                        | 0,0152  | 1,295259                         | 0,0040  |
| 22       | 1,404963             | 1,404234                        | 0,0518  | 1,404243                         | 0,0513  |
| 41       | 1,404963             | 1,404739                        | 0,0160  | 1,404873                         | 0,0064  |
| 32       | 1,570796             | 1,570433                        | 0,0231  | 1,570553                         | 0,0155  |
| 51       | 1,691799             | 1,690336                        | 0,0865  | 1,690343                         | 0,0861  |
| 42       | 1,777153             | 1,776444                        | 0,0399  | 1,776550                         | 0,0339  |
| 13       | 1,910956             | 1,910287                        | 0,0350  | 1,910785                         | 0,0090  |
| 23       | 1,986918             | 1,984342                        | 0,1296  | 1,984348                         | 0,1293  |
| 61       | 1,986918             | 1,986244                        | 0,0339  | 1,986723                         | 0,0098  |
| 52       | 2,011601             | 2,010253                        | 0,0670  | 2,010346                         | 0,0624  |
| 33       | 2,107444             | 2,106688                        | 0,0359  | 2,107139                         | 0,0145  |
| 43       | 2,265435             | 2,263072                        | 0,1043  | 2,263155                         | 0,1006  |
| 62       | 2,265435             | 2,264427                        | 0,0445  | 2,264847                         | 0,0259  |
| 71       | 2,287114             | 2,282975                        | 0,1810  | 2,282981                         | 0,1807  |
| 53       | 2,453662             | 2,452140                        | 0,0620  | 2,452528                         | 0,0462  |
| 14       | 2,532833             | 2,529003                        | 0,1512  | 2,529078                         | 0,1483  |
| 72       | 2,532833             | 2,531240                        | 0,0629  | 2,532427                         | 0,0160  |
| 24       | 2,590624             | 2,584395                        | 0,2404  | 2,584400                         | 0,2402  |
| 81       | 2,590624             | 2,589043                        | 0,0610  | 2,590204                         | 0,0162  |
| 63       | 2,665730             | 2,663338                        | 0,0897  | 2,663695                         | 0,0763  |
| 34       | 2,684178             | 2,682557                        | 0,0604  | 2,683678                         | 0,0186  |
| 44       | 2,809926             | 2,804101                        | 0,2073  | 2,804168                         | 0,2049  |
| 82       | 2,809926             | 2,808133                        | 0,0638  | 2,809203                         | 0,0257  |
| 73       | 2,896405             | 2,887486                        | 0,3079  | 2,887490                         | 0,3078  |
| 91       | 2,896405             | 2,892703                        | 0,1278  | 2,893032                         | 0,1165  |
| 54       | 2,963773             | 2,961582                        | 0,0739  | 2,962597                         | 0,0397  |
| 92       | 3,094110             | 3,085686                        | 0,2723  | 3,085747                         | 0,2703  |

Table 6.1.13: comparison between our FD code and analytic results for TE on TM grid in rectangular waveguide, when varying  $\Delta x \neq \Delta y$ .

|          |          | $\Delta x=0.01 ; \Delta y=0,05$ |         | $\Delta x=0.01 ; \Delta y=0,025$ |         |
|----------|----------|---------------------------------|---------|----------------------------------|---------|
| TE MODES | kta(TE)  | ktp(TE)                         | ep(TE)% | ktp(TE)                          | ep(TE)% |
| 10       | 0,314159 | 0,314145                        | 0,0046  | 0,314145                         | 0,0046  |
| 01       | 0,628319 | 0,628203                        | 0,0184  | 0,628203                         | 0,0184  |
| 20       | 0,628319 | 0,628290                        | 0,0046  | 0,628290                         | 0,0046  |
| 11       | 0,702482 | 0,702449                        | 0,0046  | 0,702449                         | 0,0046  |
| 21       | 0,888577 | 0,888474                        | 0,0115  | 0,888474                         | 0,0115  |
| 30       | 0,942478 | 0,942088                        | 0,0414  | 0,942088                         | 0,0414  |
| 31       | 1,132717 | 1,132377                        | 0,0301  | 1,132377                         | 0,0301  |
| 02       | 1,256637 | 1,255713                        | 0,0736  | 1,255713                         | 0,0736  |
| 40       | 1,256637 | 1,256406                        | 0,0184  | 1,256406                         | 0,0184  |
| 12       | 1,295312 | 1,295084                        | 0,0176  | 1,295084                         | 0,0176  |
| 22       | 1,404963 | 1,404123                        | 0,0598  | 1,404123                         | 0,0598  |
| 41       | 1,404963 | 1,404704                        | 0,0184  | 1,404704                         | 0,0184  |
| 50       | 1,570796 | 1,568993                        | 0,1148  | 1,568993                         | 0,1148  |
| 32       | 1,570796 | 1,570377                        | 0,0267  | 1,570377                         | 0,0267  |
| 51       | 1,691799 | 1,690114                        | 0,0996  | 1,690114                         | 0,0996  |
| 42       | 1,777153 | 1,776336                        | 0,0460  | 1,776336                         | 0,0460  |
| 03       | 1,884956 | 1,881843                        | 0,1651  | 1,881843                         | 0,1651  |
| 60       | 1,884956 | 1,884175                        | 0,0414  | 1,884175                         | 0,0414  |
| 13       | 1,910956 | 1,910184                        | 0,0404  | 1,910184                         | 0,0404  |
| 23       | 1,986918 | 1,983956                        | 0,1491  | 1,983956                         | 0,1491  |
| 61       | 1,986918 | 1,986141                        | 0,0391  | 1,986141                         | 0,0391  |
| 52       | 2,011601 | 2,010048                        | 0,0772  | 2,010048                         | 0,0772  |
| 33       | 2,107444 | 2,106572                        | 0,0414  | 2,106572                         | 0,0414  |
| 70       | 2,199115 | 2,194179                        | 0,2244  | 2,194179                         | 0,2244  |
| 43       | 2,265435 | 2,262717                        | 0,1200  | 2,262717                         | 0,1200  |
| 62       | 2,265435 | 2,264272                        | 0,0513  | 2,264272                         | 0,0513  |
| 71       | 2,287114 | 2,282361                        | 0,2078  | 2,282361                         | 0,2078  |
| 53       | 2,453662 | 2,451908                        | 0,0715  | 2,451908                         | 0,0715  |
| 04       | 2,513274 | 2,505920                        | 0,2926  | 2,505920                         | 0,2926  |
| 80       | 2,513274 | 2,511425                        | 0,0736  | 2,511425                         | 0,0736  |

Table 6.1.14: comparison between our FD code and analytic results for TM on TM grid in rectangular waveguide, when varying  $\Delta x \neq \Delta y$

|          |          | $\Delta x=0.01 ; \Delta y=0,05$ |         | $\Delta x=0.01 ; \Delta y=0,025$ |         |
|----------|----------|---------------------------------|---------|----------------------------------|---------|
| TM MODES | kta(TM)  | ktp(TM)                         | ep(TM)% | ktp(TM)                          | ep(TM)% |
| 11       | 0,702482 | 0,702453                        | 0,0041  | 0,702453                         | 0,0041  |
| 21       | 0,888577 | 0,888485                        | 0,0103  | 0,888485                         | 0,0103  |
| 31       | 1,132717 | 1,132413                        | 0,0269  | 1,132413                         | 0,0269  |
| 12       | 1,295312 | 1,295108                        | 0,0157  | 1,295108                         | 0,0157  |
| 22       | 1,404963 | 1,404212                        | 0,0534  | 1,404212                         | 0,0534  |
| 41       | 1,404963 | 1,404732                        | 0,0164  | 1,404732                         | 0,0164  |
| 32       | 1,570796 | 1,570422                        | 0,0238  | 1,570422                         | 0,0238  |
| 51       | 1,691799 | 1,690291                        | 0,0892  | 1,690291                         | 0,0892  |
| 42       | 1,777153 | 1,776423                        | 0,0411  | 1,776423                         | 0,0411  |
| 13       | 1,910956 | 1,910266                        | 0,0361  | 1,910266                         | 0,0361  |
| 23       | 1,986918 | 1,984263                        | 0,1336  | 1,984263                         | 0,1336  |
| 61       | 1,986918 | 1,986223                        | 0,0350  | 1,986223                         | 0,0350  |
| 52       | 2,011601 | 2,010211                        | 0,0691  | 2,010211                         | 0,0691  |
| 33       | 2,107444 | 2,106665                        | 0,0370  | 2,106665                         | 0,0370  |
| 43       | 2,265435 | 2,263000                        | 0,1075  | 2,263000                         | 0,1075  |
| 62       | 2,265435 | 2,264396                        | 0,0459  | 2,264396                         | 0,0459  |
| 71       | 2,287114 | 2,282849                        | 0,1865  | 2,282849                         | 0,1865  |
| 53       | 2,453662 | 2,452093                        | 0,0640  | 2,452093                         | 0,0640  |
| 14       | 2,532833 | 2,528886                        | 0,1558  | 2,528886                         | 0,1558  |
| 72       | 2,532833 | 2,531191                        | 0,0648  | 2,531191                         | 0,0648  |
| 24       | 2,590624 | 2,584206                        | 0,2477  | 2,584206                         | 0,2477  |
| 81       | 2,590624 | 2,588995                        | 0,0629  | 2,588995                         | 0,0629  |
| 63       | 2,665730 | 2,663265                        | 0,0925  | 2,663265                         | 0,0925  |
| 34       | 2,684178 | 2,682507                        | 0,0622  | 2,682507                         | 0,0622  |
| 44       | 2,809926 | 2,803923                        | 0,2136  | 2,803923                         | 0,2136  |
| 82       | 2,809926 | 2,808077                        | 0,0658  | 2,808077                         | 0,0658  |
| 73       | 2,896405 | 2,887216                        | 0,3173  | 2,887216                         | 0,3173  |
| 91       | 2,896405 | 2,892590                        | 0,1317  | 2,892590                         | 0,1317  |
| 54       | 2,963773 | 2,961515                        | 0,0762  | 2,961515                         | 0,0762  |
| 92       | 3,094110 | 3,085430                        | 0,2805  | 3,085430                         | 0,2805  |



We have made several tests by varying the steps ( $\Delta x, \Delta y$ ). The results of the tables 6.1.1 to 6.1.14 shows that our technique has a very low error, as long as the steps are small

## **6.2) FD IN CIRCULAR AND ELLIPTICAL WAVEGUIDE**

In this paragraph we will show the results of techniques presented in the paragraph 4.1 and 4.2 To assess the proposed technique, we will analyze both circular and elliptical waveguide.

In the table 6.2.1 you can see the  $k_t$  of TE and TM modes calculated on the TE grids.

Data of the circular waveguide:

$r=4, \Delta\theta=1^\circ \quad \Delta r=0.079208$

$k_{ta}=k_t$  analytical

$k_{tp}=k_t$  of the program

$ep$ = percentage (relative) error

Total points of the grid: 18001

In the table 6.2.2 , 6.2.3 you can see the  $k_t$  of TE and TM modes calculated on the TE grids where varying  $\Delta r$

Data of the circular waveguide:

$r=4, \Delta\theta=1^\circ$

$k_{ta}=k_t$  analytical

$k_{tp}=k_t$  of the program

$ep$ = percentage (relative) error

In the table 6.2.4 , 6.2.5 you can see the  $k_t$  of TE and TM modes calculated on the TE grids where varying  $\Delta\theta$

Data of the circular waveguide:

$r=4, \Delta r= 0.079208$

$k_{ta}=k_t$  analytical

ktp=kt of the program

ep= percentage (relative) error

Table 6.2.1: comparison between our FD code and analytic results for TE and TM modes on TE grid in circular waveguide

| TE MODES | Kta       | Ktp      | ep%    |
|----------|-----------|----------|--------|
| 11       | 0,460296  | 0,460292 | 0,0008 |
| 11       | 0,460296  | 0,460292 | 0,0008 |
| 21       | 0,7635592 | 0,763531 | 0,0037 |
| 21       | 0,7635592 | 0,763531 | 0,0037 |
| 01       | 0,9579265 | 0,957697 | 0,0240 |
| 31       | 1,0502972 | 1,050204 | 0,0088 |
| 31       | 1,0502972 | 1,050204 | 0,0088 |
| 41       | 1,3293883 | 1,329170 | 0,0164 |
| 41       | 1,3293883 | 1,329170 | 0,0164 |
| 12       | 1,3328607 | 1,332475 | 0,0290 |
| 12       | 1,3328607 | 1,332475 | 0,0290 |
| 51       | 1,6039041 | 1,603482 | 0,0263 |
| 51       | 1,6039041 | 1,603482 | 0,0263 |
| 22       | 1,6765333 | 1,675952 | 0,0347 |
| 22       | 1,6765333 | 1,675952 | 0,0347 |
| 02       | 1,7538967 | 1,752487 | 0,0804 |
| 61       | 1,8753165 | 1,874590 | 0,0387 |
| 61       | 1,8753165 | 1,874590 | 0,0387 |
| 32       | 2,0038092 | 2,002971 | 0,0418 |
| 32       | 2,0038092 | 2,002971 | 0,0418 |
| 13       | 2,1340791 | 2,132172 | 0,0894 |
| 13       | 2,1340791 | 2,132172 | 0,0894 |
| 71       | 2,1444591 | 2,143311 | 0,0536 |
| 71       | 2,1444591 | 2,143311 | 0,0536 |
| 42       | 2,3205991 | 2,319424 | 0,0506 |
| 42       | 2,3205991 | 2,319424 | 0,0506 |
| 81       | 2,4118554 | 2,410147 | 0,0708 |
| 81       | 2,4118554 | 2,410147 | 0,0708 |
| 23       | 2,492367  | 2,489910 | 0,0986 |

| TM MODES | Kta      | Ktp      | ep%    |
|----------|----------|----------|--------|
| 01       | 0,601200 | 0,601141 | 0,0098 |
| 11       | 0,957925 | 0,957796 | 0,0135 |
| 11       | 0,957925 | 0,957796 | 0,0135 |
| 21       | 1,283900 | 1,283680 | 0,0171 |
| 21       | 1,283900 | 1,283680 | 0,0171 |
| 02       | 1,380025 | 1,379330 | 0,0504 |
| 31       | 1,595050 | 1,594670 | 0,0238 |
| 31       | 1,595050 | 1,594670 | 0,0238 |
| 12       | 1,753900 | 1,752912 | 0,0563 |
| 12       | 1,753900 | 1,752912 | 0,0563 |
| 41       | 1,897075 | 1,896501 | 0,0302 |
| 41       | 1,897075 | 1,896501 | 0,0302 |
| 22       | 2,104300 | 2,102992 | 0,0622 |
| 22       | 2,104300 | 2,102992 | 0,0622 |
| 03       | 2,163425 | 2,160829 | 0,1200 |
| 51       | 2,192875 | 2,191983 | 0,0407 |
| 51       | 2,192875 | 2,191983 | 0,0407 |
| 32       | 2,440250 | 2,438539 | 0,0701 |
| 32       | 2,440250 | 2,438539 | 0,0701 |
| 61       | 2,484025 | 2,482728 | 0,0522 |
| 61       | 2,484025 | 2,482728 | 0,0522 |
| 13       | 2,543375 | 2,540060 | 0,1303 |
| 13       | 2,543375 | 2,540060 | 0,1303 |
| 42       | 2,766175 | 2,763979 | 0,0794 |
| 42       | 2,766175 | 2,763979 | 0,0794 |
| 71       | 2,771593 | 2,769754 | 0,0663 |
| 71       | 2,771593 | 2,769754 | 0,0663 |
| 23       | 2,904950 | 2,900901 | 0,1394 |
| 23       | 2,904950 | 2,900901 | 0,1394 |

Table 6.2.2: comparison between our FD code and analytic results for TE modes on TE grid in circular waveguide , when varying  $\Delta r$

| TE MODES | Kta      | $\Delta r=0.156863$ |        | $\Delta r=0.079208$ |        | $\Delta r=0.039409$ |        |
|----------|----------|---------------------|--------|---------------------|--------|---------------------|--------|
|          |          | Ktp                 | ep%    | Ktp                 | ep%    | Ktp                 | ep%    |
| 11       | 0,460296 | 0,460294            | 0,0005 | 0,460292            | 0,0008 | 0,460292            | 0,0009 |
| 11       | 0,460296 | 0,460294            | 0,0005 | 0,460292            | 0,0008 | 0,460292            | 0,0009 |
| 21       | 0,763559 | 0,763537            | 0,0030 | 0,763531            | 0,0037 | 0,763530            | 0,0038 |
| 21       | 0,763559 | 0,763537            | 0,0030 | 0,763531            | 0,0037 | 0,763530            | 0,0038 |
| 01       | 0,957927 | 0,957026            | 0,0940 | 0,957697            | 0,0240 | 0,957870            | 0,0059 |
| 31       | 1,050297 | 1,050216            | 0,0077 | 1,050204            | 0,0088 | 1,050202            | 0,0091 |
| 31       | 1,050297 | 1,050216            | 0,0077 | 1,050204            | 0,0088 | 1,050202            | 0,0091 |
| 41       | 1,329388 | 1,329191            | 0,0149 | 1,329170            | 0,0164 | 1,329165            | 0,0168 |
| 41       | 1,329388 | 1,329191            | 0,0149 | 1,329170            | 0,0164 | 1,329165            | 0,0168 |
| 12       | 1,332861 | 1,331358            | 0,1128 | 1,332475            | 0,0290 | 1,332762            | 0,0074 |
| 12       | 1,332861 | 1,331358            | 0,1128 | 1,332475            | 0,0290 | 1,332762            | 0,0074 |
| 51       | 1,603904 | 1,603513            | 0,0244 | 1,603482            | 0,0263 | 1,603474            | 0,0268 |
| 51       | 1,603904 | 1,603513            | 0,0244 | 1,603482            | 0,0263 | 1,603474            | 0,0268 |
| 22       | 1,676533 | 1,674350            | 0,1302 | 1,675952            | 0,0347 | 1,676364            | 0,0101 |
| 22       | 1,676533 | 1,674350            | 0,1302 | 1,675952            | 0,0347 | 1,676364            | 0,0101 |
| 02       | 1,753897 | 1,748379            | 0,3146 | 1,752487            | 0,0804 | 1,753548            | 0,0199 |
| 61       | 1,875317 | 1,874634            | 0,0364 | 1,874590            | 0,0387 | 1,874579            | 0,0393 |
| 61       | 1,875317 | 1,874634            | 0,0364 | 1,874590            | 0,0387 | 1,874579            | 0,0393 |
| 32       | 2,003809 | 2,000842            | 0,1481 | 2,002971            | 0,0418 | 2,003519            | 0,0145 |
| 32       | 2,003809 | 2,000842            | 0,1481 | 2,002971            | 0,0418 | 2,003519            | 0,0145 |
| 13       | 2,134079 | 2,126606            | 0,3502 | 2,132172            | 0,0894 | 2,133604            | 0,0223 |
| 13       | 2,134079 | 2,126606            | 0,3502 | 2,132172            | 0,0894 | 2,133604            | 0,0223 |
| 71       | 2,144459 | 2,143369            | 0,0508 | 2,143311            | 0,0536 | 2,143296            | 0,0542 |
| 71       | 2,144459 | 2,143369            | 0,0508 | 2,143311            | 0,0536 | 2,143296            | 0,0542 |
| 42       | 2,320599 | 2,316728            | 0,1668 | 2,319424            | 0,0506 | 2,320117            | 0,0208 |
| 42       | 2,320599 | 2,316728            | 0,1668 | 2,319424            | 0,0506 | 2,320117            | 0,0208 |
| 81       | 2,411855 | 2,410222            | 0,0677 | 2,410147            | 0,0708 | 2,410129            | 0,0716 |
| 81       | 2,411855 | 2,410222            | 0,0677 | 2,410147            | 0,0708 | 2,410129            | 0,0716 |
| 23       | 2,492367 | 2,482826            | 0,3828 | 2,489910            | 0,0986 | 2,491732            | 0,0255 |

Table 6.2.3: comparison between our FD code and analytic results for TM modes on TE grid in circular waveguide , when varying  $\Delta r$

| TM MODES | Kta      | $\Delta r=0.156863$ |        | $\Delta r=0.079208$ |        | $\Delta r=0.039409$ |        |
|----------|----------|---------------------|--------|---------------------|--------|---------------------|--------|
|          |          | Ktp                 | ep%    | Ktp                 | ep%    | Ktp                 | ep%    |
| 01       | 0,601200 | 0,600954            | 0,0409 | 0,601141            | 0,0098 | 0,601190            | 0,0017 |
| 11       | 0,957925 | 0,957447            | 0,0499 | 0,957796            | 0,0135 | 0,957890            | 0,0036 |
| 11       | 0,957925 | 0,957447            | 0,0499 | 0,957796            | 0,0135 | 0,957890            | 0,0036 |
| 21       | 1,283900 | 1,283164            | 0,0573 | 1,283680            | 0,0171 | 1,283824            | 0,0059 |
| 21       | 1,283900 | 1,283164            | 0,0573 | 1,283680            | 0,0171 | 1,283824            | 0,0059 |
| 02       | 1,380025 | 1,377392            | 0,1908 | 1,379330            | 0,0504 | 1,379846            | 0,0130 |
| 31       | 1,595050 | 1,593983            | 0,0669 | 1,594670            | 0,0238 | 1,594867            | 0,0115 |
| 31       | 1,595050 | 1,593983            | 0,0669 | 1,594670            | 0,0238 | 1,594867            | 0,0115 |
| 12       | 1,753900 | 1,750200            | 0,2110 | 1,752912            | 0,0563 | 1,753645            | 0,0146 |
| 12       | 1,753900 | 1,750200            | 0,2110 | 1,752912            | 0,0563 | 1,753645            | 0,0146 |
| 41       | 1,897075 | 1,895640            | 0,0756 | 1,896501            | 0,0302 | 1,896754            | 0,0169 |
| 41       | 1,897075 | 1,895640            | 0,0756 | 1,896501            | 0,0302 | 1,896754            | 0,0169 |
| 22       | 2,104300 | 2,099493            | 0,2285 | 2,102992            | 0,0622 | 2,103950            | 0,0166 |
| 22       | 2,104300 | 2,099493            | 0,2285 | 2,102992            | 0,0622 | 2,103950            | 0,0166 |
| 03       | 2,163425 | 2,153543            | 0,4568 | 2,160829            | 0,1200 | 2,162778            | 0,0299 |
| 51       | 2,192875 | 2,190948            | 0,0879 | 2,191983            | 0,0407 | 2,192295            | 0,0265 |
| 51       | 2,192875 | 2,190948            | 0,0879 | 2,191983            | 0,0407 | 2,192295            | 0,0265 |
| 32       | 2,440250 | 2,434227            | 0,2468 | 2,438539            | 0,0701 | 2,439733            | 0,0212 |
| 32       | 2,440250 | 2,434227            | 0,2468 | 2,438539            | 0,0701 | 2,439733            | 0,0212 |
| 61       | 2,484025 | 2,481520            | 0,1009 | 2,482728            | 0,0522 | 2,483100            | 0,0372 |
| 61       | 2,484025 | 2,481520            | 0,1009 | 2,482728            | 0,0522 | 2,483100            | 0,0372 |
| 13       | 2,543375 | 2,530872            | 0,4916 | 2,540060            | 0,1303 | 2,542530            | 0,0332 |
| 13       | 2,543375 | 2,530872            | 0,4916 | 2,540060            | 0,1303 | 2,542530            | 0,0332 |
| 42       | 2,766175 | 2,758834            | 0,2654 | 2,763979            | 0,0794 | 2,765419            | 0,0273 |
| 42       | 2,766175 | 2,758834            | 0,2654 | 2,763979            | 0,0794 | 2,765419            | 0,0273 |
| 71       | 2,771593 | 2,768374            | 0,1161 | 2,769754            | 0,0663 | 2,770189            | 0,0506 |
| 71       | 2,771593 | 2,768374            | 0,1161 | 2,769754            | 0,0663 | 2,770189            | 0,0506 |
| 23       | 2,904950 | 2,889818            | 0,5209 | 2,900901            | 0,1394 | 2,903906            | 0,0359 |
| 23       | 2,904950 | 2,889818            | 0,5209 | 2,900901            | 0,1394 | 2,903906            | 0,0359 |

Table 6.2.4: comparison between our FD code and analytic results for TE modes on TE grid in circular waveguide , when varying  $\Delta\theta$

| TE MODES | $\Delta\theta=2^\circ$ |          |        | $\Delta\theta=1^\circ$ |        | $\Delta\theta=0.5^\circ$ |        |
|----------|------------------------|----------|--------|------------------------|--------|--------------------------|--------|
|          | Kta                    | Ktp      | ep%    | Ktp                    | ep%    | Ktp                      | ep%    |
| 11       | 0,460296               | 0,460280 | 0,0034 | 0,460292               | 0,0008 | 0,460295                 | 0,0001 |
| 11       | 0,460296               | 0,460280 | 0,0034 | 0,460292               | 0,0008 | 0,460295                 | 0,0001 |
| 21       | 0,763559               | 0,763442 | 0,0153 | 0,763531               | 0,0037 | 0,763554                 | 0,0007 |
| 21       | 0,763559               | 0,763442 | 0,0153 | 0,763531               | 0,0037 | 0,763554                 | 0,0007 |
| 01       | 0,957927               | 0,957697 | 0,0240 | 0,957697               | 0,0240 | 0,957697                 | 0,0240 |
| 31       | 1,050297               | 1,049914 | 0,0364 | 1,050204               | 0,0088 | 1,050277                 | 0,0019 |
| 31       | 1,050297               | 1,049914 | 0,0364 | 1,050204               | 0,0088 | 1,050277                 | 0,0019 |
| 41       | 1,329388               | 1,328497 | 0,0671 | 1,329170               | 0,0164 | 1,329339                 | 0,0037 |
| 41       | 1,329388               | 1,328497 | 0,0671 | 1,329170               | 0,0164 | 1,329339                 | 0,0037 |
| 12       | 1,332861               | 1,332461 | 0,0300 | 1,332475               | 0,0290 | 1,332478                 | 0,0287 |
| 12       | 1,332861               | 1,332461 | 0,0300 | 1,332475               | 0,0290 | 1,332478                 | 0,0287 |
| 51       | 1,603904               | 1,602184 | 0,1073 | 1,603482               | 0,0263 | 1,603806                 | 0,0061 |
| 51       | 1,603904               | 1,602184 | 0,1073 | 1,603482               | 0,0263 | 1,603806                 | 0,0061 |
| 22       | 1,676533               | 1,675850 | 0,0408 | 1,675952               | 0,0347 | 1,675977                 | 0,0332 |
| 22       | 1,676533               | 1,675850 | 0,0408 | 1,675952               | 0,0347 | 1,675977                 | 0,0332 |
| 02       | 1,753897               | 1,752487 | 0,0804 | 1,752487               | 0,0804 | 1,752487                 | 0,0804 |
| 61       | 1,875317               | 1,872370 | 0,1571 | 1,874590               | 0,0387 | 1,875146                 | 0,0091 |
| 61       | 1,875317               | 1,872370 | 0,1571 | 1,874590               | 0,0387 | 1,875146                 | 0,0091 |
| 32       | 2,003809               | 2,002641 | 0,0583 | 2,002971               | 0,0418 | 2,003054                 | 0,0377 |
| 32       | 2,003809               | 2,002641 | 0,0583 | 2,002971               | 0,0418 | 2,003054                 | 0,0377 |
| 13       | 2,134079               | 2,132158 | 0,0900 | 2,132172               | 0,0894 | 2,132176                 | 0,0892 |
| 13       | 2,134079               | 2,132158 | 0,0900 | 2,132172               | 0,0894 | 2,132176                 | 0,0892 |
| 71       | 2,144459               | 2,139811 | 0,2168 | 2,143311               | 0,0536 | 2,144186                 | 0,0127 |
| 71       | 2,144459               | 2,139811 | 0,2168 | 2,143311               | 0,0536 | 2,144186                 | 0,0127 |
| 42       | 2,320599               | 2,318663 | 0,0834 | 2,319424               | 0,0506 | 2,319615                 | 0,0424 |
| 42       | 2,320599               | 2,318663 | 0,0834 | 2,319424               | 0,0506 | 2,319615                 | 0,0424 |
| 81       | 2,411855               | 2,404954 | 0,2861 | 2,410147               | 0,0708 | 2,411446                 | 0,0170 |
| 81       | 2,411855               | 2,404954 | 0,2861 | 2,410147               | 0,0708 | 2,411446                 | 0,0170 |
| 23       | 2,492367               | 2,489804 | 0,1028 | 2,489910               | 0,0986 | 2,489937                 | 0,0975 |

Table 6.2.5: comparison between our FD code and analytic results for TM modes on TE grid in circular waveguide , when varying  $\Delta\theta$

| TM MODES | Kta      | $\Delta\theta=2^\circ$ |        | $\Delta\theta=1^\circ$ |        | $\Delta\theta=0.5^\circ$ |        |
|----------|----------|------------------------|--------|------------------------|--------|--------------------------|--------|
|          |          | Ktp                    | ep%    | Ktp                    | ep%    | Ktp                      | ep%    |
| 01       | 0,601200 | 0,601141               | 0,0098 | 0,601141               | 0,0098 | 0,601141                 | 0,0098 |
| 11       | 0,957925 | 0,957783               | 0,0148 | 0,957796               | 0,0135 | 0,957799                 | 0,0132 |
| 11       | 0,957925 | 0,957783               | 0,0148 | 0,957796               | 0,0135 | 0,957799                 | 0,0132 |
| 21       | 1,283900 | 1,283583               | 0,0247 | 1,283680               | 0,0171 | 1,283704                 | 0,0153 |
| 21       | 1,283900 | 1,283583               | 0,0247 | 1,283680               | 0,0171 | 1,283704                 | 0,0153 |
| 02       | 1,380025 | 1,379330               | 0,0504 | 1,379330               | 0,0504 | 1,379330                 | 0,0504 |
| 31       | 1,595050 | 1,594356               | 0,0435 | 1,594670               | 0,0238 | 1,594749                 | 0,0189 |
| 31       | 1,595050 | 1,594356               | 0,0435 | 1,594670               | 0,0238 | 1,594749                 | 0,0189 |
| 12       | 1,753900 | 1,752899               | 0,0571 | 1,752912               | 0,0563 | 1,752916                 | 0,0561 |
| 12       | 1,753900 | 1,752899               | 0,0571 | 1,752912               | 0,0563 | 1,752916                 | 0,0561 |
| 41       | 1,897075 | 1,895774               | 0,0686 | 1,896501               | 0,0302 | 1,896683                 | 0,0207 |
| 41       | 1,897075 | 1,895774               | 0,0686 | 1,896501               | 0,0302 | 1,896683                 | 0,0207 |
| 22       | 2,104300 | 2,102888               | 0,0671 | 2,102992               | 0,0622 | 2,103018                 | 0,0609 |
| 22       | 2,104300 | 2,102888               | 0,0671 | 2,102992               | 0,0622 | 2,103018                 | 0,0609 |
| 03       | 2,163425 | 2,160829               | 0,1200 | 2,160829               | 0,1200 | 2,160829                 | 0,1200 |
| 51       | 2,192875 | 2,190588               | 0,1043 | 2,191983               | 0,0407 | 2,192332                 | 0,0248 |
| 51       | 2,192875 | 2,190588               | 0,1043 | 2,191983               | 0,0407 | 2,192332                 | 0,0248 |
| 32       | 2,440250 | 2,438199               | 0,0840 | 2,438539               | 0,0701 | 2,438624                 | 0,0667 |
| 32       | 2,440250 | 2,438199               | 0,0840 | 2,438539               | 0,0701 | 2,438624                 | 0,0667 |
| 61       | 2,484025 | 2,480352               | 0,1479 | 2,482728               | 0,0522 | 2,483323                 | 0,0283 |
| 61       | 2,484025 | 2,480352               | 0,1479 | 2,482728               | 0,0522 | 2,483323                 | 0,0283 |
| 13       | 2,543375 | 2,540046               | 0,1309 | 2,540060               | 0,1303 | 2,540064                 | 0,1302 |
| 13       | 2,543375 | 2,540046               | 0,1309 | 2,540060               | 0,1303 | 2,540064                 | 0,1302 |
| 42       | 2,766175 | 2,763195               | 0,1077 | 2,763979               | 0,0794 | 2,764174                 | 0,0723 |
| 42       | 2,766175 | 2,763195               | 0,1077 | 2,763979               | 0,0794 | 2,764174                 | 0,0723 |
| 71       | 2,771593 | 2,766023               | 0,2010 | 2,769754               | 0,0663 | 2,770687                 | 0,0327 |
| 71       | 2,771593 | 2,766023               | 0,2010 | 2,769754               | 0,0663 | 2,770687                 | 0,0327 |
| 23       | 2,904950 | 2,900794               | 0,1431 | 2,900901               | 0,1394 | 2,900928                 | 0,1384 |
| 23       | 2,904950 | 2,900794               | 0,1431 | 2,900901               | 0,1394 | 2,900928                 | 0,1384 |

In the table 6.2.6 , 6.2.7 you can see the  $k_t$  of TE and TM modes calculated on the TM grids when varying  $\Delta r$

Data of the circular waveguide:

$r=4$ ,  $\Delta\theta=1^\circ$

$k_{ta}=k_t$  analytical

$k_{tp}=k_t$  of the program

$ep$ = percentage (relative) error

In the table 6.2.8 , 6.2.9 you can see the  $k_t$  of TE and TM modes calculated on the TM grids when varying  $\Delta\theta$

Data of the circular waveguide:

$r=4$ ,  $\Delta r= 0.079208$

$k_{ta}=k_t$  analytical

$k_{tp}=k_t$  of the program

$ep$ = percentage (relative) error

In the Figures 6.2.1, 6.2.2. comparison between our FD code and analytic results and FIT(CST) results for TE modes in circular waveguide calculated on the TE grids.

Data of the circular waveguide figure 6.2.1:

$r=4$ ,  $\Delta\theta=1^\circ$                        $\Delta r=0.079208$

Data of the circular waveguide figure 6.2.2:

$r=4$ ,  $\Delta\theta=0.5^\circ$                        $\Delta r=0.079208$

Table 6.2.6: comparison between our FD code and analytic results for TM modes on TM grid in circular waveguide , when varying  $\Delta r$

| TM MODES | Kta      | $\Delta r=0.153846$ |        | $\Delta r=0.078431$ |        | $\Delta r=0.039604$ |        |
|----------|----------|---------------------|--------|---------------------|--------|---------------------|--------|
|          |          | Ktp                 | ep%    | Ktp                 | ep%    | Ktp                 | ep%    |
| 01       | 0,601200 | 0,600970            | 0,0382 | 0,601143            | 0,0094 | 0,601190            | 0,0017 |
| 11       | 0,957925 | 0,957439            | 0,0507 | 0,957796            | 0,0135 | 0,957890            | 0,0037 |
| 11       | 0,957925 | 0,957439            | 0,0507 | 0,957796            | 0,0135 | 0,957890            | 0,0037 |
| 21       | 1,283900 | 1,283103            | 0,0621 | 1,283674            | 0,0176 | 1,283822            | 0,0060 |
| 21       | 1,283900 | 1,283103            | 0,0621 | 1,283674            | 0,0176 | 1,283822            | 0,0060 |
| 02       | 1,380025 | 1,377342            | 0,1944 | 1,379326            | 0,0506 | 1,379843            | 0,0132 |
| 31       | 1,595050 | 1,593839            | 0,0759 | 1,594655            | 0,0247 | 1,594864            | 0,0117 |
| 31       | 1,595050 | 1,593839            | 0,0759 | 1,594655            | 0,0247 | 1,594864            | 0,0117 |
| 12       | 1,753900 | 1,750000            | 0,2224 | 1,752893            | 0,0574 | 1,753638            | 0,0150 |
| 12       | 1,753900 | 1,750000            | 0,2224 | 1,752893            | 0,0574 | 1,753638            | 0,0150 |
| 41       | 1,897075 | 1,895385            | 0,0891 | 1,896474            | 0,0317 | 1,896749            | 0,0172 |
| 41       | 1,897075 | 1,895385            | 0,0891 | 1,896474            | 0,0317 | 1,896749            | 0,0172 |
| 22       | 2,104300 | 2,099080            | 0,2480 | 2,102949            | 0,0642 | 2,103939            | 0,0172 |
| 22       | 2,104300 | 2,099080            | 0,2480 | 2,102949            | 0,0642 | 2,103939            | 0,0172 |
| 03       | 2,163425 | 2,153229            | 0,4713 | 2,160800            | 0,1213 | 2,162762            | 0,0307 |
| 51       | 2,192875 | 2,190552            | 0,1059 | 2,191940            | 0,0426 | 2,192287            | 0,0268 |
| 51       | 2,192875 | 2,190552            | 0,1059 | 2,191940            | 0,0426 | 2,192287            | 0,0268 |
| 32       | 2,440250 | 2,433541            | 0,2749 | 2,438465            | 0,0731 | 2,439717            | 0,0218 |
| 32       | 2,440250 | 2,433541            | 0,2749 | 2,438465            | 0,0731 | 2,439717            | 0,0218 |
| 61       | 2,484025 | 2,480953            | 0,1237 | 2,482665            | 0,0548 | 2,483090            | 0,0376 |
| 61       | 2,484025 | 2,480953            | 0,1237 | 2,482665            | 0,0548 | 2,483090            | 0,0376 |
| 13       | 2,543375 | 2,530209            | 0,5177 | 2,539993            | 0,1330 | 2,542506            | 0,0342 |
| 13       | 2,543375 | 2,530209            | 0,5177 | 2,539993            | 0,1330 | 2,542506            | 0,0342 |
| 42       | 2,766175 | 2,757814            | 0,3023 | 2,763867            | 0,0834 | 2,765397            | 0,0281 |
| 42       | 2,766175 | 2,757814            | 0,3023 | 2,763867            | 0,0834 | 2,765397            | 0,0281 |
| 71       | 2,771593 | 2,767606            | 0,1438 | 2,769667            | 0,0695 | 2,770176            | 0,0511 |
| 71       | 2,771593 | 2,767606            | 0,1438 | 2,769667            | 0,0695 | 2,770176            | 0,0511 |
| 23       | 2,904950 | 2,888710            | 0,5590 | 2,900784            | 0,1434 | 2,903873            | 0,0371 |
| 23       | 2,904950 | 2,888710            | 0,5590 | 2,900784            | 0,1434 | 2,903873            | 0,0371 |



Table 6.2.7: comparison between our FD code and analytic results for TE modes on TM grid in circular waveguide , when varying  $\Delta r$

| TE MODES | Kta      | $\Delta r=0.153846$ |        | $\Delta r=0.078431$ |        | $\Delta r=0.039604$ |        |
|----------|----------|---------------------|--------|---------------------|--------|---------------------|--------|
|          |          | Ktp                 | ep%    | Ktp                 | ep%    | Ktp                 | ep%    |
| 11       | 0,460296 | 0,460271            | 0,0054 | 0,460289            | 0,0015 | 0,460291            | 0,0010 |
| 11       | 0,460296 | 0,460271            | 0,0054 | 0,460289            | 0,0015 | 0,460291            | 0,0010 |
| 21       | 0,763559 | 0,763432            | 0,0166 | 0,763522            | 0,0049 | 0,763530            | 0,0039 |
| 21       | 0,763559 | 0,763432            | 0,0166 | 0,763522            | 0,0049 | 0,763530            | 0,0039 |
| 01       | 0,957927 | 0,956850            | 0,1124 | 0,957669            | 0,0269 | 0,957863            | 0,0066 |
| 31       | 1,050297 | 1,049995            | 0,0288 | 1,050185            | 0,0106 | 1,050201            | 0,0091 |
| 31       | 1,050297 | 1,049995            | 0,0288 | 1,050185            | 0,0106 | 1,050201            | 0,0091 |
| 41       | 1,329388 | 1,328828            | 0,0421 | 1,329139            | 0,0187 | 1,329166            | 0,0167 |
| 41       | 1,329388 | 1,328828            | 0,0421 | 1,329139            | 0,0187 | 1,329166            | 0,0167 |
| 12       | 1,332861 | 1,330816            | 0,1534 | 1,332400            | 0,0345 | 1,332748            | 0,0084 |
| 12       | 1,332861 | 1,330816            | 0,1534 | 1,332400            | 0,0345 | 1,332748            | 0,0084 |
| 51       | 1,603904 | 1,602992            | 0,0569 | 1,603436            | 0,0292 | 1,603475            | 0,0268 |
| 51       | 1,603904 | 1,602992            | 0,0569 | 1,603436            | 0,0292 | 1,603475            | 0,0268 |
| 22       | 1,676533 | 1,673297            | 0,1930 | 1,675813            | 0,0430 | 1,676341            | 0,0114 |
| 22       | 1,676533 | 1,673297            | 0,1930 | 1,675813            | 0,0430 | 1,676341            | 0,0114 |
| 02       | 1,753897 | 1,747142            | 0,3851 | 1,752325            | 0,0896 | 1,753517            | 0,0216 |
| 61       | 1,875317 | 1,873948            | 0,0730 | 1,874528            | 0,0421 | 1,874581            | 0,0392 |
| 61       | 1,875317 | 1,873948            | 0,0730 | 1,874528            | 0,0421 | 1,874581            | 0,0392 |
| 32       | 2,003809 | 1,999156            | 0,2322 | 2,002750            | 0,0529 | 2,003485            | 0,0162 |
| 32       | 2,003809 | 1,999156            | 0,2322 | 2,002750            | 0,0529 | 2,003485            | 0,0162 |
| 13       | 2,134079 | 2,124348            | 0,4560 | 2,131877            | 0,1032 | 2,133554            | 0,0246 |
| 13       | 2,134079 | 2,124348            | 0,4560 | 2,131877            | 0,1032 | 2,133554            | 0,0246 |
| 71       | 2,144459 | 2,142518            | 0,0905 | 2,143230            | 0,0573 | 2,143298            | 0,0541 |
| 71       | 2,144459 | 2,142518            | 0,0905 | 2,143230            | 0,0573 | 2,143298            | 0,0541 |
| 42       | 2,320599 | 2,314304            | 0,2713 | 2,319103            | 0,0645 | 2,320070            | 0,0228 |
| 42       | 2,320599 | 2,314304            | 0,2713 | 2,319103            | 0,0645 | 2,320070            | 0,0228 |
| 81       | 2,411855 | 2,409212            | 0,1096 | 2,410047            | 0,0750 | 2,410131            | 0,0715 |
| 81       | 2,411855 | 2,409212            | 0,1096 | 2,410047            | 0,0750 | 2,410131            | 0,0715 |
| 23       | 2,492367 | 2,479353            | 0,5221 | 2,489451            | 0,1170 | 2,491659            | 0,0284 |

Table 6.2.8: comparison between our FD code and analytic results for TM modes on TM grid in circular waveguide , when varying  $\Delta\theta$

| TM MODES | $\Delta\theta=2^\circ$ |          |        | $\Delta\theta=1^\circ$ |        | $\Delta\theta=0.5^\circ$ |        |
|----------|------------------------|----------|--------|------------------------|--------|--------------------------|--------|
|          | Kta                    | Ktp      | ep%    | Ktp                    | ep%    | Ktp                      | ep%    |
| 01       | 0,601200               | 0,601143 | 0,0094 | 0,601143               | 0,0094 | 0,601143                 | 0,0094 |
| 11       | 0,957925               | 0,957783 | 0,0149 | 0,957796               | 0,0135 | 0,957799                 | 0,0132 |
| 11       | 0,957925               | 0,957783 | 0,0149 | 0,957796               | 0,0135 | 0,957799                 | 0,0132 |
| 21       | 1,283900               | 1,283578 | 0,0251 | 1,283674               | 0,0176 | 1,283698                 | 0,0157 |
| 21       | 1,283900               | 1,283578 | 0,0251 | 1,283674               | 0,0176 | 1,283698                 | 0,0157 |
| 02       | 1,380025               | 1,379326 | 0,0506 | 1,379326               | 0,0506 | 1,379326                 | 0,0506 |
| 31       | 1,595050               | 1,594341 | 0,0445 | 1,594655               | 0,0247 | 1,594734                 | 0,0198 |
| 31       | 1,595050               | 1,594341 | 0,0445 | 1,594655               | 0,0247 | 1,594734                 | 0,0198 |
| 12       | 1,753900               | 1,752879 | 0,0582 | 1,752893               | 0,0574 | 1,752896                 | 0,0572 |
| 12       | 1,753900               | 1,752879 | 0,0582 | 1,752893               | 0,0574 | 1,752896                 | 0,0572 |
| 41       | 1,897075               | 1,895747 | 0,0700 | 1,896474               | 0,0317 | 1,896656                 | 0,0221 |
| 41       | 1,897075               | 1,895747 | 0,0700 | 1,896474               | 0,0317 | 1,896656                 | 0,0221 |
| 22       | 2,104300               | 2,102845 | 0,0691 | 2,102949               | 0,0642 | 2,102975                 | 0,0629 |
| 22       | 2,104300               | 2,102845 | 0,0691 | 2,102949               | 0,0642 | 2,102975                 | 0,0629 |
| 03       | 2,163425               | 2,160800 | 0,1213 | 2,160800               | 0,1213 | 2,160800                 | 0,1213 |
| 51       | 2,192875               | 2,190545 | 0,1063 | 2,191940               | 0,0426 | 2,192289                 | 0,0267 |
| 51       | 2,192875               | 2,190545 | 0,1063 | 2,191940               | 0,0426 | 2,192289                 | 0,0267 |
| 32       | 2,440250               | 2,438126 | 0,0870 | 2,438465               | 0,0731 | 2,438550                 | 0,0697 |
| 32       | 2,440250               | 2,438126 | 0,0870 | 2,438465               | 0,0731 | 2,438550                 | 0,0697 |
| 61       | 2,484025               | 2,480288 | 0,1504 | 2,482665               | 0,0548 | 2,483259                 | 0,0308 |
| 61       | 2,484025               | 2,480288 | 0,1504 | 2,482665               | 0,0548 | 2,483259                 | 0,0308 |
| 13       | 2,543375               | 2,539979 | 0,1335 | 2,539993               | 0,1330 | 2,539996                 | 0,1328 |
| 13       | 2,543375               | 2,539979 | 0,1335 | 2,539993               | 0,1330 | 2,539996                 | 0,1328 |
| 42       | 2,766175               | 2,763084 | 0,1118 | 2,763867               | 0,0834 | 2,764063                 | 0,0764 |
| 42       | 2,766175               | 2,763084 | 0,1118 | 2,763867               | 0,0834 | 2,764063                 | 0,0764 |
| 71       | 2,771593               | 2,765936 | 0,2041 | 2,769667               | 0,0695 | 2,770601                 | 0,0358 |
| 71       | 2,771593               | 2,765936 | 0,2041 | 2,769667               | 0,0695 | 2,770601                 | 0,0358 |
| 23       | 2,904950               | 2,900676 | 0,1471 | 2,900784               | 0,1434 | 2,900810                 | 0,1425 |
| 23       | 2,904950               | 2,900676 | 0,1471 | 2,900784               | 0,1434 | 2,900810                 | 0,1425 |

Table 6.2.9: comparison between our FD code and analytic results for TE modes on TM grid in circular waveguide , when varying  $\Delta\theta$

| TE MODES | $\Delta\theta=2^\circ$ |          |        | $\Delta\theta=1^\circ$ |        | $\Delta\theta=0.5^\circ$ |        |
|----------|------------------------|----------|--------|------------------------|--------|--------------------------|--------|
|          | Kta                    | Ktp      | ep%    | Ktp                    | ep%    | Ktp                      | ep%    |
| 11       | 0,460296               | 0,460277 | 0,0042 | 0,460289               | 0,0015 | 0,460292                 | 0,0009 |
| 11       | 0,460296               | 0,460277 | 0,0042 | 0,460289               | 0,0015 | 0,460292                 | 0,0009 |
| 21       | 0,763559               | 0,763433 | 0,0166 | 0,763522               | 0,0049 | 0,763544                 | 0,0020 |
| 21       | 0,763559               | 0,763433 | 0,0166 | 0,763522               | 0,0049 | 0,763544                 | 0,0020 |
| 01       | 0,957927               | 0,957669 | 0,0269 | 0,957669               | 0,0269 | 0,957669                 | 0,0269 |
| 31       | 1,050297               | 1,049895 | 0,0383 | 1,050185               | 0,0106 | 1,050258                 | 0,0037 |
| 31       | 1,050297               | 1,049895 | 0,0383 | 1,050185               | 0,0106 | 1,050258                 | 0,0037 |
| 41       | 1,329388               | 1,328466 | 0,0694 | 1,329139               | 0,0187 | 1,329308                 | 0,0061 |
| 41       | 1,329388               | 1,328466 | 0,0694 | 1,329139               | 0,0187 | 1,329308                 | 0,0061 |
| 12       | 1,332861               | 1,332387 | 0,0356 | 1,332400               | 0,0345 | 1,332404                 | 0,0343 |
| 12       | 1,332861               | 1,332387 | 0,0356 | 1,332400               | 0,0345 | 1,332404                 | 0,0343 |
| 51       | 1,603904               | 1,602138 | 0,1101 | 1,603436               | 0,0292 | 1,603760                 | 0,0090 |
| 51       | 1,603904               | 1,602138 | 0,1101 | 1,603436               | 0,0292 | 1,603760                 | 0,0090 |
| 22       | 1,676533               | 1,675711 | 0,0490 | 1,675813               | 0,0430 | 1,675838                 | 0,0415 |
| 22       | 1,676533               | 1,675711 | 0,0490 | 1,675813               | 0,0430 | 1,675838                 | 0,0415 |
| 02       | 1,753897               | 1,752325 | 0,0896 | 1,752325               | 0,0896 | 1,752325                 | 0,0896 |
| 61       | 1,875317               | 1,872307 | 0,1605 | 1,874528               | 0,0421 | 1,875083                 | 0,0124 |
| 61       | 1,875317               | 1,872307 | 0,1605 | 1,874528               | 0,0421 | 1,875083                 | 0,0124 |
| 32       | 2,003809               | 2,002420 | 0,0693 | 2,002750               | 0,0529 | 2,002833                 | 0,0487 |
| 32       | 2,003809               | 2,002420 | 0,0693 | 2,002750               | 0,0529 | 2,002833                 | 0,0487 |
| 13       | 2,134079               | 2,131863 | 0,1038 | 2,131877               | 0,1032 | 2,131881                 | 0,1030 |
| 13       | 2,134079               | 2,131863 | 0,1038 | 2,131877               | 0,1032 | 2,131881                 | 0,1030 |
| 71       | 2,144459               | 2,139730 | 0,2205 | 2,143230               | 0,0573 | 2,144105                 | 0,0165 |
| 71       | 2,144459               | 2,139730 | 0,2205 | 2,143230               | 0,0573 | 2,144105                 | 0,0165 |
| 42       | 2,320599               | 2,318342 | 0,0973 | 2,319103               | 0,0645 | 2,319293                 | 0,0563 |
| 42       | 2,320599               | 2,318342 | 0,0973 | 2,319103               | 0,0645 | 2,319293                 | 0,0563 |
| 81       | 2,411855               | 2,404854 | 0,2903 | 2,410047               | 0,0750 | 2,411346                 | 0,0211 |
| 81       | 2,411855               | 2,404854 | 0,2903 | 2,410047               | 0,0750 | 2,411346                 | 0,0211 |
| 23       | 2,492367               | 2,489344 | 0,1213 | 2,489451               | 0,1170 | 2,489477                 | 0,1159 |

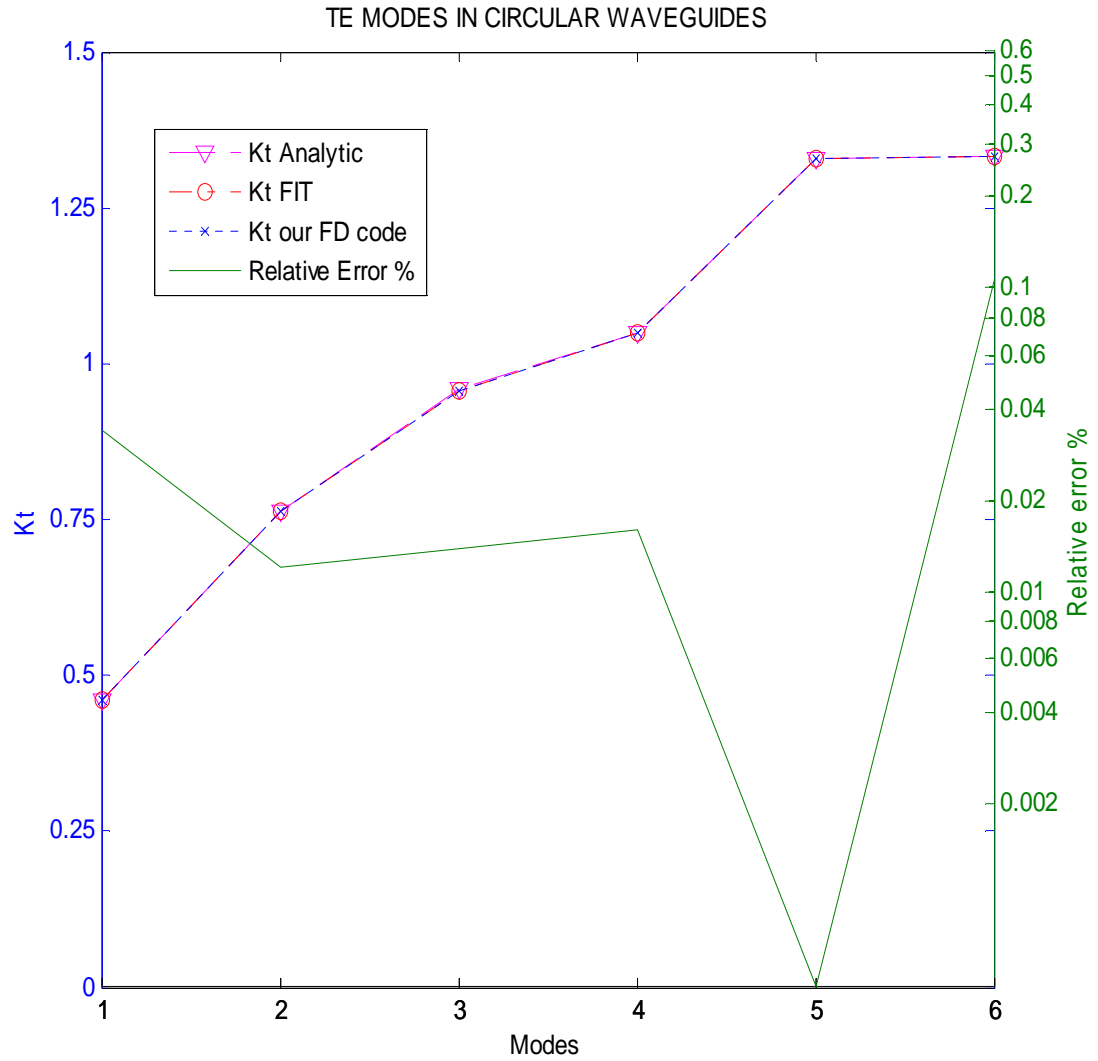


Fig. 6.2.1. Comparison between our FD code and analytic results and FIT(CST) results for TE modes in circular wave guide with  $r=4$  mm  $\Delta r=0.0792$  mm and  $\theta=1^\circ$ ;

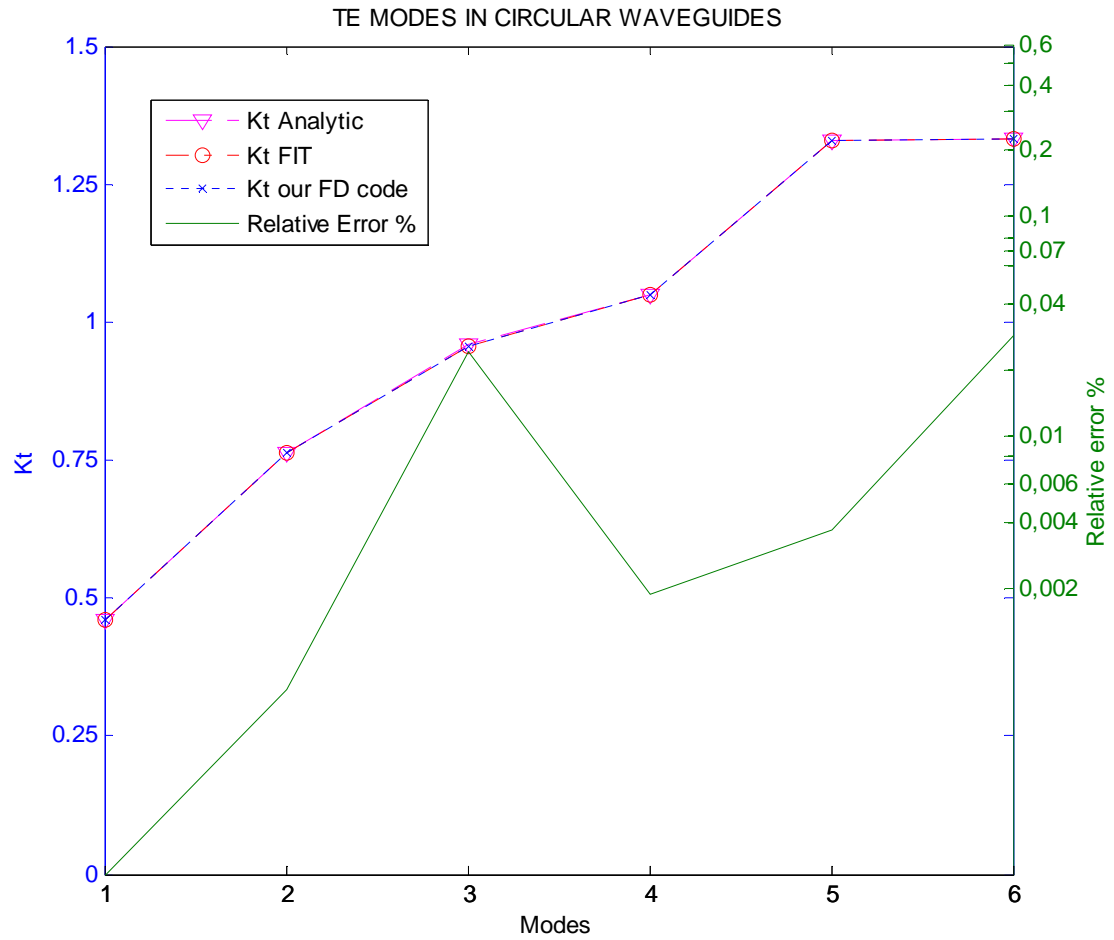


Fig. 6.2. Comparison between our FD code and analitic results and FIT(CST) results for TE modes in circular wave guide with  $r=4$  mm  $\Delta r=0.0792$  mm and  $\Delta\theta =0,5^\circ$ ,

We have made several tests by varying the steps ( $\Delta r, \Delta\theta$ ). The results of the tables and Figures (6.2.1,6.2.2) shows that our technique has a very low error, as long as the steps are small. When compared to CST our results are better, and can be obtained in a fraction of the computational time required by the former. However, the comparison of FIT and analytical results show that CST is

quite accurate, too, and can be used to test our approach for waveguide. S without known analytical solutions.

In the table 6.2.10 you can see the  $k_t$  of TE and TM modes calculated on the TE grids, where varying  $\Delta u$ .

Data of the elliptic waveguide:

major axis=8.6558

minor axis=4

eccentricity=0.8868

$\Delta v=1^\circ$

$k_{tcst}=k_t$  of CST

$k_{tp}=k_t$  of the program

ep= percentage (relative) error

In the table 6.2.11 you can see the  $k_t$  of TE and TM modes calculated on the TE grids, where varying  $\Delta v$ .

Data of the elliptic waveguide:

major axis=8.6558

minor axis=4

eccentricity=0.8868

$\Delta u= 0,002488$

$k_{tcst}=k_t$  of CST

$k_{tp}=k_t$  of the program

ep= percentage (relative) error

Table 6.2.10: comparison between our FD code and FIT (CST) results for TE and TM modes on TE grid in elliptic waveguide , with different  $\Delta u$

|          |          | Du=0,009804 |        | Du=0,00495 |        | Du=0,002488 |        |
|----------|----------|-------------|--------|------------|--------|-------------|--------|
| TE MODES | Ktcst    | Ktp         | ep%    | Ktp        | ep%    | Ktp         | ep%    |
| I        | 0,216761 | 0,216519    | 0,1118 | 0,216590   | 0,0793 | 0,216635    | 0,0582 |
| II       | 0,396308 | 0,395816    | 0,1241 | 0,395990   | 0,0801 | 0,396100    | 0,0524 |
| III      | 0,439542 | 0,439368    | 0,0396 | 0,439382   | 0,0364 | 0,439391    | 0,0345 |
| IV       | 0,566608 | 0,566490    | 0,0208 | 0,566483   | 0,0222 | 0,566489    | 0,0211 |
| V        | 0,572023 | 0,571366    | 0,1149 | 0,571657   | 0,0640 | 0,571839    | 0,0322 |
| VI       | 0,703570 | 0,703502    | 0,0097 | 0,703468   | 0,0144 | 0,703472    | 0,0139 |
| VII      | 0,745401 | 0,744851    | 0,0738 | 0,745251   | 0,0200 | 0,745499    | 0,0133 |
| VIII     | 0,840046 | 0,840037    | 0,0011 | 0,840362   | 0,0376 | 0,840452    | 0,0483 |
| IX       | 0,847613 | 0,847548    | 0,0076 | 0,847488   | 0,0147 | 0,847488    | 0,0147 |
| X        | 0,917454 | 0,916716    | 0,0804 | 0,917201   | 0,0275 | 0,917499    | 0,0049 |

|          |          | Du=0,009804 |        | Du=0,00495 |        | Du=0,002488 |        |
|----------|----------|-------------|--------|------------|--------|-------------|--------|
| TM MODES | Ktcst    | Ktp         | ep%    | Ktp        | ep%    | Ktp         | ep%    |
| I        | 0,464520 | 0,464404    | 0,0251 | 0,464440   | 0,0172 | 0,464453    | 0,0145 |
| II       | 0,604530 | 0,604413    | 0,0194 | 0,604491   | 0,0066 | 0,604510    | 0,0034 |
| III      | 0,754913 | 0,754794    | 0,0159 | 0,754979   | 0,0086 | 0,755022    | 0,0144 |
| IV       | 0,849685 | 0,849803    | 0,0139 | 0,850105   | 0,0494 | 0,850197    | 0,0602 |
| V        | 0,911798 | 0,911963    | 0,0181 | 0,912364   | 0,0621 | 0,912465    | 0,0732 |
| VI       | 0,979441 | 0,978743    | 0,0712 | 0,979020   | 0,0429 | 0,979111    | 0,0337 |
| VII      | 1,075333 | 1,073525    | 0,1682 | 1,074296   | 0,0964 | 1,074508    | 0,0768 |
| VIII     | 1,115153 | 1,114329    | 0,0739 | 1,114573   | 0,0521 | 1,114662    | 0,0441 |
| IX       | 1,241573 | 1,237907    | 0,2953 | 1,239242   | 0,1877 | 1,239628    | 0,1566 |
| X        | 1,241775 | 1,239674    | 0,1692 | 1,240780   | 0,0801 | 1,241088    | 0,0553 |

Table 6.2.11: comparison between our FD code and FIT (CST) results for TE and TM modes on TE grid in elliptic waveguide , when varying  $\Delta\theta$

|          |          | Dv=2°    |        | Dv=1°    |        | Dv=0,5°  |        |
|----------|----------|----------|--------|----------|--------|----------|--------|
| TE MODES | Ktcst    | Ktp      | ep%    | Ktp      | ep%    | Ktp      | ep%    |
| I        | 0,216761 | 0,216608 | 0,0708 | 0,216635 | 0,0582 | 0,216645 | 0,0539 |
| II       | 0,396308 | 0,395976 | 0,0839 | 0,396100 | 0,0524 | 0,396138 | 0,0430 |
| III      | 0,439542 | 0,439381 | 0,0366 | 0,439391 | 0,0345 | 0,439393 | 0,0340 |
| IV       | 0,566608 | 0,566423 | 0,0327 | 0,566489 | 0,0211 | 0,566505 | 0,0182 |
| V        | 0,572023 | 0,571502 | 0,0911 | 0,571839 | 0,0322 | 0,571933 | 0,0158 |
| VI       | 0,703570 | 0,703247 | 0,0458 | 0,703472 | 0,0139 | 0,703527 | 0,0060 |
| VII      | 0,745401 | 0,744793 | 0,0815 | 0,745500 | 0,0133 | 0,745689 | 0,0387 |
| VIII     | 0,840046 | 0,840431 | 0,0458 | 0,840452 | 0,0483 | 0,840457 | 0,0489 |
| IX       | 0,847613 | 0,846957 | 0,0774 | 0,847488 | 0,0147 | 0,847620 | 0,0009 |
| X        | 0,917454 | 0,916227 | 0,1337 | 0,917499 | 0,0049 | 0,917833 | 0,0413 |

|          |          | Dv=2°    |        | Dv=1°    |        | Dv=0,5°  |        |
|----------|----------|----------|--------|----------|--------|----------|--------|
| TM MODES | Ktcst    | Ktp      | ep%    | Ktp      | ep%    | Ktp      | ep%    |
| I        | 0,464520 | 0,464441 | 0,0170 | 0,464453 | 0,0145 | 0,464456 | 0,0139 |
| II       | 0,604530 | 0,604430 | 0,0166 | 0,604510 | 0,0034 | 0,604530 | 0,0000 |
| III      | 0,754913 | 0,754756 | 0,0209 | 0,755022 | 0,0144 | 0,755089 | 0,0233 |
| IV       | 0,849685 | 0,850176 | 0,0577 | 0,850197 | 0,0602 | 0,850202 | 0,0608 |
| V        | 0,911798 | 0,911843 | 0,0049 | 0,912465 | 0,0732 | 0,912624 | 0,0906 |
| VI       | 0,979441 | 0,978984 | 0,0466 | 0,979111 | 0,0337 | 0,979143 | 0,0304 |
| VII      | 1,075333 | 1,073307 | 0,1885 | 1,074508 | 0,0768 | 1,074815 | 0,0482 |
| VIII     | 1,115153 | 1,114278 | 0,0785 | 1,114662 | 0,0441 | 1,114757 | 0,0355 |
| IX       | 1,241573 | 1,237575 | 0,3220 | 1,239628 | 0,1566 | 1,240155 | 0,1142 |
| X        | 1,241775 | 1,241056 | 0,0579 | 1,241088 | 0,0553 | 1,241096 | 0,0547 |

For elliptic waveguide we have considered different axial ratios and we compared our FD results only with FIT simulations. We present her only this case of an axial ratio of 2, giving a relative error of less that 0.2% but other aspect ratios gives comparable accuracy.



### 6.3) FD IN ROUNDED-END WAVEGUIDE

In this paragraph we will show the results of techniques presented in the paragraph 5.2. To assess our FD code in this case, we have evaluated a few TE modes, for different structures.

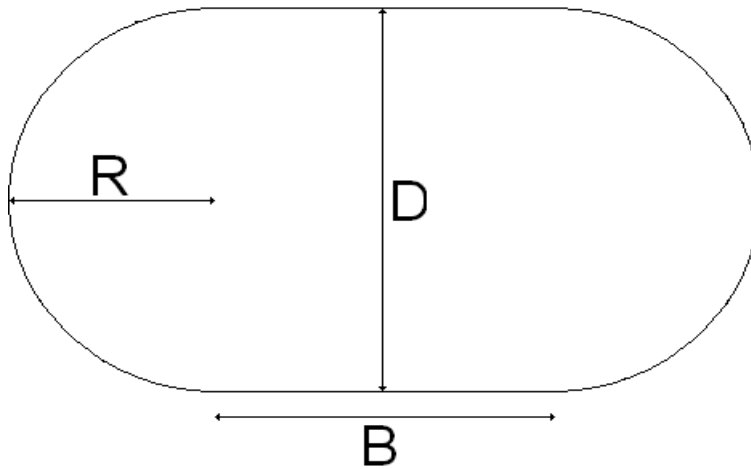


Fig.6.3.1 – 6.3.6 shows the comparison between our results and CST ones.

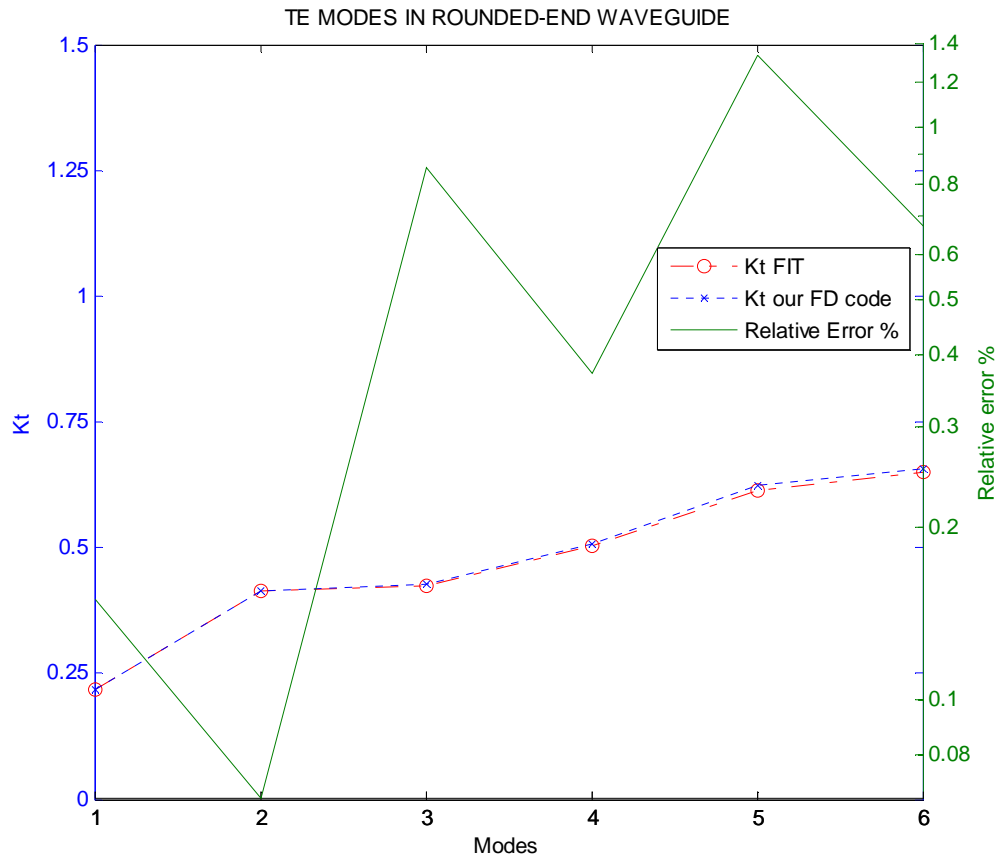


Fig. 6.3.1. Comparison between our FD code and and FIT (CST) results for TE modes in Rounded-end wave guide with  $\Delta x = \Delta y = \Delta r = 0,1569$  mm  $D=B=8$  mm and  $\theta=1^\circ$ ;

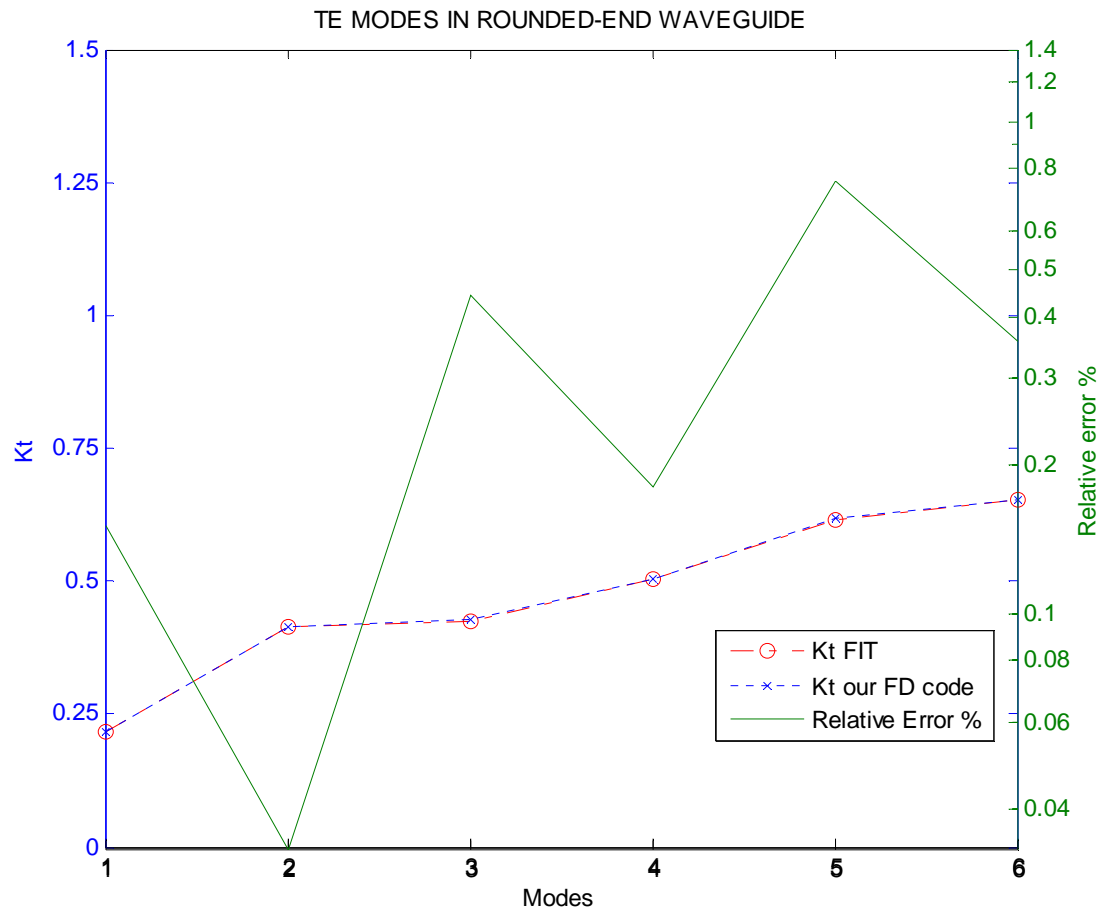


Fig. 6.3.2. Comparison between our FD code and FIT (CST) results for TE modes in Rounded-end wave guide with  $\Delta x = \Delta y = \Delta r = 0,0792$  mm  $D=B=8$  mm and  $\Delta\theta=1^\circ$ ;

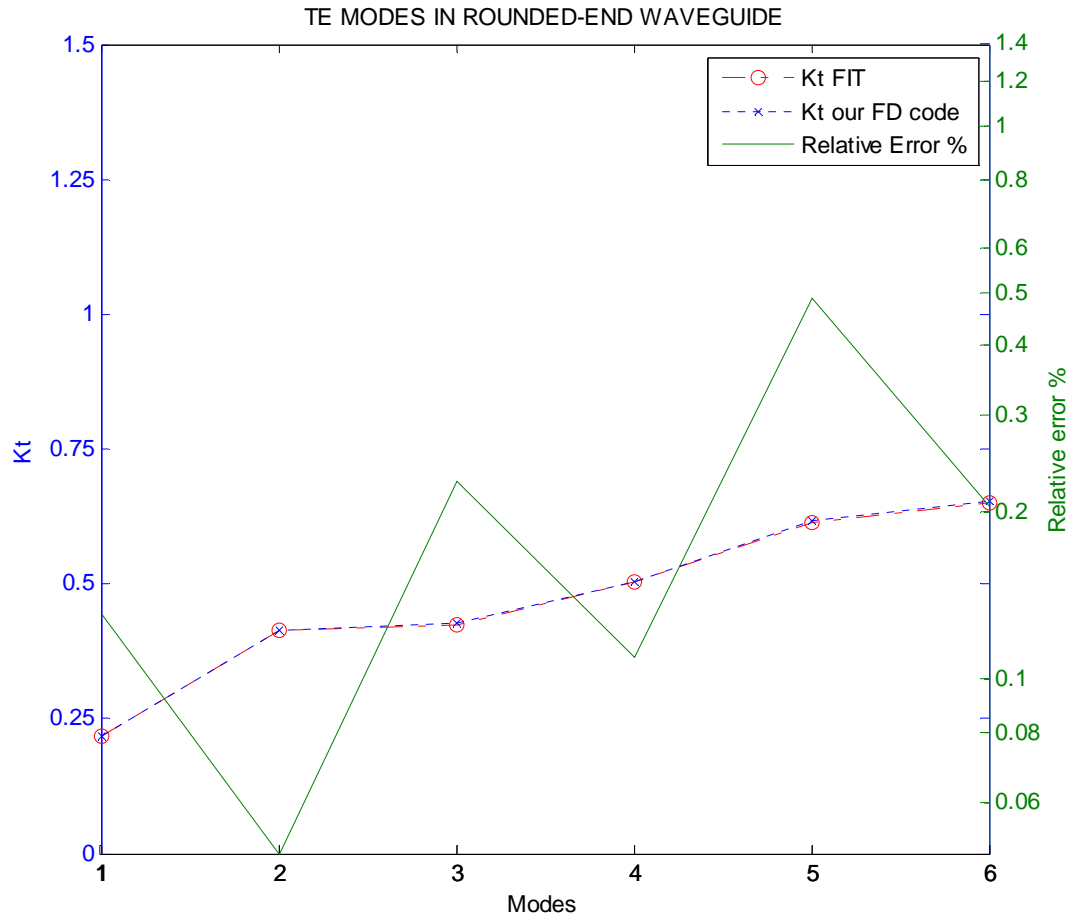


Fig. 6.3.3. Comparison between our FD code and and FIT (CST) results for TE modes in Rounded-end wave guide with  $\Delta x = \Delta y = \Delta r = 0,03980$  mm  $D=B=8$  mm and  $\theta=1^\circ$ ;

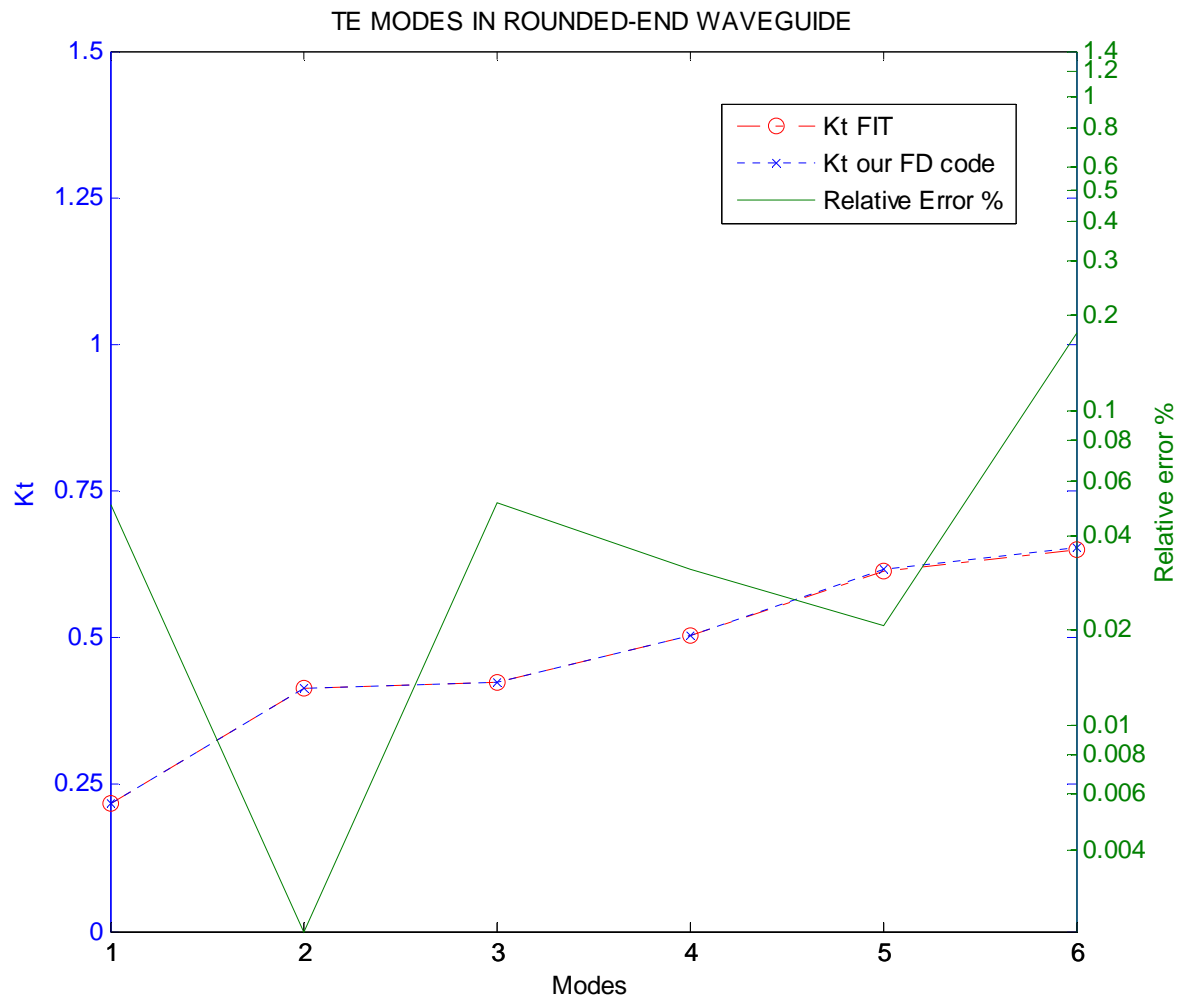


Fig. 6.3.4. Comparison between our FD code and and FIT (CST) results for TE modes in Rounded-end wave guide with  $\Delta x = \Delta y = \Delta r = 0,01995$  mm  $D=B=8$  mm and  $\theta=1^\circ$ ;

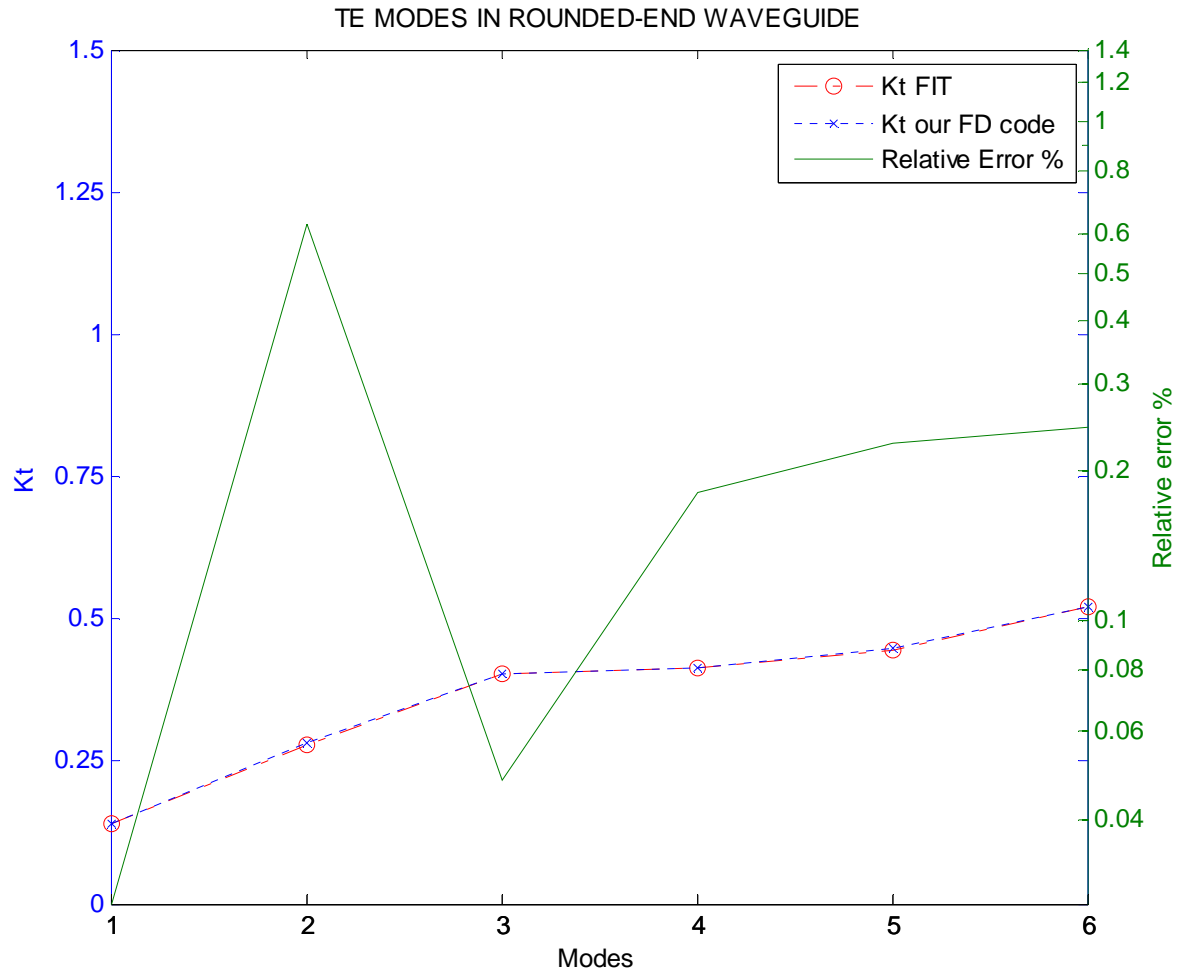


Fig. 6.3.5. Comparison between our FD code and and FIT (CST) results for TE modes in Rounded-end wave guide with  $\Delta x = \Delta y = \Delta r = 0,0792$  mm  $D=8$  mm  $B=16$  mm and  $\theta=1^\circ$ ;

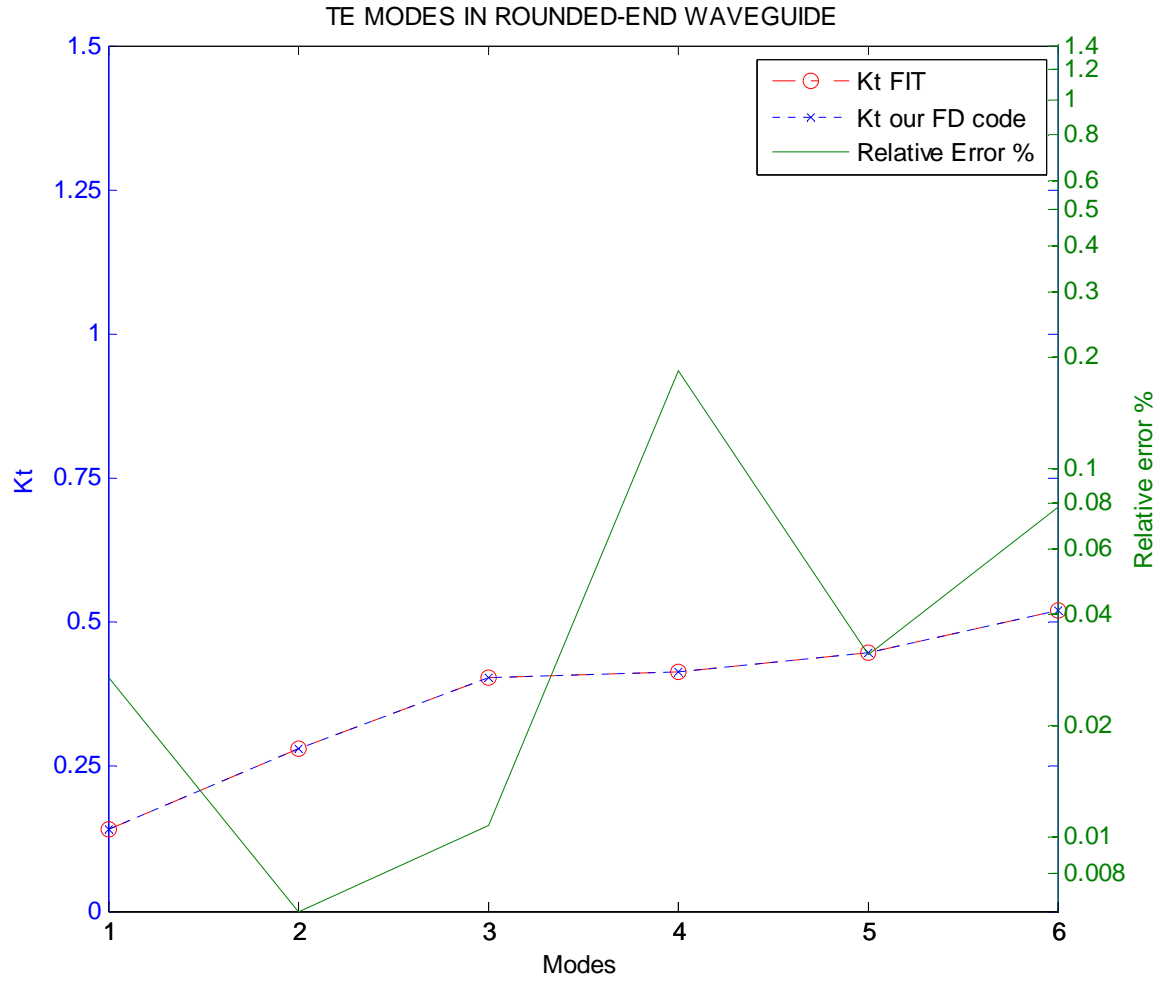


Fig. 6.3.6. Comparison between our FD code and and FIT (CST) results for TE modes in Rounded-end wave guide with  $\Delta x = \Delta y = \Delta r = 0,03980$  mm  $D=8$  mm  $B=16$  mm and  $\theta=1^\circ$ ;

The results shows that our FD approach allows an high accuracy, when the discretization step is suitably chosen. But even a quite large steps, as in the case of Figure 6.3.3, allows a quite accurate mode evaluation.

#### **6.4) VECTOR FD IN RECTANGULAR WAVEGUIDE**

In this paragraph we will show the results of techniques presented in the paragraph 3.4. To assess the proposed technique we have analyzed a Rectangular waveguide and compared the eigenvalues and eigenvectors of the first few TE modes with their exact values. In the table 6.4.1 you can see the  $k_t$  and Max eigenvectors error percentage of TE modes calculated on the TE grids.

Data of the rectangular waveguide:

$a=3.35$ ,  $b=1.65$        $\Delta x=\Delta y=0.05$

$k_{ta}=k_t$  analytical

$k_{tps}=k_t$  of the program use scalar FD

$k_{tpv}=k_t$  of the program use vector FD

$epv$ = percentage (relative) error between  $k_{ta}$  and  $k_{tpv}$

Max eigenvectors error%= Max eigenvectors error percentage of TE modes calculated.



Table 6.4.1: comparison between our vector FD code and analytic results for TE modes on TE grid in rectangular waveguide

| TE MODES | Kta      | Ktps     | Ktpv     | epv%     | Max eigenvectors error % |
|----------|----------|----------|----------|----------|--------------------------|
| 10       | 0,937789 | 0,937703 | 0,937707 | 0,008211 | 0,000634                 |
| 20       | 1,875578 | 1,874890 | 1,874921 | 0,065649 | 0,005065                 |
| 01       | 1,903996 | 1,903277 | 1,903342 | 0,065364 | 0,005218                 |
| 11       | 2,122415 | 2,121732 | 2,121742 | 0,067299 | 0,054902                 |
| 21       | 2,672637 | 2,671643 | 2,671576 | 0,106113 | 0,017336                 |
| 30       | 2,813367 | 2,811048 | 2,811151 | 0,221568 | 0,017055                 |
| 31       | 3,397092 | 3,394768 | 3,394683 | 0,240807 | 0,124122                 |
| 40       | 3,751155 | 3,745660 | 3,745904 | 0,525173 | 0,040353                 |
| 02       | 3,807991 | 3,802242 | 3,802760 | 0,523096 | 0,041615                 |
| 12       | 3,921765 | 3,916163 | 3,916553 | 0,521283 | 0,153269                 |
| 41       | 4,206705 | 4,201479 | 4,201458 | 0,524732 | 0,233309                 |
| 22       | 4,244831 | 4,239370 | 4,239449 | 0,538210 | 0,244167                 |
| 50       | 4,688944 | 4,678213 | 4,678687 | 1,025698 | 0,078287                 |
| 32       | 4,734536 | 4,728534 | 4,728267 | 0,626906 | 0,240676                 |
| 51       | 5,060770 | 5,050558 | 5,050698 | 1,007252 | 0,322581                 |
| 42       | 5,345275 | 5,337322 | 5,336782 | 0,849241 | 0,142042                 |

Data of the rectangular waveguide:

$a=3.35$ ,  $b=1.65$        $\Delta x=\Delta y=0.025$

kta=kt analytical

ktps=kt of the program use scalar FD

ktpv=kt of the program use vector FD

epv= percentage (relative) error between kta and Ktpv

Max eigenvectors error%= Max eigenvectors error percentage of TE modes calculated.

Table 6.4.2: comparison between our vector FD code and analytic results for TE modes on TE grid in rectangular waveguide

| TE MODES | Kta      | Ktps     | Ktpv     | epv%   | Max eigenvectors<br>relative error% |
|----------|----------|----------|----------|--------|-------------------------------------|
| 10       | 0,937789 | 0,937767 | 0,937768 | 0,0021 | 0,0001                              |
| 20       | 1,875578 | 1,875406 | 1,875410 | 0,0168 | 0,0006                              |
| 01       | 1,903996 | 1,903816 | 1,903824 | 0,0172 | 0,0007                              |
| 11       | 2,122415 | 2,122245 | 2,122246 | 0,0170 | 0,0139                              |
| 21       | 2,672637 | 2,672389 | 2,672380 | 0,0257 | 0,0021                              |
| 30       | 2,813367 | 2,812787 | 2,812800 | 0,0567 | 0,0022                              |
| 31       | 3,397092 | 3,396511 | 3,396500 | 0,0592 | 0,0313                              |
| 40       | 3,751155 | 3,749781 | 3,749812 | 0,1344 | 0,0051                              |
| 02       | 3,807991 | 3,806553 | 3,806618 | 0,1373 | 0,0053                              |
| 12       | 3,921765 | 3,920364 | 3,920413 | 0,1352 | 0,0361                              |
| 41       | 4,206705 | 4,205398 | 4,205395 | 0,1310 | 0,0557                              |
| 22       | 4,244831 | 4,243465 | 4,243474 | 0,1356 | 0,0583                              |
| 50       | 4,688944 | 4,686260 | 4,686320 | 0,2624 | 0,0100                              |
| 32       | 4,734536 | 4,733035 | 4,733001 | 0,1535 | 0,0544                              |
| 51       | 5,060770 | 5,058216 | 5,058233 | 0,2537 | 0,0806                              |
| 42       | 5,345275 | 5,343286 | 5,343218 | 0,2056 | 0,0174                              |

The results of Tables 6.4.1, 6.4.2 shows that our technique has a very low error, as long as the discretization steps are small.

## 6.5) VECTOR FD IN CIRCULAR WAVEGUIDE

In this paragraph we will show the results of techniques presented in the paragraph 4.3. To assess the proposed technique we have analyzed a Circular waveguide and compared the eigenvalues and eigenvectors of the first few TE modes with their exact values. In the table 6.5.1 you can see the  $k_t$  and RMS error on eigenvectors of TE modes calculated on the TE grids.

Table 6.5.1: comparison between our vector FD code and analytic results for TE modes on TE grid in circular waveguide

| n,p | Kta      | Ktpv     | ep%      | RMS_error *1.0e-006 |
|-----|----------|----------|----------|---------------------|
| 11  | 0,460296 | 0,460292 | 0,000793 | 0.0001              |
| 21  | 0,763559 | 0,763531 | 0,003656 | 0.0007              |
| 01  | 0,957927 | 0,957697 | 0,023982 | 0.0008              |
| 31  | 1,050297 | 1,050204 | 0,008831 | 0.0011              |
| 41  | 1,329388 | 1,329170 | 0,016382 | 0.0013              |
| 12  | 1,332861 | 1,332475 | 0,028974 | 0.0173              |
| 51  | 1,603904 | 1,603482 | 0,026341 | 0.0015              |
| 22  | 1,676533 | 1,675952 | 0,034689 | 0.0682              |
| 02  | 1,753897 | 1,752487 | 0,080364 | 0.0012              |
| 61  | 1,875317 | 1,874590 | 0,038724 | 0.0015              |
| 32  | 2,003809 | 2,002971 | 0,041806 | 0.1195              |
| 13  | 2,134079 | 2,132172 | 0,089353 | 0.1302              |
| 71  | 2,144459 | 2,143311 | 0,053550 | 0.0016              |
| 42  | 2,320599 | 2,319424 | 0,050620 | 0.1734              |
| 81  | 2,411855 | 2,410147 | 0,070825 | 0.0017              |

The same comparison has been made in Table 6.5.1 for a circular waveguide, with a radius equal to 4 (in normalized units), and using discretization steps of  $\Delta r = 0.0396$ ,  $\Delta \vartheta = 1^\circ$ . In both tables  $k_{ta}$  and  $k_{tpv}$  are the eigenvalues computed analytically [6] and using our approach,  $ep\%$  is the percentage error between them, and the last column shows the RMS difference between analytical mode vectors, and those computed using (I.9).

From these data, it appears that our technique is able to give all mode data with a very small error, both on eigenvalues and on eigenvectors. The error on the forms is significantly smaller for the circular case. The RMS error on normalized modes is even smaller, being less than  $5 \cdot 10^{-8}$  in circular case.

## 6.6) VECTOR FD IN ELLIPTIC WAVEGUIDE

In this paragraph we will show the results of techniques presented in the paragraph 4.4. To assess the proposed technique we have analyzed a Elliptical waveguide and compared the eigenvalues and eigenvectors of the first few TE modes with their exact values. Tables 6.6.1,6.6.2,6.6.3 shows the validation test for an elliptic waveguide, with a length of the minor axis (in normalized units) equal to 4, and different eccentricities  $ex$ , discretized with  $\Delta\nu = 1^\circ$ , and a different number  $Nu$  of discretization ellipses. Though an analytical solution is available for elliptic waveguides [11], its effectiveness is very poor, and many numerical techniques have been proposed in the literature. As in many of those papers, we use, for our comparison, the eigenvalues  $k_{ta}$  obtained from the cut-off wavelength data reported in [36]. From the data in Tables 6.6.1,6.6.2,6.6.3, it is clear that, for all cases shown, the eigenvalues  $k_{tpv}$  computed from our techniques are very accurate.

Table 6.6.1: comparison between our vector FD code and analytic results for TE modes on TE grid in elliptic waveguide with  $\epsilon_x=0,1$  ,  $\Delta v = 1^\circ$  and  $\Delta u$  variable.

| $\epsilon_x=0,1$ | hta       | Nu=100    | e%     | Nu=200    | e%     | Nu=400    | e%     |
|------------------|-----------|-----------|--------|-----------|--------|-----------|--------|
| TEc1-1           | 0,4581763 | 0,4582208 | 0,0097 | 0,4581167 | 0,0130 | 0,4580902 | 0,0188 |
| TEs1-1           | 0,4602013 | 0,4603401 | 0,0302 | 0,4602356 | 0,0074 | 0,4602092 | 0,0017 |
| TEc2-1           | 0,7616249 | 0,7618597 | 0,0308 | 0,7616784 | 0,0070 | 0,7616328 | 0,0010 |
| TEs2-1           | 0,7616464 | 0,7618813 | 0,0308 | 0,7616999 | 0,0070 | 0,7616542 | 0,0010 |
| TEc0-1           | 0,9555448 | 0,9551314 | 0,0433 | 0,9554371 | 0,0113 | 0,9555118 | 0,0035 |
| TEc3-1           | 1,0476538 | 1,0479783 | 0,0310 | 1,0477170 | 0,0060 | 1,0476516 | 0,0002 |
| TEs3-1           | 1,0476539 | 1,0479785 | 0,0310 | 1,0477172 | 0,0060 | 1,0476517 | 0,0002 |
| TEc4-1           | 1,3260436 | 1,3264481 | 0,0305 | 1,3261025 | 0,0044 | 1,3260164 | 0,0021 |
| TEs4-1           | 1,3260436 | 1,3264481 | 0,0305 | 1,3261025 | 0,0044 | 1,3260164 | 0,0021 |
| TEc1-2           | 1,3277392 | 1,3265297 | 0,0911 | 1,3274329 | 0,0231 | 1,3276602 | 0,0059 |
| TEs1-2           | 1,3313232 | 1,3300634 | 0,0946 | 1,3310037 | 0,0240 | 1,3312421 | 0,0061 |
| TEc5-1           | 1,5998694 | 1,6003400 | 0,0294 | 1,5999051 | 0,0022 | 1,5997974 | 0,0045 |
| TEs5-1           | 1,5998694 | 1,6003400 | 0,0294 | 1,5999051 | 0,0022 | 1,5997974 | 0,0045 |
| TEc2-2           | 1,6722143 | 1,6699783 | 0,1337 | 1,6716427 | 0,0342 | 1,6720643 | 0,0090 |
| TEs2-2           | 1,6723449 | 1,6701076 | 0,1338 | 1,6717729 | 0,0342 | 1,6721948 | 0,0090 |
| TEc0-2           | 1,7496312 | 1,7459051 | 0,2130 | 1,7486822 | 0,0542 | 1,7493761 | 0,0146 |
| TEc2-3           | 2,4857717 | 2,4763404 | 0,3794 | 2,4836944 | 0,0836 | 2,4855461 | 0,0091 |
| TEs6-2           | 2,9263444 | 2,9185745 | 0,2655 | 2,9242314 | 0,0722 | 2,9256595 | 0,0234 |
| TEc11-1          | 3,1985589 | 3,2154367 | 0,5277 | 3,1977907 | 0,0240 | 3,1975337 | 0,0321 |

Table 6.6.2: comparison between our vector FD code and analytic results for TE modes on TE grid in elliptic waveguide with  $ex=0,5$  ,  $\Delta v = 1^\circ$  and  $\Delta u$  variable.

| ex=0,5 | kta       | Nu=100    | e%     | Nu=200    | e%     | Nu=400    | e%     |
|--------|-----------|-----------|--------|-----------|--------|-----------|--------|
| TEc1-1 | 0,4007537 | 0,4007794 | 0,0064 | 0,4007558 | 0,0005 | 0,4007477 | 0,0015 |
| TEs1-1 | 0,4573402 | 0,4573597 | 0,0043 | 0,4573447 | 0,0010 | 0,4573409 | 0,0001 |
| TEc2-1 | 0,6977267 | 0,6977632 | 0,0052 | 0,6977281 | 0,0002 | 0,6977169 | 0,0014 |
| TEs2-1 | 0,7129897 | 0,7130268 | 0,0052 | 0,7129942 | 0,0006 | 0,7129861 | 0,0005 |
| TEc0-1 | 0,9072690 | 0,9071392 | 0,0143 | 0,9072289 | 0,0044 | 0,9072557 | 0,0015 |
| TEc3-1 | 0,9697687 | 0,9698069 | 0,0039 | 0,9697602 | 0,0009 | 0,9697479 | 0,0021 |
| TEs3-1 | 0,9731326 | 0,9731735 | 0,0042 | 0,9731259 | 0,0007 | 0,9731138 | 0,0019 |
| TEc1-2 | 1,2056011 | 1,2053633 | 0,0197 | 1,2054972 | 0,0086 | 1,2055450 | 0,0047 |
| TEc4-1 | 1,2301100 | 1,2301380 | 0,0023 | 1,2300769 | 0,0027 | 1,2300614 | 0,0040 |
| TEs4-1 | 1,2307620 | 1,2307916 | 0,0024 | 1,2307297 | 0,0026 | 1,2307142 | 0,0039 |
| TEs1-2 | 1,2982175 | 1,2977695 | 0,0345 | 1,2981032 | 0,0088 | 1,2981879 | 0,0023 |
| TEc5-1 | 1,4849816 | 1,4849813 | 0,0000 | 1,4849048 | 0,0052 | 1,4848852 | 0,0065 |
| TEs5-1 | 1,4850990 | 1,4850993 | 0,0000 | 1,4850225 | 0,0052 | 1,4850033 | 0,0064 |
| TEc2-2 | 1,5162727 | 1,5158575 | 0,0274 | 1,5160720 | 0,0132 | 1,5161445 | 0,0085 |
| TEs2-2 | 1,5741075 | 1,5735833 | 0,0333 | 1,5739680 | 0,0089 | 1,5740659 | 0,0026 |
| TEc0-2 | 1,6945503 | 1,6934183 | 0,0668 | 1,6942624 | 0,0170 | 1,6944732 | 0,0046 |
| TEc1-4 | 2,0884337 | 2,0861798 | 0,1079 | 2,0878626 | 0,0273 | 2,0882878 | 0,0070 |
| TEs6-2 | 2,7535930 | 2,7493575 | 0,1538 | 2,7525100 | 0,0393 | 2,7533090 | 0,0103 |
| TEc0-4 | 3,2687699 | 3,2595013 | 0,2835 | 3,2663930 | 0,0727 | 3,2681693 | 0,0184 |

Table 6.6.3: comparison between our vector FD code and analytic results for TE modes on TE grid in elliptic waveguide with  $\epsilon_x=0,9$  ,  $\Delta v = 1^\circ$  and  $\Delta u$  variable.

| $\epsilon_x=0,9$ | kta       | Nu=100    | e%     | Nu=200    | e%     | Nu=400    | e%     |
|------------------|-----------|-----------|--------|-----------|--------|-----------|--------|
| TEc1-1           | 0,2044955 | 0,2044593 | 0,0177 | 0,2044777 | 0,0087 | 0,2044887 | 0,0033 |
| TEc2-1           | 0,3744120 | 0,3743190 | 0,0248 | 0,3743640 | 0,0128 | 0,3743908 | 0,0057 |
| TEs1-1           | 0,4375153 | 0,4375027 | 0,0029 | 0,4375116 | 0,0009 | 0,4375138 | 0,0004 |
| TEc3-1           | 0,5410773 | 0,5409102 | 0,0309 | 0,5409863 | 0,0168 | 0,5410313 | 0,0085 |
| TEs2-1           | 0,5570149 | 0,5570002 | 0,0027 | 0,5570071 | 0,0014 | 0,5570088 | 0,0011 |
| TEs3-1           | 0,6856484 | 0,6856239 | 0,0036 | 0,6856284 | 0,0029 | 0,6856296 | 0,0028 |
| TEc4-1           | 0,7060436 | 0,7057903 | 0,0359 | 0,7058971 | 0,0208 | 0,7059600 | 0,0118 |
| TEs4-1           | 0,8209958 | 0,8209498 | 0,0056 | 0,8209517 | 0,0054 | 0,8209522 | 0,0053 |
| TEc0-1           | 0,8373801 | 0,8372581 | 0,0146 | 0,8373480 | 0,0038 | 0,8373707 | 0,0011 |
| TEc5-1           | 0,8697291 | 0,8693819 | 0,0399 | 0,8695147 | 0,0247 | 0,8695927 | 0,0157 |
| TEc1-2           | 0,9562268 | 0,9560986 | 0,0134 | 0,9561867 | 0,0042 | 0,9562090 | 0,0019 |
| TEs5-1           | 0,9612009 | 0,9611177 | 0,0087 | 0,9611169 | 0,0087 | 0,9611166 | 0,0088 |
| TEc6-1           | 1,0322693 | 1,0318234 | 0,0432 | 1,0319741 | 0,0286 | 1,0320626 | 0,0200 |
| TEc2-2           | 1,0813326 | 1,0811866 | 0,0135 | 1,0812725 | 0,0056 | 1,0812943 | 0,0035 |
| TEs6-1           | 1,1048916 | 1,1047514 | 0,0127 | 1,1047479 | 0,0130 | 1,1047470 | 0,0131 |
| TEc7-1           | 1,1937006 | 1,1931511 | 0,0460 | 1,1933100 | 0,0327 | 1,1934033 | 0,0249 |
| TEs7-1           | 1,2510720 | 1,2508515 | 0,0176 | 1,2508455 | 0,0181 | 1,2508440 | 0,0182 |
| TEc5-2           | 1,4870521 | 1,4867331 | 0,0215 | 1,4868168 | 0,0158 | 1,4868391 | 0,0143 |
| TEc12-1          | 1,9845625 | 1,9832412 | 0,0666 | 1,9833291 | 0,0621 | 1,9835141 | 0,0528 |
| TEc4-3           | 2,1094353 | 2,1082575 | 0,0558 | 2,1089925 | 0,0210 | 2,1091784 | 0,0122 |

## 6.7) EXTENSION TO 3D PROBLEM

In this paragraph we will show the results of techniques presented in the paragraph 3.7. In the table 6.6.4 you can see the  $k_t$  of modes calculated on the Newmann grid. Data of the rectangular cavite waveguide:

$a=10, b=2, c=2 \quad \Delta x=\Delta y=\Delta z=0.1$

$k_{ta}=k_t$  analytical

$k_{tp}=k_t$  of the program

ep= percentage (relative) error

Total points of the grid: 40000



Table 6.6.4: comparison between our 3D FD code and analytic results for modes on Newmann grid in a rectangular cavity.

| n | p | z | kta(Newmann) | ktp(Newmann) | ep(Newmann)% |
|---|---|---|--------------|--------------|--------------|
| 1 | 0 | 0 | 0,3141593    | 0,3141463    | 0,0013       |
| 2 | 0 | 0 | 0,6283185    | 0,6282152    | 0,0103       |
| 3 | 0 | 0 | 0,9424778    | 0,9421290    | 0,0349       |
| 4 | 0 | 0 | 1,2566371    | 1,2558104    | 0,0827       |
| 0 | 0 | 1 | 1,5707963    | 1,5691819    | 0,1614       |
| 0 | 1 | 0 | 1,5707963    | 1,5691819    | 0,1614       |
| 5 | 0 | 0 | 1,5707963    | 1,5691819    | 0,1614       |
| 1 | 0 | 1 | 1,6019042    | 1,6003187    | 0,1586       |
| 1 | 1 | 0 | 1,6019042    | 1,6003187    | 0,1586       |
| 2 | 0 | 1 | 1,6917994    | 1,6902622    | 0,1537       |
| 2 | 1 | 0 | 1,6917994    | 1,6902622    | 0,1537       |
| 3 | 0 | 1 | 1,8318476    | 1,8302838    | 0,1564       |
| 3 | 1 | 0 | 1,8318476    | 1,8302838    | 0,1564       |
| 6 | 0 | 0 | 1,8849556    | 1,8821663    | 0,2789       |
| 4 | 0 | 1 | 2,0116008    | 2,0098238    | 0,1777       |
| 4 | 1 | 0 | 2,0116008    | 2,0098238    | 0,1777       |
| 7 | 0 | 0 | 2,1991149    | 2,1946862    | 0,4429       |
| 0 | 1 | 1 | 2,2214415    | 2,2191583    | 0,2283       |
| 5 | 0 | 1 | 2,2214415    | 2,2191583    | 0,2283       |
| 5 | 1 | 0 | 2,2214415    | 2,2191583    | 0,2283       |
| 1 | 1 | 1 | 2,2435459    | 2,2412835    | 0,2262       |
| 2 | 1 | 1 | 2,3085897    | 2,3063647    | 0,2225       |
| 3 | 1 | 1 | 2,4131031    | 2,4108652    | 0,2238       |
| 6 | 0 | 1 | 2,4536623    | 2,4504860    | 0,3176       |
| 6 | 1 | 0 | 2,4536623    | 2,4504860    | 0,3176       |
| 8 | 0 | 0 | 2,5132741    | 2,5066647    | 0,6609       |
| 4 | 1 | 1 | 2,5522419    | 2,5498477    | 0,2394       |
| 7 | 0 | 1 | 2,7025002    | 2,6979584    | 0,4542       |
| 7 | 1 | 0 | 2,7025002    | 2,6979584    | 0,4542       |

## 6.8) ELABORATION TIME

The elaboration time in the scalar case is shown in table 6.5.1 for TE eigenvalue of a rectangular structure. This time is sum of the filling matrix time( program in Fortran code) and the time needed to extract eigenvalue and eigenvectors of the matrix (Matlab code). The characteristics of the PC where we performed the simulations are: Intel(R) Core(TM) 2 CPU 6600 @ 2.40 Ghz and 4,00 GB RAM with Win Xp 64 bit and Matlab version r2009b.

$N_p$ = number of points for rectangular structure

$T_{fm}$ = Time (s) of filling matrix

Time extract TE= time (s) needed to extract eigenvalue and eigenvectors TE of the matrix

Time extract TM= time (s) needed to extract eigenvalue and eigenvectors TM of the matrix

| $N_p$ | $T_{fm}$ | Time extract TE | Time extract TM |
|-------|----------|-----------------|-----------------|
| 2000  | 0,28     | 0,38            | 0,24            |
| 5000  | 0,83     | 0,49            | 0,35            |
| 10000 | 1,83     | 0,77            | 0,62            |
| 20000 | 3,71     | 1,26            | 1,15            |
| 40000 | 7,24     | 2,75            | 2,47            |

The latter is very small since we deal with highly sparse matrix. It is worth noting that the filling time scales with the number of grid point. The eigenvectors computation time, on the other hand, increases very slowly with it. The same behavior is obtained for all other structures.

For the vector FD, instead, the computation time of eigenvectors is two order of magnitude large than the scalar case, since the matrix is full. However, the total time is still smaller than that required by CST

## **Chapter VII**

### **CONCLUSION**

In this thesis the use of a finite differences approach for the computation of the modes of electromagnetic structures with arbitrary geometry has been discussed. We have considered essentially the computation of waveguide modes, but the extension to 3D structure has been partly considered.

The main point is how to overcome the main drawbacks of FD, to get an effective strategy.

The standard discretization through a cartesian grid is derived from the expression of the Laplace operator in Cartesian coordinates. In this work, a different grid polar and elliptic deriving from the Laplace operator written in a form suitable to different structures under test, has been proposed.

The first test involved a circular guide, using the Laplace operator and a discretization grid in polar coordinates. Good results have been obtained with a low computational load, compared to FEM technique; and an high precision, comparable, with analytic results. In particular, as shown in chapter IV, this approach can be extended to elliptic waveguides.

Another problem, described in chapter 3, has been the redefinition of the Laplace operator based on boundary conditions in order to use a single grid for both TE and TM modes.

In chapter V it has been presented a FD technique for the computation of modes and eigenvalues of a waveguide whose boundary are irregular, such as polygonal, or consisting of segments and circular arcs, taking exactly into account the boundary of the waveguide and therefore with no loss of accuracy.

As an extension of scalar FD described in the paragraphs (3.4),(3.5),(3.7),(4.3), the Vector finite differences method has been proposed. In this case the computation of the TE and TM modes has been obtained by solving the vector

Helmholtz equation. The problem is reduced to a constrained eigenvalues problem. The vector finite difference approximation of the vector Helmholtz eigenvalues equation both on a Cartesian and on a curvilinear grid have been considered.

The results obtained analysing different cases of scalar and vector FD are very accurate. From these data, it appears that the proposed techniques are able to evaluate modes with a very small error, both on eigenvalues and on eigenvectors. The error on the eigenvalue is no larger than 0.3% . The RMS error on normalized modes is even small, being less than  $5 \cdot 10^{-8}$  in all cases, as shown in the tests reported in chapter VI. Future developments of this thesis are the extension of FD:

- to 3D cases for the study of close structures, in particular to evaluate modes of the resonant cavities
- to optical fibers and dielectric guides..

## Appendix

### I) CONSTRAINED EIGENVALUE PROBLEMS

The constrained eigenvalue problems is:

$$\text{I.1.} \quad \begin{cases} Ax = \lambda x \\ C^T x = 0 \end{cases}$$

where A is a  $(2n, 2n)$  matrix, and C is  $(2n, m)$  with  $n > m$  and  $\lambda = -k_t^2$ .

We can solve (I.1) using the QR factorization  $C = Q \cdot R$  where Q is an orthogonal  $(2n, 2n)$  matrix ( $Q^{-1} = Q^T$ ) and R is a upper triangular matrix  $(2n, m)$  that form is ; then substitute in second equation of (I.1):

$$\text{I.2.} \quad C^T \cdot x = (Q \cdot R)^T \cdot x = R^T \cdot Q^T \cdot x = R^T \cdot (Q^T \cdot x) = 0$$

which suggest to change the unknown as:

$$\text{I.3.} \quad y = Q^T \cdot x \Rightarrow x = Q \cdot y$$

(I.2) becomes:

$$\text{I.4.} \quad C^T \cdot x = R^T \cdot y = 0$$

Replacing  $x = Q \cdot y$  in the first of (I.1) and multiplying all member to  $Q^T$  we obtaine:

$$\text{I.5.} \quad A \cdot Q \cdot y = \lambda \cdot Q \cdot y \Rightarrow Q^T \cdot A \cdot Q \cdot y = Q^T \cdot \lambda \cdot Q \cdot y \Rightarrow By = \lambda y$$

where  $B = Q^T \cdot A \cdot Q$  is a  $(2n, 2n)$  matrix. The unknown can be partitioned in two vector  $y = \begin{bmatrix} u \\ v \end{bmatrix}$ , where  $u$  and  $v$  are  $(n, 1)$  vector. Then equations (I.4), (I.5) on rewritten in portioned form as::

$$\text{I.6.} \quad \begin{cases} B \cdot y = \lambda \cdot y \\ R^T \cdot y = 0 \end{cases} \Rightarrow \begin{cases} \begin{bmatrix} B_{11} & B_{12} \\ B_{21} & B_{22} \end{bmatrix} \cdot \begin{bmatrix} u \\ v \end{bmatrix} = \lambda \cdot \begin{bmatrix} u \\ v \end{bmatrix} \\ \begin{bmatrix} T_1 & 0 \end{bmatrix} \cdot \begin{bmatrix} u \\ v \end{bmatrix} = 0 \end{cases}$$

where  $B_{ij}$  is a  $(n, n)$  matrix.  $T_1$ , are (invertible) triangular matrix . The second equation of (I.6) becomes:

$$\text{I.7.} \quad T_1 \cdot u = 0 \quad \rightarrow u = 0$$

Therefore the first of I.7 becomes:

$$\text{I.8.} \quad B_{22} \cdot v = \lambda v$$

and we need to extract the eigenvalues of  $B_{22}$ .

This discretized eigenvalues problem must be solved by numerical routine and, the full matrix routines of Matlab have been used. The waveguide modes can then be obtained as

$$\text{I.9.} \quad x = Q \cdot \begin{bmatrix} 0 \\ v \end{bmatrix}$$

## **List of papers by the author**

### **Journal Paper:**

- [1] A.FANTI, G.MAZZARELLA. "A Finite Difference Polar-Cartesian Grid Approach For Mode Computation in Rounded-End Waveguides", *Aces Journal* , Vol.26, no. 9, September 2011.

### **Submitted Journal Paper:**

- [2] A. FANTI, G. MAZZARELLA,, " Computation of TE and TM Modes of Circular and Elliptic Waveguides with Curvilinear Finite Difference", (submitted to *IEEE Trans. Microwave Theory and Techniques*)
- [3] A. FANTI, G. MAZZARELLA, G. MONTISCI, "Curvilinear Vector Finite Difference Approach to the Computation of Waveguide Modes", (submitted to *ADVANCED ELECTROMAGNETICS*)
- [4] A. GIFUNI, A. SORRENTINO, A. FANTI, G. FERRARA, M. MIGLIACCIO, G. MAZZARELLA, F. CORONA, "On the Evaluation of the Shielding Effectiveness of Electrically Large Enclosure", (submitted to *ADVANCED ELECTROMAGNETICS*)

### **Journal Paper (In Preparation):**

- [5] A.FANTI, G.MAZZARELLA. "Finite difference single grid evaluation of TE and TM modes in waveguides.

### **International Conference Papers:**

- 1. A.FANTI, G.MAZZARELLA. "Finite difference variable grid evaluation of TE modes in metallic ridge waveguides", *Proc. Int. Conf. Mathematical Methods in Electromagnetic Theory (MMET\*10)*, Kiev, 06–08 September 2010,WGC-5.
- 2. A.FANTI, G.MAZZARELLA. "Curvilinear Finite Difference Approach to the Computation of Modes of Circular and Elliptic Waveguides"*Proc. Int. Conf. on Applied Electromagnetics and Communications (ICECom 2010)*, Dubrovnik, Croazia, 20-23 September 2010.
- 3. A.FANTI, G.MAZZARELLA. "Finite difference single grid evaluation of TE and TM modes in metallic waveguides ", *Proc. Int. Conf. Loughborough Antennas and Propagation Conference (LAPC2010)*, UK, pp. 517-520, 08-09 Nov. 2010.
- 4. A.FANTI, G.MAZZARELLA. "A finite difference polar-cartesian grid approach for mode computation in rounded-end waveguides", *Proc. Int. Conf. Eighth International Conference on Computation in Electromagnetics (CEM2011)*,Wroclaw, Poland 11-14 April 2011
- 5. A.FANTI, G.MAZZARELLA. " Computation of TE modes with Vector finite difference in to rectangular waveguides",*Proc. 13<sup>th</sup> International Symposium on Microwave and Optical Technology ISMOT 2011* Prague, Czech Republic, EU, June 20-23, 2011

6. A.FANTI, G.MAZZARELLA. " Finite difference computation of TE and TM modes using a single grid", Proc. 13<sup>th</sup> International Symposium on Microwave and Optical Technology ISMOT 2011 Prague, Czech Republic, EU, June 20-23, 2011
7. A.FANTI, G.MAZZARELLA. " Vector Finite Difference Approach to the Computation of Circular Waveguide Modes", Proc.10<sup>th</sup> International Conference on Applied Electromagnetics - PES 2011, Nis, Serbia 25-29 September 2011
8. A.FANTI, G.MAZZARELLA. "Vector Finite Difference Approach to the Computation of TM Waveguide Modes.", Proc.Int. Conf. Loughborough Antennas and Propagation Conference (LAPC2011), UK, 14-15 Nov. 2011
9. A.CASULA, PAOLO.MAXIA, A.FANTI. "A cylindrical resonant cavity for biological experiments and chemical catalysis," Proc.Int. Conf. Loughborough Antennas and Propagation Conference (LAPC2011), UK, 14-15 Nov. 2011
10. A.GIFUNI, A.SORRENTINO, G.FERRARA, M.MIGLIACCIO, A.FANTI, G.MAZZARELLA. "Measurements on the Reflectivity of Materials in a Reverberating Chamber" , Proc.Int. Conf. Loughborough Antennas and Propagation Conference (LAPC2011), UK, 14-15 Nov. 2011
11. A. GIFUNI, A. SORRENTINO, A. FANTI, G. FERRARA, M. MIGLIACCIO, G. MAZZARELLA, F. CORONA, "On the Evaluation of the Shielding Effectiveness of Electrically Large Enclosure", Proc.Int. Conf. Advanced Electromagnetic Symposium (AES2012) 16-19 April 2012, Paris. (Accepted)
12. A. FANTI, G. MAZZARELLA, G. MONTISCI, "Curvilinear Vector Finite Difference Approach to the Computation of Waveguide Modes", Proc.Int. Conf. Advanced Electromagnetic Symposium (AES2012) 16-19 April 2012, Paris. (Accepted)
13. A. FANTI, M. FRANCESCHELLI, P.MAXIA, D. SALPIETRO,"ELU-1:Emotions Language Unified is a BCI for communication support", Proc.Int. Conf. Advanced Electromagnetic Symposium (AES2012) 16-19 April 2012, Paris. (Accepted)

#### **National Conference Papers:**

14. A.FANTI, G.MAZZARELLA. "Una tecnica di calcolo dei modi per guide d'onda e aperture non standard ". RiNEm XVII Riunione Nazionale di Elettromagnetismo. Lecce, 15-18 settembre 2008, p. #134



## Bibliography

- [1] A. Wexler, "Solution of waveguide discontinuities by modal analysis," IEEE Trans. Microwave Theory and Techniques, vol. MTT-15, pp. 508-517, September 1967.
- [2] A. Pellegrini, S. Bertini, A. Monorchio, G. Manara, "A Mode Matching - Finite Element - Spectral Decomposition Approach for the Analysis of Large Finite Arrays of Horn Antennas," ACES Journal, vol.24 no.2 pp.233-240, April 2009.
- [3] K.L.Chan and S.R.Judah, "Mode-matching analysis of a waveguide junction formed by a circular and a larger elliptic waveguide," IEEE Trans. Microwaves, Antennas and Propagation, IEE Proceedings - Vol.145, pp.123 - 127, February 1998.
- [4] Lin, S. L., L. W. Li, T. S. Yeo, and M. S. Leong, " Novel unified mode matching analysis of concentric waveguide junctions," IEEE Trans. on Antennas and Propagation, Vol. 148, No. 6, pp.369-374, December 2001.
- [5] R.Sorrentino, F.Alessandri, M.Mongiardo, G.Avitabile, L.Roselli, "Full-wave modeling of via hole grounds in microstrip by three-dimensional mode matching technique," IEEE Trans. Microwave Theory and Techniques, vol. MTT-40, no.12, pp. 2228-2234, December 1992.
- [6] Collin.R.E., "Field theory of guided waves", 2nd ed, IEEE Press,N.Y., 1991
- [7] G. Mazzarella, G. Montisci: A Rigorous Analysis of Dielectric-Covered Narrow Longitudinal Shunt Slots with Finite Wall Thickness;" Electromagnetics", Vol. 19, pp. 407-418, October 1999.
- [8] G. Montisci, M. Musa, G. Mazzarella: Waveguide slot antennas for circularly polarized radiated field; IEEE Trans. on Antennas and Propagation, vol 52, pp. 619-623, Feb 2004.
- [9] G. Mazzarella, G. Montisci: "Accurate Characterization of the Interaction between Coupling Slots and Waveguide Bends in Waveguide slot Arrays," IEEE Trans. Microwave Theory and Techniques, vol.48, issue(7), pp. 1154-1157, July 2000.
- [10] Roger F. Harrington," Time-Harmonic Electromagnetic", IEEE Press Wiley-Interscience John Wiley & Sons, INC.
- [11] L. J. Chu, "Electromagnetic waves in elliptic hollow pipes of metal," J.Appl. Phys., l. 9, pp. 583-591, Sept.1938.
- [12] N.Marcuvitz, Waveguide Handbook. London: Peter Peregrinius, 1986, pp. 80-84
- [13] J. G. Kretschmar, "Wave propagation in hollow conducting elliptical waveguides," IEEE Trans. Microwave Theory Tech., vol. MTT-18, pp.547-554, Sept. 1970.
- [14] D. A. Goldberg, L. J. Laslett, and R. A. Rimmer, "Modes of elliptical waveguides: A correction," IEEE Trans . Microwave Theory Tech., vol.MTT-38, no. 11, pp. 1603-1608, Nov. 1990.
- [15] T.Rozzi,L.Pierantoni, M.Ronzitti. "Analysis of the Suspended Strip in Elliptical Cross Section by Separation of Variables" IEEE Trans . Microwave Theory Tech., vol.MTT-45, no. 11, pp. 1778-1784, Nov. 1997.
- [16] B.K.Wang, K.Y.Lam, M S. Leong, and P.S.Kooi, "Elliptical waveguide analysis using improved polynomial approximation ," Proc.Inst.Elect.Eng., vol.141, pp.483-488, 1994.
- [17] C. Shu. "Analysis of Elliptical Waveguides by Differential Quadrature method" IEEE Trans Microwave Theory Tech., vol.48, no. 02, pp. 319-322, Feb. 2000
- [18] Bernard Dacorogna, "Direct methods in the calculus of variations", 2nd ed, Springer, 2007

- [19] Norrie, Douglas H. and Gerard De Vries, "The Finite Element Method: Fundamentals and Applications", Press, New York, 1973
- [20] K.W. Morton and D.F. Mayers, Numerical Solution of Partial Differential Equations, An Introduction. Cambridge University Press, 2005
- [21] M. J. Beaubien and A. Wexler, "An Accurate Finite-Difference Method for Higher Order Waveguide Modes," IEEE Trans. Microwave Theory and Techniques, Vol. MTT-16, no. 12, pp. 1007-1017, December 1968
- [22] A.Fanti, G.Mazzarella. "A Finite Difference Polar-Cartesian Grid Approach For Mode Computation in Rounded-End Waveguides", Aces Journal , Vol.26, no. 9, September 2011.
- [23] A.Fanti, G.Mazzarella. "Curvilinear Finite Difference Approach to the Computation of Modes of Circular and Elliptic Waveguides"Proc. Int. Conf. on Applied Electromagnetics and Communications (ICECom 2010), Dubrovnik, Croazia, 20-23 September 2010.
- [24] A.Fanti, G.Mazzarella. " Vector Finite Difference Approach to the Computation of Circular Waveguide Modes", Proc.10th International Conference on Applied Electromagnetics - PES 2011, Nis, Serbia 25-29 September 2011
- [25] A.Fanti, G.Mazzarella, G. Montisci, "Curvilinear Vector Finite Difference Approach to the Computation of Waveguide Modes", Proc. Int. Conf. Advanced Electromagnetic Symposium (AES2012) 16-19 April 2012, Paris. (Accepted)
- [26] A.Fanti, G.Mazzarella. "Finite difference single grid evaluation of TE and TM modes in metallic waveguides ", Proc. Int. Conf. Loughborough Antennas and Propagation Conference (LAPC2010), UK, pp. 517-520, 08-09 Nov. 2010.
- [27] A.Fanti, G.Mazzarella. " Finite difference computation of TE and TM modes using a single grid", Proc. 13th International Symposium on Microwave and Optical Technology ISMOT 2011 Prague, Czech Republic, EU, June 20-23, 2011.
- [28] A.Fanti, G.Mazzarella. " Computation of TE modes with Vector finite difference in to rectangular waveguides",Proc. 13th International Symposium on Microwave and Optical Technology ISMOT 2011 Prague, Czech Republic, EU, June 20-23, 2011
- [29] A.Fanti, G.Mazzarella. "Vector Finite Difference Approach to the Computation of TM Waveguide Modes.", Proc.Int. Conf. Loughborough Antennas and Propagation Conference (LAPC2011), UK, 14-15 Nov. 2011
- [30] A.Fanti, G.Mazzarella. "A finite difference polar-cartesian grid approach for mode computation in rounded-end waveguides", Proc. Int. Conf. Eighth International Conference on Computation in Electromagnetics (CEM2011),Wroclaw, Poland 11-14 April 2011
- [31] G. Franceschetti, Campi elettromagnetici, Boringhieri, Torino, 1983.
- [32] G H.Golub, C F.Van Loan," Matrix Computation" , Johns Hopkins Univ. Press, 1989.
- [33] J.Van Bladel," Electromagnetic Fields", A SUMMA Book, pp.503, hpc,1985
- [34] A.Fanti, G.Mazzarella. "Una tecnica di calcolo dei modi per guide d'onda e aperture non standard ". RiNEm XVII Riunione Nazionale di Elettromagnetismo. Lecce, 15-18 settembre 2008, p. #134
- [35] A.Fanti, G.Mazzarella. "Finite difference variable grid evaluation of TE modes in metallic ridge waveguides", Proc. Int. Conf. Mathematical Methods in Electromagnetic Theory (MMET\*10), Kiev, 06-08 September 2010,WGC-5.
- [36] Sh. Zhang, Y. Chen, Eigenmodes Sequence for an Elliptical Waveguides with Arbitrary Ellipticity, IEEE Trans. Microwave Theory and Techniques, vol.43, issue(1), pp. 227-230, Jan. 1995.

## **Acknowledgements**

I would like to thank all the people that in these years have supported me both from a scientific and human point of view. First, I would like to thank my advisor Prof. Giuseppe Mazzearella for his support along my graduate studies. He dedicated to me a lot of time and guided me during my PhD. The period in York (England) has been certainly one of the most hard periods of my Ph.D., but I will always remember it as one of the most beautiful moments of my entire life. Many people helped me in having such an enjoyable period there. Certainly without Andy, Greg, Rob, my England staying wouldn't have had the same taste. I have much appreciated that nice person which is Jaqhi Chen, who gave me his hospitality with courtesy and helpfulness. There are also other people who in that period showed me their affection even if I was more than two thousands of kilometers away. Thanks to everybody. Special thanks to Prof Andy C.Marvin and Prof Maurizio Migliaccio for their ospitality during my stay in their group and for the great opportunity to work with them.

I would like to thank Andrea Casula, Giorgio Montisci, Giampaolo Serra, Luisa Deias, Patrizia Serra, Paolo Maxia for their fruitful collaboration.

I would like to thank Prof Dan Doru Micu and Prof. Konstantina S. Nikita for reviewing this thesis. I thank all ex colleague of IT Group Vol2: Stefano Mei, Massimo Pittau, Nicola Sirena, Reinier Van Kleij for their fruitful collaboration in business. I thank the ex-colleague of Agile-Ex Eutelia, Fulvio Mattiello, Daniele Salpietro, Giuliano Uboldi for valuable advice.

I would like to thank Sebastiano, Andrea, Matteo, Roberto, Mauro, Filippo, Federico, Paolo, Antonio, Fabio, Mattia, for their invaluable friendship during last 3 years.

I would like to thank all priest: Don Felice Nuvoli, Don Chicco Locci, Padre Bruno Bisceglia for their support.

I thank all my friends for their invaluable friendship during this years. Finally, I thank my parents Augusto and Bonaria, my brother Stefano, my sisters Sara and Veronica my fiancée Alessia, for their help during all the hardest moments of my studies.